A Model *In Vitro* System to Study Heat Shock Protein 60 (HSP60) Expression in Response to Mitochondrial Impairment in Human Cells

A thesis

submitted in partial fulfilment

of the requirements for the degree

of

Master of Science in Biological Sciences

at

The University of Waikato

by

Luke Hall

THE UNIVERSITY OF
WAIKATO
Te Whare Wānanga o Waikato

2013

Abstract

Heat Shock Proteins (HSPs) are a class of ubiquitously expressed and functionally related proteins found in all living organisms from humans to bacteria. Their expression is increased in response to various cellular stressors in what is referred to as the heat shock response. The induction of one particular HSP, HSP60, has been found to be correlated with mitochondria specific cell stress. Recently HSP60 has been found to be secreted and expressed extracellularly, after first being thought to be strictly intracellular. However, the mechanisms of these mechanisms of translocation and secretion have not been clearly identified.

The aim of this study was to develop a model *in vitro* system for HSP60 expression in human cells so that treatments which resulted in mitochondrial impairment could be investigated.

This study looked at several aspects of high glucose, hydrogen peroxide (H_2O_2), and sodium azide treatment on human HeLa cells. At low levels, each treatment had a hormetic effect on HeLa cell growth; however at high concentrations growth was significantly inhibited. Additionally, high treatment concentrations resulted in increased cell lysis as determined by LDH assays. Treatment with concentrations of 100mM glucose, 200μM H_2O_2, and 50μM sodium azide were the only treatment concentrations that did not result in significantly different levels of cell lysis when compared to a control sample. Mitochondrial dehydrogenase activity was also found to be significantly decreased at high treatment concentrations as determined by MTT assays. Thus, 100mM glucose, 200μM H_2O_2, and 50μM sodium azide treatments were identified as optimal conditions for mitochondrial targeted cell stress, as each of these treatments impaired cell growth and inhibited mitochondrial activity while having no significant effect on the degree of cell lysis.

The 100mM glucose, 200μM H_2O_2, and 50μM sodium azide treatments were then investigated for the intracellular reactive oxygen species (ROS) activity they induced over treatment periods of 24 hours, 3 and 7 days. After 7 days of treatment, the 200μM H_2O_2 and 50μM sodium azide treatments resulted in an approximate three-fold increase in ROS activity, while the 100mM glucose treatment resulted in almost twice as much ROS compared to a control sample.

Finally, the effects of 100mM glucose, 200µM H_2O_2, and 50µM sodium azide treatments on HSP60 and HSP70 expression was also examined over 3 and 7 day time periods. After the 7 day treatment period, the 100mM glucose treatment had induced a 2.43 fold increase in HSP60 expression and a 2.75 fold increase in HSP70 expression, the 200µM H_2O_2 induced a 3.48 fold increase in HSP60 expression and a 3.98 fold increase in HSP70 expression, and finally the 50µM sodium azide induced a 4.74 fold increase in HSP60 expression and a 5.08 fold increase in HSP70 expression.

It can therefore be concluded that 100mM glucose, 200µM H_2O_2, and 50µM sodium azide results in the upregulation of HSP60 and HSP70 in human HeLa cells. Therefore this model may be used to investigate further aspects of HSP60 induction, such as its translocation and secretion.

Acknowledgements

I would like to thank my Master's supervisor, Dr. Ryan Martinus, for his guidance and support over the past year. I have really enjoyed his hands-off approach, letting me get on and do things as I saw fit, but still there to provide helpful advice and support when things inevitably lost their way. In doing so I feel I have learned so much more than I otherwise would have. Thank you also for putting time in to go through my thesis drafts as well.

I would also like to thank the University of Waikato for the scholarships they have awarded me throughout the course of my study. By alleviating my financial pressures I have been allowed to focus much more effectively on my work.

A big thank you goes to Kerry Allen for doing such a great job filling in as lab manager. Things would only have stuttered along without her there to smooth everything out. Thanks also to Julie Goldsbury for my crash course on cell culture. At least some of it stuck which made things a lot easier than they would otherwise have been.

Thanks heaps to Judith Burrows who really helped me find my feet through the beginning stages of this thesis and was always willing to help with anything and everything. Thanks also to Dr Gregory Jacobson and Olivia Patty in the Molecular Genetics Laboratory for letting me use their equipment and space, and providing sound advice. A special thank you goes to Richard Lobb who went through all the trials and tribulations of western blotting with me, and put in a lot of time and energy to help me get them right.

Also, thank you to my family for all the support, especially Ma and Pa. Thank you also to my sister T-dog, long may our *quid pro quo* system continue.

Table of Contents

List of Figures

List of Tables

List of Equations

List of Abbreviations

˚C, degree Celsius; ADP, Adenosine diphosphate; AGE, Advanced glycated endproduct; AIF, Apoptosis-inducing factor; APAF-1, Apoptotic protease activating factor-1; APC, Antigen presenting cell; APS, Ammonium persulphate; ATP, Adenosine triphosphate; AZT, Azidothymadine; BMI, Body mass index; CHO, Chinese hamster ovary; CLSM, Confocal laser scaning microscopy; CNS, Central nervous system; CoA, Coenzyme A; CVD, Cardiovascular disease; DC, Dendritic cell; DCF, 2, 7-dichlorofluorescin; DCFDA, 2,7-dichlorofluorescein diacetate; DNA, Deoxyribonucleic acid; ELISA, Enzyme-linked immunosorbant assay; ERK, Mitogen-activated protein kinase; FBS, Fetal bovine serum; FFA, Free fatty acid; H_2O_2, Hydrogen peroxide; HbA1c, Glycated haemoglobin; HDL, High-density lipoprotein; HSE, Heat shock element; HSF, Heat shock factor; HSF1BP, Heat shock factor-1 binding protein; HSP, Heat shock protein; HUVEC, Human umbilical vein endothelial cell; IFG, Impaired fasting glucose; IFN, Interferon; IGT, Impaired glucose tolerance; IKK, I-κB kinase; IL, Interleukin; INS, Infectious nonself; IR, Insulin resistance; JNK, c-Jun N-terminal kinase, LAL,Limulus amebocyte lysate; LDH, Lactate dehydrogenase; LDL, Low-density lipoprotein; LPS, Lipopolysaccharide; MCP-1, Monocyte chemoattractant protein-1; MHC, Major histocompatibility complex; MMP, Matrix metalloproteinase; MRS, Magnetic resonance spectroscopy; MTT, 3-(4,5-dimethylthiazol-2-yl)-2,5-diphenyl tetrazolium bromide; NADH, Nicotinamide adenine dinucleotide; NADPH, Nicotinamide adenine dinucleotide phosphate; NCD, Non-communicable disease; NO, Nitric oxide; O_2^-, Superoxide; PAMP, Pathogen-associated molecular pattern; PBMC, Peripheral blood-derived mononuclear cell; PGC, Peroxisome proliferator-activated receptor co-activator; PMSF, Phenylmethylsulfonyl fluoride; PRR, Pattern recognition receptors; ROS, Reactive oxygen species; RT, Room temperature; SNS, Self-nonself; SOD, Superoxide dismutase; T2D, Type 2 Diabetes Mellitus; TBS, Tris buffered saline; TGF, Transforming growth factor; TLR, Toll-like receptor; TNF, Tumour necrosis factor; UCP, Uncoupling protein; VCAM, Vascular cell adhesion molecule; WHO, World Health Organisation; WR, Working reagent.

1 Literature Review and Research Aims

This chapter presents a general overview of type 2 Diabetes Mellitus and obesity. A review of the current literature on the roles of heat shock protein 60 (HSP60) is also provided, with particular emphasis on its extracellular roles and involvement in the promotion of atherosclerosis. The chapter will conclude with the proposed hypothesis.

1.1 The 'Western Disease' Paradigm

The 'Western Disease' paradigm, or 'diseases of affluence', is a term sometimes given to selected non-communicable diseases (NCDs) and other health conditions which are commonly thought to be a result of increasing wealth in a society (Ezzatti *et al*., 2005). While already well-established in the 'West', these disorders are also on the rise in the developing world too, and therefore are a truly global problem. 36 million of the 57 million global deaths in 2008 were due to non-communicable diseases. 29% of NCD deaths in the developing world in 2008 were premature deaths, that being deaths before the age of 60 (World Health Organisation, 2011).

Factors associated with the increase of these conditions and illnesses appear to be, paradoxically, things which many people would regard as improvements in their lives; a reduction in menial physical activity, easy accessibility to low-cost foods, and a longer life-span. By eliminating manual tasks, people exert less energy in their everyday lives. This is accompanied by a 'Western' diet; that being low-cost, readily accessible fast food, with high fat and sugar contents, resulting in huge excess influxes of energy. This results in an energy imbalance, as people require less energy but consume an excessive amount. Due to the greater human longevity connected with the 'Western' lifestyle, associated problems have a much greater period of time to accumulate and exert their effects (Kershaw and Flier, 2004).

1.2 Type 2 Diabetes Mellitus

1.2.1 Statistics

With 346 million people worldwide diagnosed with diabetes, it is the most common metabolic disease in the world, of which type 2 diabetes (T2D) accounts for around 90%. T2D reduces projected lifespan, quality of life and has a huge financial cost; the United States alone exceeds $130 billion annually on diabetes related health care (Peterson, 2003). In 2004, an estimated 3.4 million people died from consequences of high blood sugar. The World Health Organisation (WHO) projects that diabetes related deaths will double between 2005 and 2030. (World Health Organisation, 2011). In New Zealand, the number of people diagnosed with diabetes in 1996 was 81,000 (Ministry of Health, 2007). This figure has grown, and is now estimated to be approaching 200,000, with the vast majority T2D (Ministry of Health, 2011). Additionally, people of Māori and Pacific origins have approximately 2.5 times the risk of developing T2D during their lives compared with New Zealand Europeans. They also develop diabetes 10 years earlier on average. While these figures are most marked for Māori and Pacific peoples, the rising prevalence of diabetes in the growing population descending from South Asia is also concerning (Ministry of Health, 2008). Patients with T2D have an increased risk of cardiovascular disease (CVD), which is responsible for 50-80% of deaths in people with diabetes (World Health Organisation, 2011). The common association of T2D and CVD will be reviewed in **Chapter 1.4**.

1.2.2 Definitions of Diabetes

The WHO's definitions of diabetes and intermediate hyperglycaemic states are summarised in **Table 1.1.** Impaired fasting glucose (IFG) and impaired glucose tolerance (IGT) are intermediate hyperglycaemic stages in the development of diabetes (World Health Organisation, 2006).

Table 1.1 Diagnostic criteria for diabetes and intermediate hyperglycaemia.

Condition	**Fasting plasma glucose** mmol/L (mg/dL)	**2-h plasma glucose*** mmol/L (mg/dL)
Normal	<6.1 (110)	<7.8 (140)
Impaired Fasting Glucose (IFG)	6.1-6.9 (110-125)	<7.8 (140)
Impaired Glucose Tolerance (IGT)	<7.0 (126)	≥7.8 and <11.1mmol/l (140mg/dl and 200mg/dl)
Diabetes	≥7.0 (126)	≥11.1mmol/l (200mg/dl)

*Venous plasma glucose 2 hours after 75g of glucose ingested.

An additional means of diagnosis is the detection of glycated haemoglobin (HbA1c) in the blood. HbA1c reflects average plasma glucose over the previous eight to twelve weeks, avoiding the problem of day-to-day variability of glucose values. Diagnosis of diabetes can be made if the HbA1c level is greater than 6.5%, and a level of 5.7% to 6.4% is indicative of intermediate hyperglycaemia (World Health Organisation, 2011).

1.2.3 Pathogenesis of T2D

Insulin is the principal hormone that regulates uptake of glucose from the blood into most cells. Therefore, deficiency of insulin or the insensitivity of its receptors plays a central role in all forms of Diabetes Mellitus. In the pathogenesis of T2D, insulin resistance is the symptom that occurs first in the early stages of disease progression. This leads to systemic hyperglycaemia, which eventually results in defects in insulin secretion by the pancreatic β-islet cells (Lowell and Shulman, 2005).

Glucose sensing by β-cells of the pancreatic islets of Langerhans is essential for maintaining glucose homeostasis. The β-cells act as sensors to vary insulin secretion to the predominant blood glucose level. Insulin allows skeletal muscle, liver and fat cells to take up glucose from the blood, as well as acting to promote glucose storage and inhibit glycogen breakdown.

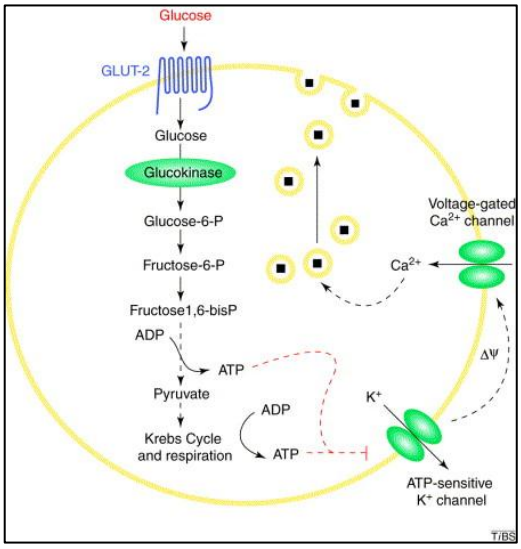

Figure 1.1- Glucose sensing in β-cells (Adapted from Rolland *et al*., 2001).

Figure 1.1 depicts the cascade of events that result from glucose sensing by β-cells. After docking at the GLUT-2 glucose transporter, the glucose monomer moves into the β-cell. It is processed through oxidative mitochondrial metabolism to produce adenosine-5'-triphosphate (ATP), increasing the net concentration of ATP in the cell at the expense of adenosine diphosphate (ADP). This increase in the ATP:ADP ratio of the cell results in the inhibition of an ATP:ADP-regulated potassium ion channel, culminating in plasma membrane depolarisation. As a result, voltage gated calcium channels open, causing an influx of calcium ions into

the β-cell. The calcium ions signal to insulin vesicles to dock at the cell membrane and expel their contents into the extracellular space (Rolland *et al*., 2001).

Insulin resistance (IR) is a condition where the primary insulin-responsive organs (skeletal muscle, the liver and adipose tissue) require higher levels of insulin for glucose sensing. Due to this impaired ability of the peripheral tissues to take up glucose, and the resulting failure of glycogen synthesis and the suppression of glucose production in the liver, hyperglycaemia ensues.

There is substantial evidence indicating that mitochondrial dysfunction also plays a role in the pathogenesis of T2D. This occurs in a number of different ways. There is a systemic increase in oxidative stress in diabetic individuals as a result of excess production of superoxide free radicals by the mitochondrial electron-transport system (Giacco and Brownlee, 2010; Rolo and Palmeira, 2006). Defects in mitochondrial fatty acid metabolism may lead to the accumulation of intracellular fatty acid metabolites, such as diacylglycerol and fatty acid acyl coenzyme As (fatty acyl CoAs). These metabolites activate protein kinase C, which sets in motion a cascade of events which culminates in suppression of insulin-stimulated glucose transport (Lowell and Shulman, 2005). Also, magnetic resonance spectroscopy (MRS) has been used to show that young IR progeny of parents with T2D have a lower ratio of type 1 (oxidative) to type 2 (glycolytic) muscle fibers when compared to insulin-sensitive controls. As type 1 fibers hold more mitochondria than type 2, it is inferred that IR individuals contain less muscle mitochondria. There is evidence that reduction in mitochondria numbers in these IR individuals is due to the down-regulation of nuclear encoded genes that regulate mitochondrial biogenesis, in particular peroxisome proliferator-activated receptor co-activators 1α and 1β (PGC-1α and PGC-1β) (Chanseaume and Morio, 2009; Lowell and Shulman, 2005). Mitochondrial dysfunction within the insulin secreting β-cells has been proposed to result in β-cell dysfunction through several means, and therefore the pathogenesis of T2D. Uncoupling protein 2 (UCP2) is an inner mitochondrial membrane protein that, when activated, leaks protons across the inner membrane space to uncouple the oxidative metabolism of glucose with ATP synthesis. It is therefore a negative regulator of glucose-stimulated insulin secretion, as an increase of the ATP:ADP ratio is required for insulin secretion, as previously mentioned. A pathogenic role in T2D has been suggested for UCP2 as both *in vitro* and *in vivo* models have

demonstrated that it is stimulated by hyperglycaemia and hyperlipidaemia, as well as superoxide radicals produced as a byproduct from the electron transport chain. β-cell mass has also been shown to be reduced in T2D individuals. While the cause of this reduction is still unknown, one garnered hypothesis is that it is due to mitochondrial mediated apoptosis, again implying mitochondrial dysfunction in the pathogenesis of T2D (Mulder and Ling, 2009; Kim *et al*., 2008; Lowell and Shulman, 2005).

1.3 Obesity

1.3.1 Statistics

In 2008, globally, more than 1.4 billion adults were overweight. Of these, over 200 million men and nearly 300 million women were obese. At least 2.8 million people die each year as a result of being overweight or obese. Over 40 million preschool children were overweight in 2008. The prevalence of obesity has nearly doubled between 1980 and 2008 (World Health Organisation, 2012). In New Zealand, in 1977, 9.4% of men and 10.8% of women were considered obese. By 2003 these figures had more than doubled; 19.9% of men and 22.1% of women were considered obese. Statistics are worse for Māori and Pacific peoples with Māori male obesity rising from 19.3% to 27.0% and Māori female obesity rising from 20.0% to 26.5% between 1989 and 2003. Extreme obesity has also been increasing. In 1977, 0.3% of males and 1.2% of females were considered extremely obese, which has risen to 2.2% and 3.0% respectively. Again, figures for Māori men are much more prevalent. Māori male extreme obesity rose from 3.2% to 7.8% and Māori female extreme obesity held at approximately 7.0% between 1989 and 2003 (Ministry of Health, 2004). Like T2D, patients with obesity have an increased risk of CVD, which is the leading cause of death in people with obesity (World Health Organisation, 2012). The common association of obesity and CVD will be reviewed in **Chapter 1.4**.

1.3.2 Definitions of Obesity

Obesity is defined as abnormal or excessive fat accumulation that may impair health. Body mass index (BMI) is a heuristic proxy for body fat defined as a person's weight in kilograms divided by the square of their height in meters (kg/m^2). Abdominal fat mass can vary considerably within a narrow range of total body fat and BMI. Therefore, waist circumference is used to complement the measurement of BMI, to identify individuals at increased risk of obesity related morbidity due to accumulation of abdominal fat. The WHO's classification of body fat based on BMI and waist circumference is summarised in **Table 1.2** (World Health Organisation, 2008; World Health Organisation, 2012).

Table 1.2 - Classifications of body fat and disease risk based on BMI and waist circumference**.**

Classification	**BMI (kg/m^2)**	**Obesity Class**	**Disease risk (relative to normal weight and waist circumference)**	
			Men < 102 cm Women < 88 cm	Men >102 cm Women >88 cm
Underweight	<18.5			
Normal	18.5-24.9			
Overweight	25-29.9		Increased	High
Obese	30-34.9 35-39.9	I II	High Very high	Very high Very high
Extremely Obese	>40	III	Extremely high	Extremely high

1.3.3 Pathogenesis of Obesity

Evolving in an environment of scarcity, the human genome has adapted to survive in such conditions. However, there has been a relatively rapid change to the availability of foodstuffs, to the point where they are now in overabundance. Poor diet and sedentary lifestyle are the predominant factors that explain most cases of obesity; however a minority of cases may be explained through genetics and other illnesses (Bray, 1999).

In most cases, obesity is simply a result of an energy imbalance, where the amount of energy coming into the body, through eating, grossly exceeds the amount of energy being expended through physical exercise. Excess energy is stored as adipocytes in the body's adipose tissues. Adipose tissue functions as a passive reservoir of energy storage, with an inherent buffering capacity; releasing energy to the body when energy levels are low and absorbing it when they are high for later use. However, with a constant net influx of energy, there is a consistent setting down of adipose tissue, resulting in an abnormally high set down of fat deposits which results in the characteristic expansion of girth in individuals with obesity (Laclaustra *et al*., 2007).

Over the past two decades it has been found that the adipose tissue also plays an important function as an endocrine organ, secreting adipocyte-derived cytokines, or adipokines. In addition, adipose tissue also expresses a number of receptors allowing it to respond to traditional hormone systems as well as the central nervous system (CNS). This implicates adipose tissue function as an integral component in an interactive endocrine network capable of communicating with distant organs and the CNS, and vice versa. Dysfunction of this endocrine component of the adipose tissue is another factor which impacts on the pathogenesis of obesity. Leptin is the most studied adipokine, known to play a number of important roles in the body. Although initially viewed as an antiobesity hormone, leptin's primary role is to serve as a signal of energy sufficiency, rather than excess, from the adipose tissue to the hypothalamus. Common forms of obesity are characterised by elevated circulating leptin levels, indicating that the body is trying to signal satiety to the brain, but the condition is not being ameliorated (Kershaw and Flier, 2004). This suggests that these common forms of obesity are consistent with a state of leptin resistance. Although the mechanism

for such resistance remains unknown, it has been postulated that it may result from the inefficient transport of leptin across the blood brain barrier (Bjorbaek and Kahn, 2004).

In an area of increasing interest, recent studies have shown that leptin inhibits insulin secretion from the pancreatic β-cells and have anti-insulin effects on liver and adipose tissue. If these effects on insulin are confirmed, leptin could play a role similar to tumour necrosis factor-α (TNFα) and could participate in the IR associated with obesity and T2D (Girard, 1997).

Grehlin, purported as the complimentary hormone to leptin, is a peptide produced in the stomach that is thought to be responsible for modulating short-term appetitive control. It acts on the hypothalamus, causing release of growth hormone from the pituitary. Chronic administration in rats results in obesity, and the fall in grehlin levels after gastric bypass surgery for obesity has been posited for the suppression of appetite seen after such operations (Flier, 2004).

Defects in the pro-opiomelanocortin receptor system, the peroxisome proliferator-activated receptor-gamma, the agouti-related peptide, hypothalamic injury following craniopharyngioma, and several rare genetic syndromes such as Prader-Willi syndrome, Bardet-Biedl syndrome, Cohen syndrome, and MOMO syndrome are also associated with human obesity. However, for most patients, it is not possible to connect obesity to any one specific cause (Bray, 1999).

An emerging trend is that obese individuals exhibit increased oxidative stress. Fat accumulation has been shown to positively correlate with systemic oxidative stress in both humans and mice. As the production of reactive oxygen species (ROS) increased, there was increased expression of NADPH oxidase and decreased expression of antioxidative enzymes. This would perhaps suggest that some degree of mitochondrial dysfunction may play some role in the pathogenesis of obesity (Furukawa *et al*., 2004).

1.4 T2D and Obesity

T2D and obesity are related diseases, as most patients with T2D are obese. However, most obese individuals do not have T2D. The causal interplay between the two is very complex and not fully understood. Whatever the relationship between T2D and obesity may be, it is recognised that both disease states lead to similar pathophysiological complications (Eckell *et al.*, 2011).

Metabolic syndrome is a combination of medical disorders that occur together to increase the risk of developing CVD. The two major disorders that contribute to metabolic syndrome are T2D and obesity. Metabolic syndrome is characterised with a number of pathophysiological conditions including hyperglycaemia, dyslipidaemia, abdominal obesity, and hypertension (Brownlee, 2001).

1.4.1 Complications of T2D

Diabetes is associated with pathophysiological conditions such as hyperglycaemia, hyperinsulinaemia, dyslipidaemia, abdominal obesity, raised blood pressure, a low-grade pro-inflammatory state, and atherosclerosis (Bailey, 2008). As previously mentioned, T2D patients have an increased risk of CVD, which is responsible for 50-80% of deaths in people with diabetes (World Health Organisation, 2011; Zarich, 2009). CVD is a collective term for both microvascular and macrovascular diseases. Microvascular diseases include various neuropathies, end-stage renal disease, and blindness; while macrovascular diseases refer to atherosclerotic events such as stroke, myocardial infarction, and limb amputation (Brownlee, 2001).

1.4.2 Complications of Obesity

A number of the major diseases associated with obesity have long been known and include hypertension, atherosclerosis, and diabetes, as well as certain types of cancer. Less well-known complications include hepatic steatosis, gallbladder disease, pulmonary function impairment, endocrine abnormalities, obstetric complications, trauma to the weight-bearing joints, gout, cutaneous disease, proteinuria, increased haemoglobin concentration, and possibly immunologic impairment (Bray, 1982). In addition, the site of obesity has long been known to impact on the severity of obesity related complications. Individuals with upper body segment obesity, that being abdominal obesity, have been found to be much

more prone to complications including glucose intolerance, hyperinsulinemia, and hypertriglyceridemia when compared to individuals with lower body segment obesity (Kissebah *et al.*, 1982). Much like in T2D, patients with obesity have an increased risk of CVD, which is also the leading cause of death in people with obesity (World Health Organisation, 2012).

1.4.3 CVD Complications

CVDs are the primary life threatening complication of T2D and obesity. The high levels of circulating free fatty acids (FFAs) associated with these disease states encourage the liver to produce more 'bad' low-density lipoprotein (LDL) cholesterol, while reducing levels of 'good' high-density lipoprotein (HDL) cholesterol. This alteration in relative cholesterol levels helps to promote atherosclerosis, which may culminate in CVD if left untreated. High circulating FFA levels also have deleterious effects on the body's blood vessels, causing constriction and hypertension. It also induces a signal to inflammatory factors, stimulating their recruitment, which can result in systemic, low-grade inflammation of the circulatory system's endothelium (Jensen, 2006).

Early stages of atherosclerotic development require recruitment of monocytes and their ultimate differentiation into macrophages (Ludewig and Laman, 2004; Beekhuizen and van Furth, 1993). Monocytes are required to cross the vascular endothelium for routine immunological surveillance of tissues and their entry into inflamed sites. This process of transendothelial migration, or diapedesis, initially involves tethering of monocytes to the endothelium, followed by loose rolling along the vascular surface. There is then the establishment of firm adhesion to the endothelium via interactions between the monocyte and a number of cellular adhesion proteins expressed on the endothelial cell surface. These adhesion proteins include vascular cell adhesion molecule-1 (VCAM-1), integrins and CD receptors, occurring at different steps along the migration. A gradient of chemoattractants is responsible for driving the subsequent monocyte migration into the endothelial intima. One of the major chemokines responsible for monocyte migration is monocyte chemoattractant protein-1 (MCP-1), which interacts with its receptor CCR2, located on the monocyte surface. After penetrating the endothelial basement membrane, the monocytes may migrate through the extracellular tissue matrix and differentiate into macrophages.

Macrophages are known to express a number of scavenger receptors, including CD36, which bind to modified forms of LDLs. Common modifications include oxidation and glycation (also referred to as non-enzymatic glycosylation). When macrophages take up these forms of LDLs they undergo several alterations, namely their morphology. They are termed foam cells due to their abnormal appearance under the microscope that resembles foam. Clusters of foam cells represent the early stages of the formation of atherosclerotic lesions. The foam cells amplify inflammatory signals from the site of the lesion through the production of ROS, cytokines and tissue damaging proteins, including the matrix metalloproteinases (MMPs). As foam cells continue to aggregate along with T helper cells and skeletal muscle cells, the lesion progresses and may lead to a thrombotic or embolic event. If the lesion were to get to a sufficient size it could occlude the vessel. If the atherosclerotic lesion were to rupture, the plaque could be carried through the bloodstream to any number of smaller capillaries which it could occlude. Depending on the site of blockage, a ruptured atherosclerotic lesion could result in myocardial infarction, stroke, or limb amputation (Maslin *et al*, 2005; Ludewig and Laman, 2004; Libby, 2002).

1.5 Heat Shock Proteins

Heat shock proteins (HSPs) are a group of highly conserved proteins found in all cells of all organisms in prokaryotic and eukaryotic life. They were first observed in 1962 by Ritossa, when a lab worker accidentally increased the incubation temperature of the fruit fly drosophila. When examining the chromosomes, Ritossa found a "puffing pattern" which was indicative of the elevated gene transcription of an unknown protein. This was later described as the 'Heat Shock Response' and the unknown proteins as the 'Heat Shock Proteins' (Ritossa, 1996). The enhanced synthesis of these proteins immediately after subjecting cells to a proteotoxic stress, such as heat shock, was first reported for drosophila cells in 1974, and the universality of the response, from bacteria to human, was recognized shortly thereafter (Schlesinger, 1990). HSPs are actually constitutively expressed, and have two main intracellular roles: a molecular chaperone function, where they act to mediate the folding, assembly or translocation across the intracellular membranes of other polypeptides; and a role in protein degradation, making up some of the essential components of the cytoplasmic ubiquitin-dependent degradative pathway (Burel *et al*., 1992). However, when exposed to a proteotoxic stressor, HSP expression is induced to prevent cellular damage and stave off apoptosis.

HSPs can be classified into six families, based on their molecular mass: the small HSPs (sHSP), HSP40, 60, 70, 90, and HSP110 (**Table 1.3**).

Table 1.3 Major mammalian HSP families (Adapted from Habich and Burkart, 2007).

Families	Size (KDa)	Prominent members	Localisation
sHSPs	12-43	B-crystallin HSP27	Cytoplasm Cytoplasm, nucleus
HSP40	~40	HSP40	Cytoplasm, nucleus
HSP60	~60	HSP60 TCP1	Mitochondria Cytoplasm
HSP70	~70	HSP70 HSC70 Grp78/BiP	Cytoplasm Nucleus Cytoplasm, ER
HSP90	~90	HSP90 (α and β) Gp96	Cytoplasm ER
HSP110	~110	HSP110	Cytoplasm

In more recent times, HSPs have been detected extracellularly, both on the cell surface and in the extracellular space. When expressed in these locations, HSPs take on an immunoregulatory role. Members of the HSP60 and HSP70 families in particular have been established as playing stimulatory roles of both the innate and adaptive immune systems when in these locales.

1.5.1 The HSP60 Family

Proteins belonging to the HSP60 family have a molecular weight of approximately 60 KDa. They also have high sequence homology between species with HSP60s of bacterial origin having homology higher than 97% while prokaryotic and human HSP60 show over 70% homology.

One of the most studied members of the HSP60 family is the *E. coli* GroEL protein. It is well documented for playing a crucial ATP-dependent role in protein folding along with its cofactor GroES, also referred to as HSP10. Crystal structures of GroEL show that it is an oligomer that forms a complex arranged as two stacked heptameric rings (Cheng *et al.,* 1990). This dual heptameric structure forms a large central cavity, which is where unfolded proteins bind through hydrophobic interactions (Fenton *et al.,* 1994).

The HSP60 subunit consists of three domains: the equatorial, intermediate, and apical domains. The equatorial domain contains the binding sites for ATP and the second heptameric ring. The intermediate domain fixes the equatorial and apical domains together. When ATP is bound, the intermediate domain undergoes a conformational change which exposes the hydrophilic regions of the protein, ensuring fidelity in protein binding. HSP10 binds to the apical domain of the ATP-bound active HSP60 complex, acting as a dome-like cap. This allows the central cavity to enlarge and aids in protein folding (Ranford *et al.,* 2000).

The amino acid sequence of HSP60 contains a series of G repeats at the C-terminal, although the structure and function of this sequence has not been conclusively defined. Like other nuclear-encoded mitochondrial proteins, the N-terminal of HSP60 contains a leader sequence of hydroxylated amino acids. This N-terminal presequence directs the protein into the mitochondria. Upon translocation to the organelle the leader sequence is cleaved off (Gupta, 1995).

In eukaryotes, HSP60 is found in the chloroplasts of plants as well as the mitochondria and cytoplasm of mammalian species. While HSP60 in *Saccaromyces cerevisiae* and chloroplasts exist and function as tetradecamers, in mitochondria HSP60 typically exists in a dynamic equilibrium between its constituents; monomers, heptamers and tetradecamers (Habich and Burkart, 2007). In the presence of ATP, mitochondrial HSP60 forms the tetradecamer complex and it dissociates into its monomers in its absence (Levy-Rimler *et al.*, 2001). In contrast, cytosolic HSP60 forms heterooligomeric ring structures and assists folding of cytoskeletal proteins, such as actin and tubulin (Llorca *et al*., 2000).

HSP60 expression been found to be induced in response to mitochondrial stress, and therefore its upregulation is a good indicator of mitochondrial impairment. This is in contrast to other HSPS, such as HSP70, where induced expression is an indicator of a general cell stress (Martinus *et al*., 1996)

More recently, HSP60 has also been documented to exist outside the cell. HSP60 has been found on the cell surface and extracellularly, such as in human circulation. When HSP60 is localised in such locations it plays an immunoregulatory role, and a possibility for cross-reactivity with microbial HSP60 has also been theorised. The localisation and function of extra-cellular HSP60 will be discussed in greater detail in later sections.

1.5.2 The HSP70 Family

Proteins belonging to the HSP70 family have a molecular weight of approximately 70 KDa. Eukaryotic organisms express several slightly different HSP70 proteins. All share the same common domain structure, but each has a unique pattern of expression or subcellular localization. These include HSC70, HSP70, BIP, and mtHSP70 (Tavaria *et al*., 1996).

HSP70 consists of three major functional domains. The N-terminal contains an ATPase domain, binding ATP and hydrolising it to ADP. This action results in conformational changes in the other two domains. The intermediate substrate binding domain contains a groove with an affinity for neutral, hydrophobic amino acid groups up to seven residues in length. The C-terminal domain is rich in alpha helices which act to enclose the substrate binding domain. When ATP is bound the helical ‘lid’ opens to bind and release peptides with relative speed. When ADP

is bound the lid closes, tightly binding peptides to the substrate binding domain (Flaherty *et al*., 1990).

HSP70 plays an important role in preventing the aggregation of newly formed proteins in the cytosol. As newly synthesised proteins emerge from the ribosomes, the intermediate substrate binding domain of HSP70 recognizes sequences of hydrophobic amino acid residues and interacts with them. The presence of peptides in the binding domain stimulates the ATPase activity of the N-terminal domain. When ATP is hydrolysed to ADP, the binding pocket of HSP70 closes, tightly binding and trapping peptide chain. By binding partially synthesized peptide sequences, HSP70 prevents them from aggregating and being rendered non-functional. Once the entire protein is synthesised, nucleotide exchange factors stimulate the release of ADP and binding of a new ATP molecule, releasing the peptide from the substrate binding domain of HSP70. The protein is then free to undergo spontaneous folding, or to be transferred to other chaperones for further processing. In much the same way, HSP70 also aids in intermembrane transport of proteins by stabilizing them in a partially folded state (Wegele *et al*., 2004; Tavaria *et al*., 1996).

HSP70 proteins also act to protect cells from a number of stressors. These stressors would normally act to damage proteins, causing partial unfolding and, potentially, aggregation. By temporarily binding to hydrophobic residues exposed by the stress, HSP70 prevents these partially denatured proteins from aggregating, and allows them to refold once the stress response has passed (Tavaria *et al*., 1996).

Finally, HSP70 also directly inhibits apoptosis by blocking the recruitment of procaspase-9 to the apoptosome complex (Beere *et al*., 2000).

Like HSP60, HSP70 has also been found to exist outside the cell, both surface bound and in the extracellular milieu. It too plays an immunoregulatory role, being reported to play roles in antigen binding and presentation to the immune system (Nishikawa *et al*., 2008).

1.5.3 Regulation of HSPs

HSPs can make up to 5-10% of the total protein content in optimal growing conditions. However, the synthesis of these proteins can be induced to make up to 15% of total protein content by stresses that induce protein unfolding, misfolding, aggregation, or a flux of newly synthesized non-native proteins (Pockley, 2003).

The inducible HSP component is regulated by heat shock factors (HSFs). These are transcription factors are that are usually negatively regulated but are activated upon cellular stress (Morimoto, 1993). When activated, these activators bind specifically to heat shock sequence elements (HSE) throughout the genome (Guertin and Lis, 2010). The HSEs are highly conserved from yeast through to humans (Guertin *et al*., 2010). Only one HSF has been identified in *Saccharomyces cerevisiae* and *Drosophila melanogaster*, however a number of HSFs exist in vertebrates and plants. This suggests that these HSF isoforms have diversified and specialised in these species (Pirkkala *et al*., 2001).

HSF-1 is the major regulator of HSP transcription in eukaryotes. Although sharing 40% structural homology to HSF-2, HSF-1 functions in response to stress stimuli whereas HSF-2 activates under early embryonic development, differentiation and by inhibition of ubiquitin-dependent proteasome (Pirkkala *et al*., 2001). In the absence of cellular stress, HSF-1 is inhibited due to its association with HSPs and is therefore maintained in an inactive state. For instance, HSP70 has been shown to play a role in HSF-1 deactivation, as has the formation of a heterocomplex involving HSP90, although each modulates different steps of the HSF-1 activation-deactivation pathway. Additionally, an 8.5kDa nuclear protein termed heat shock factor 1 binding protein (HSF1BP) has also been found to hinder the oligomerisation process of HSF-1 monomers. These several means of deactivating HSF-1 highlight the importance of HSPs, as their transcription is so tightly regulated in a number of ways by cells.

If and when a cellular stress does occur, the HSPs bind to any misfolded proteins, and subsequently dissociate from HSF-1. This allows the HSF-1 monomers to oligomerise and form active trimers, regaining their DNA binding activity. The trimers undergo stress-induced serine phosphorylation and are translocated to the nucleus (Prahlad and Morimoto, 2008). Upon nuclear localisation, HSF-1 binds

to the HSE situated upstream of heat shock responsive genes, which results in HSP gene transcription.

A number of other HSF isoforms have also been identified. HSF3 is an avian HSF and it too is a stress responsive transcription factor. HSF4 is the most recently discovered mammalian HSF, and has been found to be restricted to certain tissues. While its specific role is still unclear, it shows properties of a transcription repressor (Pirkkala *et al.*, 2001).

1.5.4 Extracellular HSP60 Locations

While HSP60 is typically localised in the mitochondria, it has also been found to exist on the surface of cells as well as in the extracellular milieu. This has been found across both prokaryotic and eukaryotic cells alike, under both normal and stress conditions.

1.5.4.1 Surface HSP60 Expression

HSP60 has been found to be expressed on the surface of cells. In 2000, Newman and Crooke used immunogold cryothin-section electron microscopy and immunofluorescence to detect the localisation of HSP60 in *E. coli*. They found that 16% of the labelled GroEL proteins were located in the membrane fraction under normal conditions, and that the density of gold-bound GroEL was in fact higher in the membrane region than in the cytosol.

In 1997, Soltys and Gupta used immunogold electron microscopy on various mammalian cell lines to detect HSP60. They found that 15-20% of the HSP60 was localised in extramitochondrial sites. These sites included the foci of the endoplasmic reticulum, on the cell membrane and other unidentified vesicles. The group went on to confirm cell membrane localisation by biotin labelling of the plasma membrane proteins, followed by immunoprecipitation and Western blots. Using much of the same methodology, Cicconi and colleagues found that approximately 10% of total cell HSP60 was expressed on the cell surface of Daudi cells (Cicconi *et al.*, 2004).

More recently, Pfister and colleagues (2005) used confocal laser scanning microscopy (CLSM) and flow cytometry to investigate the surface expression of HSP60 in human umbilical venous endothelial cells (HUVECs). The CLSM revealed that there was no production of HSP60 on the surface of unstressed cells. However, after a heat shock treatment, consisting of a 42°C treatment for 30 min and a 6 hour recovery, a significant portion of cells (10.9 ± 3.6%) had HSP60 expressed on the cell surface. This is comparable to the 9.5% they detected by flow cytometry. The number of cells that had surface expression of HSP60 had also increased from 1.1% to 9.5% following the heat stress (Pfister *et al.*, 2005).

1.5.4.2 Extracellular HSP60 Expression

In the last few decades, it has become increasingly well established that HSP60 exists not only intracellularly, but also in the extracellular space and in the circulatory system. HSP60 has been detected by enzyme-linked immunosorbant assay (ELISA) in the culture media of cells which have been stressed (Liao *et al*., 2000). In humans, circulating HSP levels have been found in systemic circulation of both healthy subjects and those experiencing disease states. HSP60 was first detected in the serum of normal individuals and elevated levels in individuals with hypertension by Pockley and colleagues in 1999, and has been further shown to be present in saliva (Fabian *et al*., 2003). Circulating HSP60 has even been documented in healthy teenagers, for which a possible association with endothelial dysfunction has been suggested (Halcox *et al.,* 2005). Studies of atherosclerosis have also reported a correlation between serum HSP60 levels and arterial intima-media thickness, suggesting that circulating levels of HSP60 may be associated with vascular injury (Ellins *et al.,* 2008; Pockley *et al*., 2003). Circulating HSP60 levels have similarly been found to be decreased with aging (Tsan and Gao, 2004), and increased in disease states characterised by chronic stress, such as T2D and obesity, which will be discussed in greater detail in **Chapter 1.5.7**.

1.5.4.3 Secretory Pathway

How HSPs are secreted into the extracellular milieu is yet to be fully characterised. At present, it is believed that HSPs are actively secreted from cells, rather than by necrosis. The postulated pathways surround exosomes and lipid rafts. Blocking common protein secretory pathways has no effect on diminishing HSP60 release. However, using exosome and lipid raft inhibitors has been used to some success, decreasing the amount of HSP60 released from cells. Lipid rafts are recognised as playing an important role in exosome formation, so it can therefore be postulated that either exosomes and lipid rafts, or exosomes alone, are the secretory pathway for HSPs (Merendino *et al*., 2010; Gupta and Knowlton, 2006).

1.5.5 Extracellular HSP60 Function

HSPs play the role of molecular chaperones when situated intracellularly. However, when expressed extracellularly, HSPs play an important immunoregulatory role, impacting on both the innate and adaptive immune systems. A number of bacterial and mammalian HSPs have had their effect on the immune system characterised, as depicted in **Table 1.4** and **Table 1.5** respectively.

Early work investigating the immunogenic properties of recombinant human HSPs found they could elicit a number of immune responses through the activation of the conserved Toll-like receptor (TLR) family. The resulting activation of the downstream Toll/Interleukin-1 (IL-1) receptor pathway led to the activation of nuclear factor-κB (NF-κB) and cytokine release; the patterns of which show close similarities to that of bacterial lipopolysaccharides (LPS). It was hence concluded that many of the reported immunogenic properties of HSPs were actually due to endotoxin contamination. There is therefore a danger that the founding data on HSPs and the immune system are actually false positives, and work done since has been based upon incorrect data. To correct this, a number of counter measures have since been introduced to overcome the problem of endotoxin contamination, including: purifying HSPs from eukaryotic hosts, using a limulus amebocyte lysate (LAL) assay to measure endotoxin levels, the treating of HSPs with polymyxin B (a potent binding agent of LPS), the heat denaturation of HSPs, and breeding lineages of mice defective for the recognition of LPS (van Wijk and Prakken, 2010; Tsan and Gao, 2009; Gao and Tsan, 2003; Bausinger *et al*., 2002).

More recent studies, free of endotoxin contamination, have reaffirmed the immunoregulatory role that HSPs play when located extracellularly. HSPs achieve this in several ways, including binding antigenic peptides and mediating their presentation to the major histocompatibility complex (MHC) proteins, acting as an endogenous danger signal under cellular stress and tissue damage, and binding to pathogen-associated molecular pattern (PAMP) molecules which culminates in signalling through pattern recognition receptors (PRRs) (Osterloh and Breloer, 2008).

Table 1.4. Activation of innate immune cells by microbial heat-shock proteins (Adapted from Wallin *et al*., 2002).

Heat-Shock Protein	Cell Type	Effect
M. leprae HSP65	Monocytes (THP-1)	Production of TNF- α, IL-6 and IL-8
M. tuberculosis HSP65	Monocytes (THP-1)	CD14-dependent production of TNF-α and IL-1β
M. bovis HSP65	Monocyte-derived macrophages	Production of TNF-α and IL-1β
L. pneumophila HSP60, *E. coli* GroEL, *M. leprae* HSP65, *M. bovis* HSP65 and *M. tuberculosis* HSP70	Peritoneal macrophages	Induction of transcription of TNF-α, IL-1α, IL-1β, IL-6 and GM-CSF mRNA, and increase in supernatant IL-1 bioactivity
Mycobacterial HSP65	Peritoneal macrophages	Production of TNF-α, IL-6 and reactive nitrogen intermediates
E. coli GroEL	Calvarial bone	Bone-resorbing activity
L. pneumophila HSP60	Macrophages	PKC- and cell-surface-receptor-dependent production of IL-1
L. pneumophila HSP60, *M. bovis* HSP65 and *M. tuberculosis* HSP71	Macrophages	Production of IL-12
Recombinant *M. bovis* HSP65	HUVECs	Increased adhesiveness to monocytes and granulocytes, and up-regulation of expression of E-selectin (CD62E), VCAM-1 (CD106) and ICAM-1 (CD54)
E. coli GroES, GroEL and DNAk	Monocytes	Production of TNF-α, IL-6 and GM-CSF
	HUVECs	Production of IL-6 and GM-CSF, and up-regulation of expression of E-selectin, ICAM-1 and VCAM-1
Recombinant chlamydial HSP60	Vascular endothelium, smooth muscle cells and macrophages	Up-regulation of expression of adhesion molecules, production of IL-6 and activation of NF-κB
Recombinant chlamydial HSP60	Macrophages and dendritic cells	Activation of the Toll/IL-1 signalling pathway

Abbreviations: *E. coli*, *Escherichia coli*; GM-CSF, granulocyte–macrophage colony-stimulating factor; HSP, heat-shock protein; HUVEC, human umbilical-vein endothelial cell; ICAM-1, intracellular adhesion molecule 1; IL, interleukin; *L. pneumophila*, *Legionella pneumophila; M. bovis, Mycobacterium bovis; M. leprae, Mycobacterium leprae; M. tuberculosis, Mycobacterium tuberculosis*; NF-κB, nuclear factor κB; PKC, protein kinase C; TNF-α, tumour necrosis factor α; VCAM-1, vascular cell adhesion molecule 1.

Table 1.5. Activation of innate immune cells by mammalian heat-shock proteins (Adapted from Wallin *et al*., 2002).

Heat-Shock Protein	Cell Type	Effect
Recombinant HSP60 and HSP70	Macrophages	Production of IL-12
HSP70	Promonocytes (U-937)	Activation of potassium channels and increased expression of the differentiation markers CD11c and CD23
Recombinant HSP60	Vascular endothelium, smooth muscle cells and macrophages	Up-regulation of expression of adhesion molecules, production of IL-6 and activation of NF-κB
Recombinant HSP60	Macrophages	Production of TNF-α, NO and IL-12
HSP70 with or without bound peptide	Splenocytes	Production of IL-1β and TNF-α
Recombinant HSP70	Dendritic cells	Production of IL-1β, IL-6, IL-12 and TNF-α, and maturation of dendritic cells
gp96	Dendritic cells	Maturation of dendritic cells, and production of IL-12 and TNF-α
HSP70, HSP90 and gp96	Macrophages and dendritic cells	Maturation of dendritic cells, production of IL-1β, IL-6, IL-12 and TNF-α, and activation of NFκB
gp96	Dendritic cells *in vivo*	*In vivo* induction of maturation and migration of CD11c+ cells
Recombinant HSP60	Macrophages and dendritic cells	Activation of the Toll/IL-1 signalling pathway
HSP70	Dendritic cells	Maturation of dendritic cells

Abbreviations: HSP, heat-shock protein; IL, interleukin; NF-κB, nuclear factor κB; NO, nitric oxide; TNF-α, tumour necrosis factor α.

1.5.5.1 HSPs as Binding Agents of Antigenic Peptides

Cytosolic HSPs, including HSP70, HSP90 and gp96, play important roles in antigen presentation, cross-presentation, and tumour immunity. Antigen presenting cells (APCs) internalise the HSP/peptide complex through CD91-mediated endocytosis, resulting in MHC I presentation and cytotoxic T lymphocyte induction (Tsan and Gao, 2004). This has a number of significant implications for the design of vaccines and therapeutics for infectious diseases and cancer. However, as HSP60 has not been implicated in this mechanism, it will not be discussed further in this review.

1.5.5.2 HSP60 as a Danger Signal

There are several theories have been proposed relating to regulation of the immune system: Burnet's Self-Nonself (SNS) theory, Janeway's Infectious Nonself (INS) theory, and Matzinger's Danger theory. Each theory has their fair share of novel and controversial elements, but each has merit.

Frank Burnet's SNS theory states that an immune response is based on the discernment of "self" and "nonself" antigens. It suggests that early lymphocytes express multiple copies of a distinctive receptor that recognises foreign antigens to initiate an immune response. As these lymphocytes clonally expand, self-reactive lymphocytes are quickly erased (Burnet, 1959). However, the SNS theory has since been modified, as it is now known that the recognition of "nonself" alone is not sufficient to trigger an immune response.

Charles Janeway's INS theory, also referred to as the Extended-SNS theory, states that the activation of an immune response depends on the discrimination between "infectious nonself" and "noninfectious self" by APCs. APCs contain a vast assortment of PRRs specific for conserved PAMPs expressed by pathogens. Upon PAMP/PRR association, APCs become activated, producing costimulatory signals, and presenting foreign antigens to T cells (Janeway, 1992). Janeway's theory has been supported by the discovery of evolutionary conserved TLRs, of which the family consists of 10 members. These receptors act as PRRs as they recognise components of bacteria, fungi and viruses to activate APCs (Akira *et al*., 2001). Both Burnet's SNS theory and Janeway's INS theory have several shortcomings however, including describing events such as transplant rejection, autoimmunity,

and tumours, where “nonself” or “infectious nonself” is absent, as identified by Matzinger (1998).

Polly Matzinger’s Danger theory states that regardless of the foreign nature of a particular compound, what really determines if an immune response occurs is if that particular compound causes damage or not. It may be seen as an extension of immune signals by “self” molecules that act as an endogenous danger signal. Danger signals are thought to be conserved, profuse and ubiquitously expressed “self” molecules that are normally housed intracellularly, in healthy cells. However, if the cells are injured, infected, abnormally stressed or necrotic, the danger signal may be released into the extracellular space. Once there, the danger signals are suspected of being recognised by APCs, mediating activation of the costimulatory signals which initiate an adaptive immune response. In this regard, the Danger theory suggests that endogenous signals that originate from cells experiencing injurious or stressful conditions are utilised to induce an effective immune response (Osterloh and Breloer, 2008; Matzinger, 1998).

HSPs, being expressed abundantly and ubiquitously, present themselves as a good candidate as endogenous danger signals as they are up-regulated during times of various cellular stresses, can be expressed on the cell surface, and can be actively secreted. As such, they may become accessible to immune cells during times of cellular danger. Many HSPs, from a variety of preparations, have been shown to be potent activators of the innate immune system. Such results include the production of a range of cytokines, including TNFα, IL-1, IL-6, IL-12, as well as the release of nitric oxide (NO) from monocytes, macrophages and APCs. An ability of HSPs to induce the maturation of APCs has also been observed, as demonstrated by the up-regulation of MHC class I and II molecules. (Tsan and Gao, 2004; Chen *et al*., 1999).

There is still considerable debate surrounding whether HSP60 is able to induce such immunoregulatory responses without endotoxin co-stimulation derived from LPS contamination. However, more recent studies still provide evidence for an immunomodulatory role of HSP60 in the innate immune response. Osterloh and colleagues have demonstrated that HSP60 has the ability to modulate immune cell function through the use of transgenic cell lines which express HSP60 on the cell surface. This surface HSP60 was found to induce the maturation of murine APCs

as well as upregulate the expression of interferon-α (IFNα). The signalling pathway was also found to enhance T cell activation, and is a distinct signalling pathway to that which is induced by LPS (Osterloh *et al*., 2007; Osterloh *et al*., 2004). Furthermore, these effects of HSP60 differ from its intracellular function in that they do not require peptide binding, ATP hydrolysis, cofactors or the assembly of a protein complex (Tsan and Gao, 2004).

1.5.5.3 HSP60 and PAMP-Signalling

Accumulating evidence suggests that HSPs are capable of binding PAMP molecules, and therefore modulate PAMP-induced stimulation of the immune system. Human and murine surface expressed HSP60 has been shown to bind tritium labelled LPS in a binding pattern that is specific, saturable, and also able to be competed for with unlabelled LPS. Furthermore, an LPS binding region has been identified on HSP60. Treatment with specific antibodies for this epitope has been shown to inhibit LPS binding, further supporting a role for HSP60 as an LPS binding protein (Habich *et al*., 2005). HSPs have been shown to associate with PRRs. Extracellular HSP60 has been shown to bind to macrophages and dendritic cells (DCs) in distinct areas that co-localise with the PRR CD14 (Osterloh *et al*., 2007).

It has been shown that highly purified HSP60 and HSP70 do not induce the release of pro-inflammatory cytokines such as TNFα (Gao and Tsan, 2003; Bausinger *et al*., 2002). It is rather believed that HSP binding to PAMP has a synergistic effect on inflammatory stimulation. Evidence for this includes that the addition of recombinant HSP60 and HSP70 has been shown to enhance LPS-induced TNFα release in macrophages (Zheng *et al*., 2004). Other studies have shown that pre-incubation of LPS with HSP60 or HSP70 causes a dose-dependent increase in TNFα secretion from peripheral blood-derived mononuclear cells (PBMCs) (Bangen *et al*., 2007). Pre-incubation with LPS has also been shown to enhance murine cell surface HSP60, LPS-induced IL-12p40 production in peritoneal macrophages and IFNγ release from T cells in a synergistic manner (Osterloh *et al*., 2007).

When considered together, this evidence suggests that HSP60 plays a role as a complex modulator of the innate immune system, while also influencing adaptive immune responses. HSP60 can act as an intracellular danger signal as well as a

sensor for PAMPs, such as LPS, providing an increased efficacy to immune responses. The additional effect of HSP60 on cytokine expression has also been purported to be a contributing factor in the pathogenesis of both autoimmune diseases and chronic inflammation (Tsan and Gao, 2004).

1.5.6 Receptor and Signalling Pathway for HSP60

The search for the HSP60 receptors is a controversial topic due to the well documented problems surrounding the possibility of endotoxin contamination even after several control methods, as well as the LPS-binding nature of HSP60. Because of this, it has been unclear whether HSP60 shared the same receptors as LPS, primarily CD14 and TLR4. As HSP70 has been shown to bind to various receptors such as CD14, TLR4, LOX-1, CD40 and CCR5 (Binder et al. 2004), it has been proposed that HSP60 may also exhibit a similar non-specific quality in receptor binding, or that some receptors have been mistakenly identified due to the aforementioned problems (Henderson and Mesher, 2007; Binder *et al*., 2004).

HSP60 has been shown to bind to a number of different cell types. Using flow cytometry, fluorescence-labelled human HSP60 has been shown to bind to murine macrophages at submicromolar concentrations. Furthermore, the binding is saturable and cannot be competed for by unrelated control proteins, confirming characteristics of specific ligand-receptor interactions. Additionally, HSP70, HSP60 and gp96 could not compete, and HSP60 binding still occurred in the absence of surface TLR4. Confocal microscopy also confirmed that HSP60 binds with endothelial and DCs (Habich *et al*., 2002). However, binding of human HSP60 to macrophages could not be competed for by HSP60 of hamster or bacterial origins. This would suggest a heterogeneous nature for the receptor binding of HSP60 (Habich *et al*., 2003).

The CD14 signalling complex has been found to be necessary but not sufficient for responsiveness to human HSP60 in Chinese hamster ovary (CHO) cells and human CD14-transfected astrocytoma cells. These are cells which would normally lack a response to LPS (Kol *et al*., 2000). This is of particular interest as TLRs have been described as components of the CD14 signalling pathway, of which TLR4 has been characterised as a co-receptor for LPS. The same group also found that p38 mitogen-activated protein kinase (MAPK) in PBMCs was activated by HSP60, much like LPS. As a result NF-κB was found to be activated, which culminated in the release of IL-6 (Triantafilou and Triantafilou, 2002).

Chlamydial and human HSP60 have been shown to induce a number of stress-activated protein kinases in murine macrophages, namely p38, c-Jun N-terminal kinases1/2 (JNK1/2), the mitogen-activated protein kinases (ERK1/2), and the I-

κB kinase (IKK). The activation of these protein kinases was found to be mediated by TLR2 and TLR4, as cells with defective versions of these receptors exhibited a diminished response. Additionally, the activation of this pathway was perturbed when cells were treated with an inhibitor known to disrupt endocytosis (Vabulas *et al*., 2001).

More recently, experiments using genetically engineered eukaryotic cells have been used to investigate the signalling pathway of HSP60. Cells engineered to express surface HSP60 have revealed that the signalling is independent of TLR4, and that previous data that suggested otherwise was due to PAMP-associated TLR signalling. Pure HSP60, that is to say HSP60 absent of endotoxin contamination, was found to not result in the expression of a number of previously reported cytokines such as IL-6, IL-12 and TNFα. However, the expression of IFNα was found to be up-regulated in APCs, which was required for the activation of T cells. Membrane bound HSP60 was also observed to enhance the release of IFNγ in TLR4-mutant APCs during T cell co-stimulation, and this effect was not observed after treatment with LPS (Osterloh *et al*., 2008).

Other groups have used novel methods to investigate HSP60 receptors, such as Henderson and Mesher (2008). They ran murine whole cell lysate through a column immobilized with *Mycobacterium tuberculosis* Cpn60.1 and analysed the bound fraction by peptide mass fingerprinting. The best matched candidates for Cpn60.1 were found to be BiP, an HSP70 localised in the lumen of the endoplasmic reticulum; VCAM-1 precursor, and polycomb protein SUZ 12. It should be emphasised that the hypothesised receptors, namely CD14 and TLR4, were not identified in this study. This may be due to possible detection limits for this novel method, or it could indicate that previously described receptors may have been falsely identified. The identification of the HSP70 isoform BiP is of particular interest as HSP70 has been proposed to act synergistically with HSP60, which would make it a likely candidate receptor (Alard *et al*., 2009).

1.5.7 HSP60 and Disease

1.5.7.1 HSP60 and T2D

Extracellular levels of HSP60 have been found to be elevated in individuals with diabetes when compared to controls. Aguilar-Zavala and colleagues (2008) screened blood samples of two groups of patients (n=151) who had been diagnosed with T2D less than a year or greater than 5 years before the study commenced for HSP60, TNFα and other markers of chronic disease. They found that HSP60 associated negatively with years since diagnosis and positively with glucose levels. This would indicate that HSP60 may be a molecular marker for the pathogenesis of early phase T2D. This is similar to the finding that HSP60 is also associated with the early stages of CVD (Pockley *et al*., 2000). The elevated levels of extracellular HSP60 may also be explained by hyperglycaemia-induced tissue damage, as indicated by its positive correlation with glucose levels. The decline of HSP60 in later phases of T2D may be explained by the induction of auto-antibodies (Hoppichler *et al*., 1996).

Shamaei-Tousi and colleagues (2006) investigated plasma HSP60 levels in T1D and T2D patients (n=855). They found that the proportion of patients who had experienced CVD or a myocardial infarction had detectable levels of circulating HSP60 compared with those patients who had not. Again this agrees with the proposed hypothesis that the release of HSP60 into the circulatory system is an early risk factor for atherosclerosis (Pockley *et al*., 2000). More recently, Yuan and colleagues (2011) observed that HSP60 is present at detectable levels in salivary secretions. They detected HSP60 in 93% of the T2D patients (n=40), compared to only 10% of the control patients (n=40) they sampled. This is of particular use and significance as this provides an easy and non-invasive way of measuring extracellular levels of HSP60, allowing for further study of HSP60 in T2D. It could also be used as a novel tool for screening of early CVD risk (Yuan *et al*., 2011).

1.5.7.2 HSP60 and Obesity

Very recently it has been observed that, like in T2D, extracellular levels of HSP60 are elevated in obese individuals. Märker and colleagues (2012) investigated the plasma concentrations of HSP60 in obese and lean individual males (n=41). They found that plasma levels of HSP60 were significantly higher in the obese individuals, and did not differ between obese individuals with and without T2D. It also correlated positively with BMI, blood pressure, leptin, and insulin resistance. The group also suggested that the origin of circulating HSP60 may be the adipose tissue, as the extracellular expression of HSP60 is increased in obese subjects compared to lean, as well as correlating with the increased expression of the adipokine leptin. The adipocyte expressed HSP60 was observed to exert a pro-inflammatory autocrine/paracrine effect on adipocytes. This is of particular interest as it is strikingly similar to other reported effects of HSP60 on vascular endothelial cells.

1.5.7.3 HSP60 and Atherosclerosis

A number of studies have revealed that extracellular HSP60 exerts powerful immunogenic and immunomodulatory effects in several experimental models including arthritis, T1D, T2D, obesity and atherosclerosis (Märker *et al*, 2012).

HSP60 has been shown to be present in the serum of normal individuals (Pockley *et al*., 1999), and serum HSP60 levels have been observed to correlate with the presence of early atherosclerosis (Pockley *et al*., 2000; Xu *et al*., 2000). A number of well-known atherosclerosis risk factors, such as diabetes, smoking, hypertension, and hyperlipidemia, have also been identified as potent inducers of HSP60 expression in vascular smooth muscle cells (Liao *et al*, 2000). Shear stress, particularly in the arterial system and especially when blood pressure is raised, is another factor which has been shown to induce the expression of HSP60 in cultured human endothelial cells (Hochleitner *et al*., 2000). As oxidised LDLs play such an important part in the development of atherosclerotic lesions, generating foam cells, it is of interest that human monocyte cell lines exposed to oxidised LDLs *in vitro* also induce HSP60 expression. Therefore it is likely that foam cells situated within the atherosclerotic plaque express HSP60. Early vascular inflammation also sees augmented expression of a number of cytokines including IL-6, VCAM-1 and MCP-1. As a result, the increased HSP60 expression may also be explained by the oxidative stress resulting from leukocytes traversing the vascular endothelium (Pockley, 2002).

As discussed in **Chapter 1.5.5** extracellularly expressed HSPs are capable of inducing the nonspecific innate immune system and promoting the adaptive immune system. It is perhaps not surprising then that raised levels of anti-HSP antibodies have also been found to be associated with the presence and progression of CVDs. Levels of antibodies to human HSP60 are increased in peripheral vascular disease and elevated levels of mycobacterial HSP65 are also documented in various CVDs (Wright *et al*., 2000). Conjecture continues to surround the nature of these antibodies, particularly in regard to vascular injury and pathogenesis. There are two schools of thought: one being that self-HSP antibodies play a direct pro-inflammatory role in autoimmune disease, and the other that immunoregulatory T cells which can differentiate self and non-self

HSP60s are present and exert different outcomes according to the different HSP epitopes (Pockley, 2002).

Microbial HSP60s may also be a driving force in the progression of atherosclerosis. Given that they are known powerful immunogens involved in the pathogenesis of infectious diseases, it is likely that they are present alongside autologous HSP60 under atherosclerotic-driving conditions. This is supported by the observation that HSP60 of *Chlamydial pneumoniae* often co-localises with human HSP60 in the macrophages at the site of atherosclerotic lesions (Tsan and Gao, 2004; Pockley, 2002). It has been proposed that since the bacterial HSP60 elicits pro-inflammatory TH1 responses, the co-existing autologous HSP60 may be inducing regulatory T cells to stimulate B cell antibody production and shift to a Th2 anti-inflammatory response (Pockley, 2002).

Figure 1.2 summarises how HSP60 is postulated to promote atherosclerosis (Grundtman and Wick, 2011).

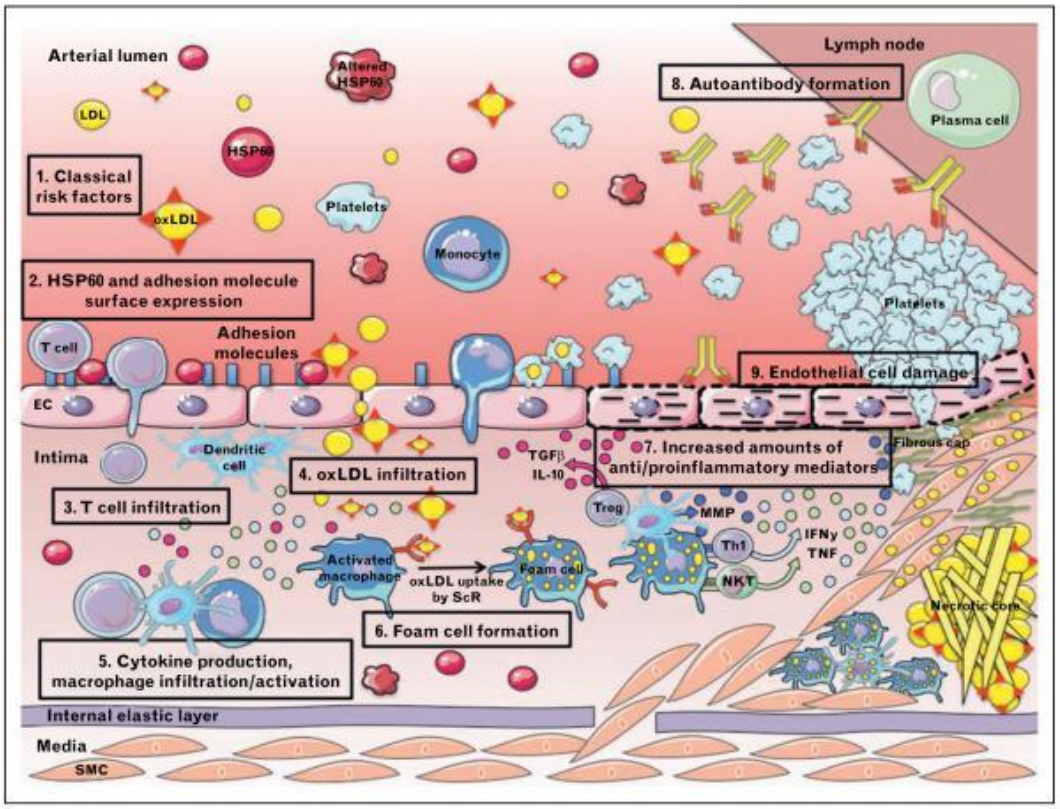

Figure 1.2- The role of HSP60 in atherosclerotic plaque formation (adapted from Grundtman and Wick, 2011).

Arterial vascular endothelial cells are more prone to atherosclerotic lesions compared to venous endothelial cells as they experience a much higher

mechanical stress due to high arterial blood pressure and flow conditions. Branching points in the arterial system are subjected to the greatest stress as there is an increased turbulent haemodynamic shear stress at these sites, predisposing them for the development of atherosclerotic lesions. The classical atherosclerotic risk factors that stress the endothelial cells result in the expression of HSP60 and adhesion molecules. T cells migrate into the intima by binding to the expressed adhesion molecules. In the intima, cytokine production occurs. This attracts monocytes, causing them to infiltrate into the intima too. It is yet to be ascertained whether monocytes bind oxidised LDLs in the circulation or after infiltration of the intima. In either case, once the monocytes reach the primary T-cell dominated inflammatory intima they differentiate into macrophages. Smooth muscle cells also infiltrate the intima from the media. Both the smooth muscle cells and the macrophages express scavenger receptors which allow the cells to take up oxidised LDLs and become foam cells. There is a subsequent imbalance of pro- and anti-inflammatory mediators, as well as autoantibody production which accelerates the disease (Grundtman and Wick, 2011).

Given that HSP60 is known to stimulate both the innate and adaptive immune systems, and its high sequence homology with prokaryotic HSP60s, Grundtman and colleagues (2011) have proposed a theory tying a lot of the unanswered questions surrounding the purpose of extracellular HSP60 together, and related it back to atherosclerosis. Immunity to microbial HSP60 is beneficial, acquired by infection or vaccination. Therefore autoimmunity to epitopes of autologous HSP60 is present in all humans. Intracellularly expressed HSP60 plays crucial cytoprotective roles, while extracellularly expressed HSP60 acts as a danger signal for immune reactions. Known atherosclerotic risk factors result in the expression of HSP60 by vascular endothelial cells. Therefore, pre-existing anti-HSP60 antibodies may have to be ‘paid for’ by cross-reactive autoimmune attack on cells, such as endothelial cells exposed to atherosclerotic risk factors which express HSP60.

In summary, intracellular HSP60 expression is upregulated under a number of cellular stresses, where it performs several cytoprotective roles. It has also been identified that HSP60 is not purely a mitochondrial protein, and that extracellularly expressed HSP60, be it surface expressed or in circulation, plays a number of powerful immunomodulatory functions. Human HSP60 has been

shown to modulate APC function in a way distinct to that of LPS. Furthermore, HSP60 has been shown to be capable of binding to LPS and augmenting its signal. The immune-stimulatory effects of HSP60, possibly due to cross-reactivity to microbial HSPs, have been implicated in the development of atherosclerosis. Both T2D and obesity are high risk factors for the development of CVDs. Therefore, the presence of HSP60 in individuals with T2D and obesity is not only an indicator of physiological stresses, but also a marker for early stage atherosclerosis development.

1.6 Aims and Objectives

HSP60 is known to be present on the surface of cells and in systemic circulation. Increases in these extracellular levels of HSP60 are known to be associated with mitochondrial stress, damage, or impairment. Therefore, the aim of this study was to develop a model system for investigating HSP60 expression at the protein level during conditions which lead to mitochondria impairment.

To achieve this, a set of stressors had to be established which resulted in impairment of mitochondrial function without inducing necrotic cell death. The treatments selected were high glucose and H_2O_2, to simulate some of the physiological states associated with obesity and T2D, as these metabolic conditions have been found to correlate with increased extracellular HSP60 expression. A specific mitochondrial electron transport chain inhibitor, sodium azide, was also used.

To find optimal mitochondria specific cell stress conditions several assays were implemented. Concentrations of each of the three treatments had to be identified that inhibited cell growth but did not increase necrotic cell death relative to control cells, as determined by LDH assays. Furthermore, these known stressor concentrations had to inhibit mitochondrial function relative to control cells, inferred through mitochondrial dehydrogenase activity, as determined by MTT assays. Once an optimal stress concentration was identified for each treatment, it had to be shown that HSP60 expression was indeed induced as a result. This was achieved through western blotting.

By establishing a model system for the expression of HSP60, further downstream effects, such as the mechanisms of translocation and secretion of extracellular HSP60, can be investigated. As extracellular HSP60 has been implicated in numerous autoimmune diseases, in particular atherosclerosis, a clear understanding of the mechanisms that lead to the expression of extracellular HSP60 may result in better treatment and prevention of these disease states.

2 Materials and Methods

2.1 Cell Culture

2.1.1 HeLa Cell Culture

The human cervical cancer HeLa cell line was purchased from the American Tissue Culture Collection (ATCC) (No. CCL-2). The cells were grown in DMEM media (Gibco) supplemented with 10% fetal bovine serum (FBS), 1X MEM non-essential amino acid solution (Gibco), 100X penicillin/streptomycin and 3.75mg of sodium bicarbonate**,** and filter sterilized through a 0.2μm filter syringe (Minisart). Cells were grown at 37°C, 5% CO_2, in a humidified incubator (standard incubation conditions). Cells were harvested every 7 days by the addition of 2mL trypsin/EDTA, followed by a short incubation period and mechanical attrition to suspend the cells. 8mLs of DMEM media was then added to neutralise remaining trypsin/EDTA. The suspended cells were then centrifuged (Megafuge 1.0) at 400 rcf. The pellet was re-suspended in pre-warmed DMEM, and DMEM was changed 3 days after passage. All experiments were carried out using exponentially growing and near-confluent cells which had been passaged 3 days prior to experiments.

2.1.2 Dose Response Curves

Dose response curves were generated for the HeLa cells over 7 day periods. The cells were grown in full DMEM media in 24 well plates. Dose treatments included high glucose (25-125mM), H_2O_2 (50-250μM) and sodium azide (1-100μM). The media was changed after 3 days. Each day, 3 wells per dose treatment were counted with a haemocytometer using the trypan blue exclusion method. The three counts were averaged and plotted to generate a growth curve. Best fit lines were also generated during the time of exponential cell growth and the slope was taken as an indication of the rate cell growth.

2.2 Cytotoxicity Assays

2.2.1 LDH Assay

Lactate dehydrogenase (LDH) is a cytosolic enzyme that is only found extracellularly due to necrotic cells. The Promega CytoTox96 NonRadioactive Cytotoxicity Assay kit was used to determine levels of LDH present in the media. Following the manufacturer's protocol, each duplicate sample was treated identically in a 96-well culture plate (Nunc) until the end of cell culture. The cell culture period lasted 3 days to acquire cells in the exponential growth phase. At the end of the culture period, 10x lysis solution was added to the maximum control and the cells were returned to standard incubating conditions for a further 45 minutes. The cells were then centrifuged at 250 x *g* for 5 minutes at room temperature (RT) to pellet cell debris. 50µL of the supernatant from each well of the culture plate was transferred to the corresponding well of a 96-well enzymatic assay plate (Greiner Bio-One). Assay substrate was reconstituted by warming both the substrate vial and buffer to RT, and then 12mL of buffer was added to dissolve the substrate. The reconstituted substrate remained at RT until the time of the assay. 50µL of reconstituted substrate was added to the supernatant in each well of the assay plate. The plate was then covered and incubated at RT, protected from light, for 30 minutes. The assay was terminated by the addition of 50µL of Stop Solution to each well of the plate. Air bubbles were then removed from all wells with a needle and the absorbance was read at 490nm using a Model 680 Microplate Reader (Bio-Rad).

To obtain the percentage of LDH content relative to the maximum control, the data was first averaged and then subtracted with the averaged media blank reading. The maximum control was multiplied by 1.1 to account for the dilution factor due to the addition of the lysis solution. The sample recording were normalised to the maximum control using **Equation 2.1.** The final data is presented as a percentage and can be interpreted as the percentage of dead cells present in the original cell culture, assuming all cells released an equal amount of LDH.

$$\% \text{ Cytotoxicity} = \frac{\text{Experimental LDH release (OD490)}}{\text{Experimental LDH release (OD490)}}$$

Equation 2.1 – Calculating relative cytotoxicity.

2.2.2 MTT Assay

MTT [3-(4,5-dimethylthiazol-2-yl)-2,5-diphenyl tetrazolium bromide] is a tetrazolium dye. When MTT is reduced by cellular dehydrogenases, it forms blue crystals intracellularly. The crystals can then be dissolved and quantified using spectrometry, and is indicative of mitochondrial dehydrogenase activity. The Sigma MTT Based *In vitro* Toxicology Assay Kit was used as per the manufacturer's protocol. MTT was dissolved in DMEM at a concentration of 5mg/mL and pre-warmed to 37°C. Each duplicate sample was treated identically in a 96-well culture plate (Nunc) until the end of cell culture, again 3 days to acquire cells in the exponential growth phase, at which time the media was removed and replaced with reconstituted MTT in an amount equal to 10% of the culture medium volume. The plate was then incubated at standard incubation conditions for 2 hours. After the incubation period, the culture fluid was removed and disposed, followed by the addition of MTT Solubilisation Solution in an amount equal to the original culture medium volume. The plate was then placed on a minishaker for 10 minutes to assist in dissolving the crystals. Air bubbles were removed from all wells with a needle and the absorbance was read at 570nm and the background read at 655nm using a Model 680 Microplate Reader (Bio-Rad). After subtracting the averaged 655nm reading from the averaged 570nm reading, the averaged blank was also subtracted, as per **Equation 2.2.**

$$\text{Absorbance (corrected)} = (\text{Sample OD570-655nm}) - (\text{Blank OD570-655nm})$$

Equation 2.2 – Calculating corrected MTT absorbance.

Experimental values were then normalised to the control and expressed as a percentage of mitochondrial dehydrogenase activity (**Equation 2.3),** since dehydrogenases are predominantly situated in the mitochondria.

$$\text{Dehydrogenase activity (\%)} = 100\% \times \frac{\text{Experimental sample absorbance (corrected)}}{\text{Control sample absorbance (corrected)}}$$

Equation 2.3 – Calculating mitochondrial dehydrogenase activity.

2.2.3 DCFDA Assay

DCFDA (2,7-dichlorofluorescein diacetate) is a fluorogenic dye that measures hydroxyl, peroxyl and other ROS activity within cells. It is a reagent capable of permeating cells, and after which, is deacetylated by cellular esterases to a non-fluorescent compound which is incapable of diffusing back out of the cell. It is later oxidized by ROS into the highly fluorescent 2, 7-dichlorofluorescin (DCF). Each duplicate sample was treated identically in a 96-well black culture plate (Greiner Bio One) until the end of the cell culture, either after 24 hours, 3 days or 7 days. Media was replaced after 3 days. At the end of the culture period, the DMEM media was removed and the cells were washed twice with pre-warmed PBS. The cells were then incubated for a further hour in Opti-MEM containing only 2% FBS and further supplemented with 10μM DCFDA. After the one hour incubation period, the media was again removed and the cells washed twice with PBS. Opti-MEM containing 2% FBS was added and the plate was left to stand at RT. 10μM H_2O_2 was added to each well immediately before reading the fluorescence intensity over a 30 minute period using a Fluostar Optima plate reader (BMG Labtechnologies) at excitation and emission wavelengths of 485nm and 520nm respectively. Data was standardised to the control analysis done in the absence of H_2O_2, and then expressed as relative fluorescence units to the control, as in **Equation 2.4**.

$$\text{ROS activity (\%)} = 100\% \times \frac{\text{(Experimental sample fluorescence/No } H_2O_2 \text{ fuorescence)}}{\text{(Control sample fluorescence/ No } H_2O_2 \text{ fuorescence)}}$$

Equation 2.4 – Calculating relative ROS activity.

2.3 Quantification of HSP60 Expression

2.3.1 Protein Extraction

Total protein was isolated using TENT buffer containing 250mM NaCl, 50mM Tris (pH 7.5), 5 mM EDTA (pH 8.0), 1% Triton X-100, and freshly added 0.4mM phenylmethylsulfonyl fluoride (PMSF) as a protease inhibitor. HeLa cells treated with hydrogen peroxide (200μM), glucose (100μM), and a control sample grown over 3 and 7 days were treated with trypsin/EDTA and then pelleted at 400 rcf for 5 minutes. Samples were ruptured with 100μL TENT buffer by vortexing, and were subsequently incubated at 4°C for 30 minutes. After this incubation period, samples were spun at 10,000 rcf for 5 minutes at 4°C to pellet cell debris. The supernatant was transferred to a new tube and stored at -20°C.

2.3.2 Protein Estimation

Protein concentration was estimated using the BCA Protein Assay kit (Pierce) following the manufacturers protocol. A working reagent (WR) was prepared constituting of 50 parts of reagent A with 1 part of reagent B. A standard curve comprised of known concentrations of serially diluted bovine serum albumin (BSA) (Pierce) in tris buffered saline (TBS) was assayed along with samples of unknown concentrations and a blank containing only TBS. 25μL of each sample standard and unknown was transferred to a 96 well plate in triplicate followed by the addition of 200μL WR to each well. The plate was then mixed briefly on a minishaker for 30 seconds before incubating at 37°C for 30 minutes. The plate was then read at 570nm using the Microplate Reader and the concentration of sample calculated from the standard curve.

2.3.3 Protein Separation and Transfer

Gel Preparation

Total protein was separated on a discontinuous gel (0.76mm). The 10% resolving polyacrylamide gel was prepared by adding 4.1mL distilled water, 3.3mL acrylamide-bis stock (Bio-Rad), 2.5mL 1.5M Tris (pH 8.8), and 100μL 10% SDS. Directly before casting, 50μL of freshly prepared 10% ammonium persulphate (APS) (Bio-Rad) and 10 μL TEMED (Bio-Rad) were added to the mixture in a fume hood, and the mixture was inserted between the plates. A layer of 70% ethanol was then gently overlaid. The resolving gel was left to set for 30 minutes.

The stacking gel was prepared by adding 6.1mL distilled water, 1.3mL acrylamide-bis stock (Bio-Rad), 2.5mL 0.5M Tris (pH 6.8), and 100µL 10% SDS. Again, immediately before casting, 50µL of 10% APS and 10 µL TEMED were added to the mixture in a fume hood. The mixture was cast on top of the resolving gel and the comb was gently inserted. The stacking gel was left to set for a further 30 minutes. The gel was then assembled in a Mini-Protean 3 Cell gel tank (Bio-Rad) buffered with 1X electrode buffer.

Sample Preparation

Each sample containing 20µg total protein was made up to 20µL with protein loading buffer. The samples were denatured in boiling water for approximately 5 minutes before loading into the wells. 2µL of protein Kaleidoscope ladder (Bio-Rad) was also added alongside the samples. The gel was electrophoresed at a constant 20mA as the bands ran through the stacking gel, and 30mA through the resolving gel. The end point was determined as when the loading dye ran off the gel.

Semi-Dry Transfer

Semi-dry transfer was completed using a 3-buffer system containing cathode, anode I and anode II buffers. The polyacrylamide gel was removed from the plates and cut to an appropriate size before being left to equilibrate in cathode buffer for 10 minutes. A sheet of PVDF membrane (Millipore) was cut to the same size as the gel. It was then wet with methanol for approximately 15 seconds before being allowed to soak in distilled water for 2 minutes. It was then left to equilibrate in anode buffer II for 10 minutes. Six pieces of extra thick filter paper (Bio-Rad) were cut to a size marginally bigger than the membrane. 3 pieces were soaked in cathode buffer, 2 in anode buffer I, and 1 in anode buffer II, all for 10 minutes before the transfer sandwich was compiled, as in **Figure 2.1**. Air bubbles were removed by rolling a falcon tube over the top of the stack. The cathode plate and safety plate were then replaced on top of the transfer sandwich, and the transfer cell (Bio-Rad) was run at 15V for 35 minutes.

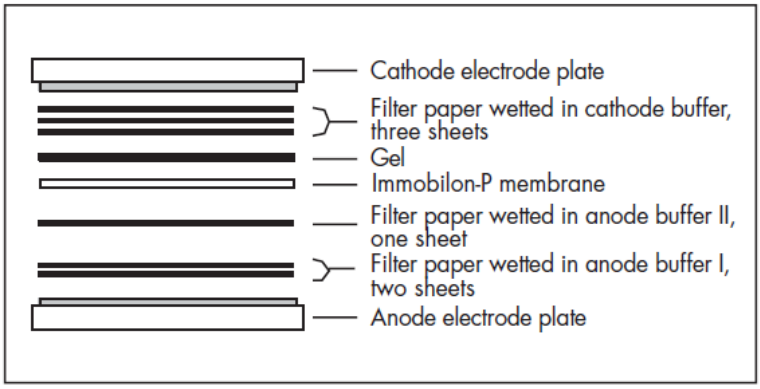

Figure 2.1 –Assembly of a semi-dry transfer sandwich (image adapted from Millipore Immobilon-P user guide).

After the transfer was complete, the membrane was briefly rinsed in distilled water before being stained with Ponceau S for 15 seconds to ascertain whether efficient transfer had occurred. The stain was then washed out with distilled water.

2.3.4 Western Blotting

The membrane was blocked in 10% skim milk in TBST overnight at 4°C. The following day, the membrane was washed 6 times for 5 minutes in TBST on a gyro rocker (Stuart). The membrane was then incubated in the primary polyclonal rabbit HSP60, HSP70 or actin antibody (Sapphire Bioscience) 1: 250 in 5% skim milk in TBST overnight at 4° in a humidified chamber. After a further 6 X 5 minute washes in TBST on a gyro rocker, the membrane was incubated in peroxidase conjugated goat anti-rabbit IgG (Sigma) 1:1000 in 5% skim milk in TBST for 5 hours in a humidified chamber on a gyro rocker. After a further 6 X 5 minute washes in TBST on a gyro rocker, the membrane was transferred onto a glass plate and incubated for 1 minute with SuperSignal West Pico Chemiluminescent Substrate (Pierce). It was then covered with a plastic sheet. The membrane was visualised using the LAS-100 Plus Gel Documentation System (Fujifilm), and the intensity of the bands was measured using Gel Quant software. The generated values represented the intensity of the band of the protein of interest less the background intensity per square millimetre. The Quant values generated for the proteins of interest were normalised to the house keeper gene actin after probing the same membrane with the anti-actin antibody.

After visualising, membranes were stripped for re-probing. Membranes were covered in membrane stripping buffer and incubated at room temperature for 10

minutes on a gyro rocker. The buffer was discarded and the membranes were again incubated for 10 minutes in fresh stripping buffer. They were then washed twice for 10 minutes in PBS, and then twice for 5 minutes in TBST, at which point the membranes were ready for blocking.

2.4 Media, Reagents & Common Solutions Preparation

Name	Composition
Full HeLa media	2mL penicillin/streptomycin (100X). 2.5mL sodium bicarbonate 1.5g/100mL. 1mL MEM non-essential amino acids (100X). 10mL FBS. Bring volume to 100mL with DMEM medium then filter through a 0.2μm filter. Store at 4˚C.
Phosphate buffered saline (PBS)	8g NaCl (137mM). 0.2g KCl (2.7mM). 1.44g Na2HPO4 (4.0mM). 0.24g KH2PO4 (1.7mM). Dissolve in 800mL ddH_2O and adjust to pH 7, bring to 1L.
1.5M Tris-HCl pH 8.8	45.42g Tris. Dissolve in 200 mL ddH2O, adjust to pH 8.8 and bring to 250mL.
0.5M Tris-HCl pH 6.8	15.14g Tris. Dissolve in 200mL ddH2O, adjust to pH 6.8 and bring to 250mL.
10% SDS	5g SDS Make up to 50mL with ddH2O water.
5x Electrode buffer	15g Tris (124mM). 72g glycine (959mM). 50 mL of 10% SDS (0.5%). Make up to 1L with ddH_2O.
Protein loading buffer	3mL 10% SDS. 1mL 1M Tris pH6.8. 0.2mL 2% bromophenol blue. 4mL glycerol. 0.8mL ddH_2O. Mix well and store in 1mL aliquots at -20˚C.

Commassie Blue stain	0.5g Brilliant Blue R-250 (0.1%) Dissolve in 500mL of fixative/destain and filter through filter paper.
Gel fixative/destain	400mL methanol (40%). 100mL acetic acid (10%). 500mL of ddH_2O.
Cathode buffer	0.303g Tris 0.3g glycine 10mL methanol Dissolve in 80mL ddH_2O, adjust to pH 9.4 and bring to 100mL.
Anode buffer I	3.63g Tris. 10mL methanol. Dissolve in 80mL ddH_2O, adjust to pH 10.4 and bring to 100mL.
Anode buffer II	0.303g Tris. 10mL methanol. Dissolve in 80mL ddH_2O, adjust to pH 10.4 and bring to 100mL.
Membrane stripping buffer	15g glycine. 1g SDS. 10mL Tween20. Dissolve in 800mL ddH_2O, adjust to pH 2.2 and bring to 1L.
10x Tris buffered saline (TBS)	12.10g Tris (0.1M). 87.66g NaCl (1.5M). Dissolve in 800mL ddH_2O, adjust to pH 7.7 and bring to 1L.
Ponceau S.	Add in the order: 10mL MQ water. 0.3mL glacial acetic acid. 33mg Ponceau S. Bring to 30mL with MQ water and store at RT.

TBS-Tween (TBST)	100mL 10x TBS. 0.5mL Tween20 (0.05%). Make up to 1 L with ddH_2O.
TENT buffer	1.51g Tris (50 mM). 10.96g NaCl (150 mM). 0.37g EDTA (5 mM). 0.75 mL TritonX-100 (0.25%). Dissolve in 200 mL ddH_2O, adjust to pH 7.4 and bring to 250mL. Supplement with 0.4 mM phenylmethylsulfonyl fluoride fresh.
400μM DCFDA	2.12mg DCFDA. Dissolve in 10ml dimethyl sulphoxide (DMSO).
Opti-MEM media	1mL penicillin/streptomycin (5000X). 1.25mL sodium bicarbonate 1.5g/100mL. 0.5mL MEM non-essential amino acids (100X). 1mL FBS. Bring volume to 50mL with OptiMEM medium then filter through a 0.2μm filter. Store at 4˚C.
1M Glucose	1.80g Glucose. Dissolve in 10mL dd ddH_2O.
1mM Sodium azide	1.30mg Sodium Azide. Dissolve in 20mL ddH_2O.
1M H_2O_2	1mL H_2O_2 (27%). Add to 6.97mL ddH_2O.
1mM H_2O_2	10μL 1M H_2O_2. Add to 10mL ddH_2O.
HeLa media absent of glucose	2mL penicillin/streptomycin (100X). 2.5mL sodium bicarbonate 1.5g/100mL. 1mL MEM non-essential amino acids (100X). 11mg Sodium pyruvate. 10mL FBS. Bring volume to 100mL with DMEM medium containing no glucose, then filter through a 0.2μm filter. Store at 4˚C.

2.5 Statistical Analysis

All statistical analysis in this study was carried out using Microsoft Excel. Data was averaged where appropriate, and the standard error of the mean (S.E.M.) was calculated using **Equation 2.5** in Excel.

```
S.E.M. = STDEV (A1:A2) / SQRT (COUNT (A1:A2))
```

Equation 2.5 – Calculating standard error of the mean in Excel.

A two-tailed student's t-test was carried out to determine the significance of the data. The accepted level of significance was $p < 0.05$, which was denoted as '*'.

3 Effects of Glucose, H_2O_2 and Sodium Azide on HeLa Cell Growth

3.1 Introduction

T2D and obesity are disease states which are both associated with chronic, low-level, systemic inflammation as well as elevated levels of circulating HSP60. Therefore these patients are at a high risk of developing CVDs. Both hyperglycaemia and increased oxidative stress have also been associated with these disorders, as well as being linked to mitochondrial dysfunction (**Chapters 1.2.3** and **1.3.3**). The cytotoxic effects of H_2O_2 on HeLa cells have been previously documented (Singh *et al*., 2007; Nakamura *et al*., 2003), however the majority of evidence of glucose cytotoxicity pertains to the human pancreatic β islet cells (Robertson *et al*., 2003) and tissues where glucose can passively enter. Using HeLa cells allows for the development of a peripheral tissue model, and by using high glucose and H_2O_2, the treatments reflect two of the most pertinent T2D and obesity conditions.

In addition, a known mitochondrial inhibitor was also used in these experiments. Sodium azide is a highly toxic inorganic compound which inhibits complex IV of the mitochondrial electron transport chain. It achieves this due to the azide anion binding irreversibly to the heme cofactor of cytochrome c oxidase, a process similar to the action of carbon monoxide (Kaal *et al*., 2000; Varming *et al.*, 1996). Sodium azide has an LD_{50} of 27 mg/kg when administered orally to rats, compared to potassium cyanide which has an LD_{50} of 5 mg/kg. In humans, lethal doses have been reported for exposure greater than 10mg/kg, while nonlethal doses have been reported for exposures less than 2 mg/kg (Chang and Lamm, 2003).

Other researchers have used various concentrations of these three compounds in cell cultures but due to the differences in the cell type, the constant changes to the culture population through clonal selection of cells through each passage, as well as the nature of further experiments, the first task of this project was to test the inhibitory effects on cell growth of glucose, H_2O_2, and sodium azide on HeLa cells. This was done at a number of different glucose (25-125mM), H_2O_2 (0-250μM), and sodium azide (0-100μM) concentrations to generate dose response

growth curves by monitoring cell growth every 24 hours by trypan blue exclusion assay. The slopes of the curves through the exponential growth phase were also used to provide an indication of growth rate.

3.2 Methods

3.2.1 Cell Culture and Dose Response Curves

Stock solutions of 1M glucose, 1mM H_2O_2 and 1mM sodium azide were prepared in ddH_2O as in **Chapter 2.4**. HeLa cells were seeded at a density of approximately 60,000 cells/mL onto a 24 hour plate containing 1mL glucose-free HeLa media which was supplemented with 25, 50, 75, 100, 125mM glucose in triplicate. Cells were also seeded at a density of approximately 60,000 cells/mL onto 24 hour plates containing 1mL full HeLa media with added 0, 50, 100, 150, 200, 250mM H_2O_2 and 0, 1, 10, 25, 50, 100mM sodium azide, again in triplicate. The plates were then placed back into standard incubation conditions. Cell density was estimated by the trypan blue exclusion method every 24 hours.

3.3 Results

3.3.1 Dose Response for Glucose Treatment

Cells treated with 50 and 75mM glucose showed a slightly reduced growth rate compared with the control, while the 100 and 125mM groups had considerably reduced growth rate through to the end of the culture period, shown in **Figure 3.1**.

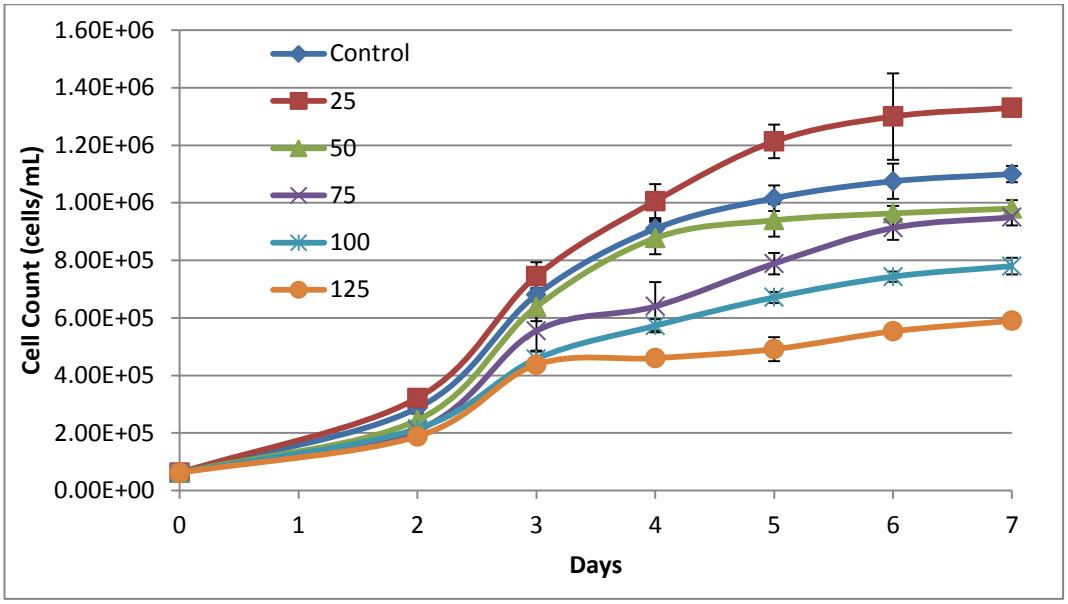

Figure 3.1- Cell growth in glucose (mM). Error bars showing S.E.M.

To compare cell growth across treatments, the number of cells at each time point was normalised to the number of control cells. The rate of cell growth was determined during the exponential growth phase between days 3 and 5 of the culture period. The slopes were taken from the graph over this time period, as shown in **Figure 3.2**. The gradient of the lines of best fit are expressed in **Table 3.1**. The degree of growth rate inhibition was then determined, as shown in **Figure 3.3**.

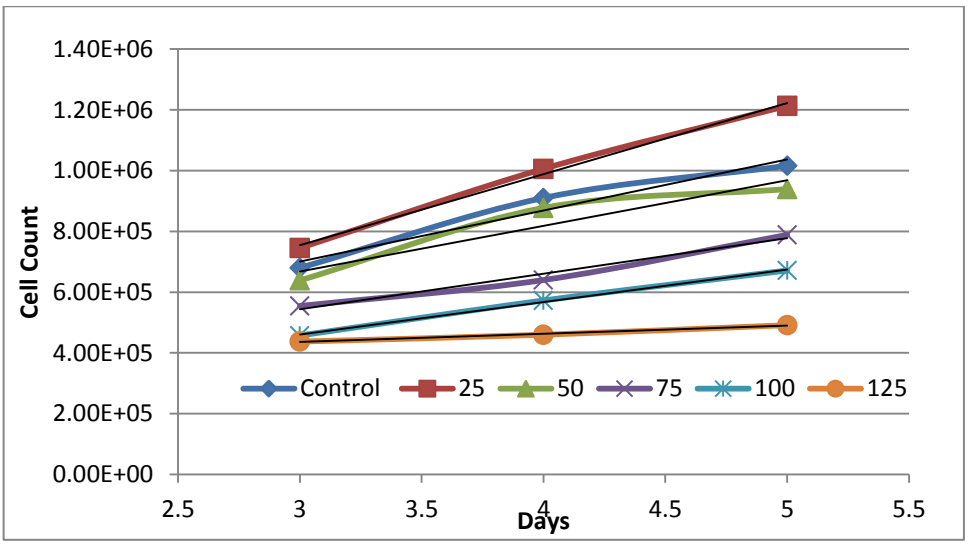

Figure 3.2- Cell growth in glucose with lines of best fit.

Glucose (mM)	Relative Growth Rate
Control	1
25	1.39
50	0.89
75	0.7
100	0.64
125	0.16

Table 3.1- Gradients of lines of best fit from **Figure 3.2** relative to control.

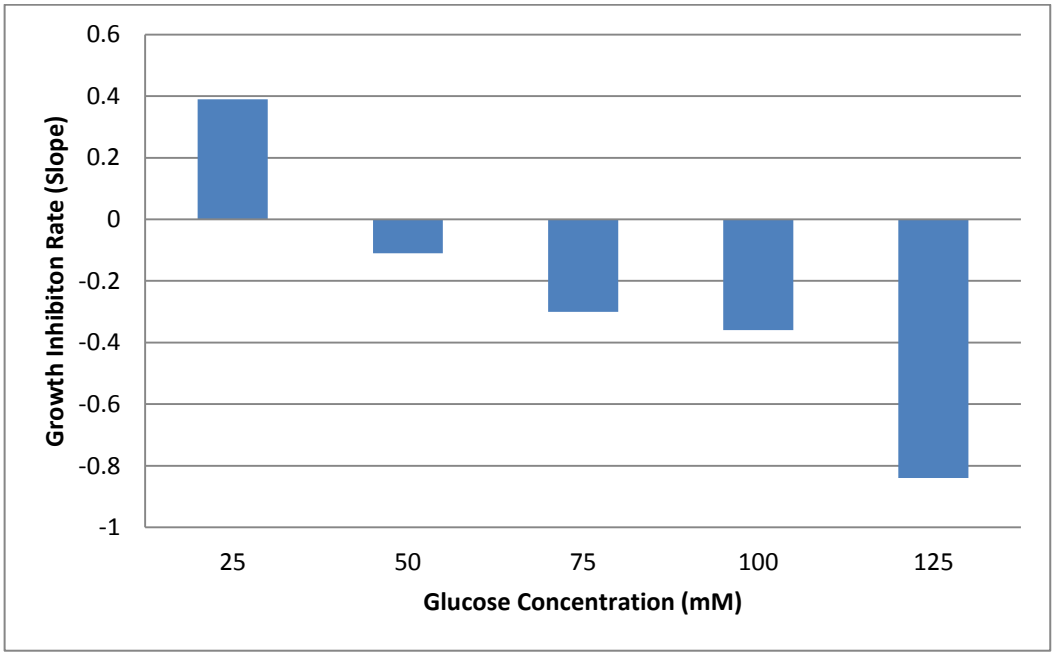

Figure 3.3- Rates of growth inhibition relative to control in glucose.

3.3.2 Dose Response for H_2O_2 Treatment

As shown in **Figure 3.4**, Cells treated with 50, 100 and 150µM H_2O_2 showed growth rates comparable, if not greater than, with the control, while the 200 and 250µM groups had considerably reduced growth rate through to the end of the culture period.

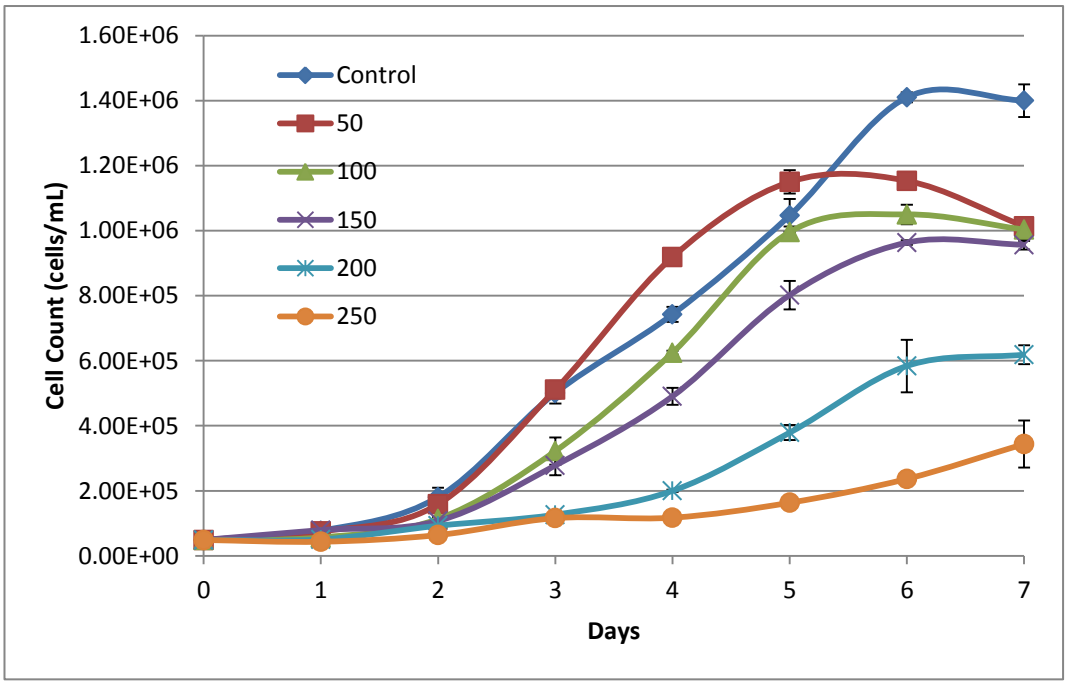

Figure 3.4- Cell growth in H_2O_2 (µM). Error bars showing S.E.M.

To compare cell growth across treatments, the number of cells at each time point was normalised to the number of control cells. The rate of cell growth was determined during the exponential growth phase between days 3 and 5 of the culture period. The slopes were taken from the graph over this time period, as shown in **Figure 3.5**. The gradient of the lines of best fit are expressed in **Table 3.2**. The degree of growth rate inhibition was then determined, as shown in **Figure 3.6**.

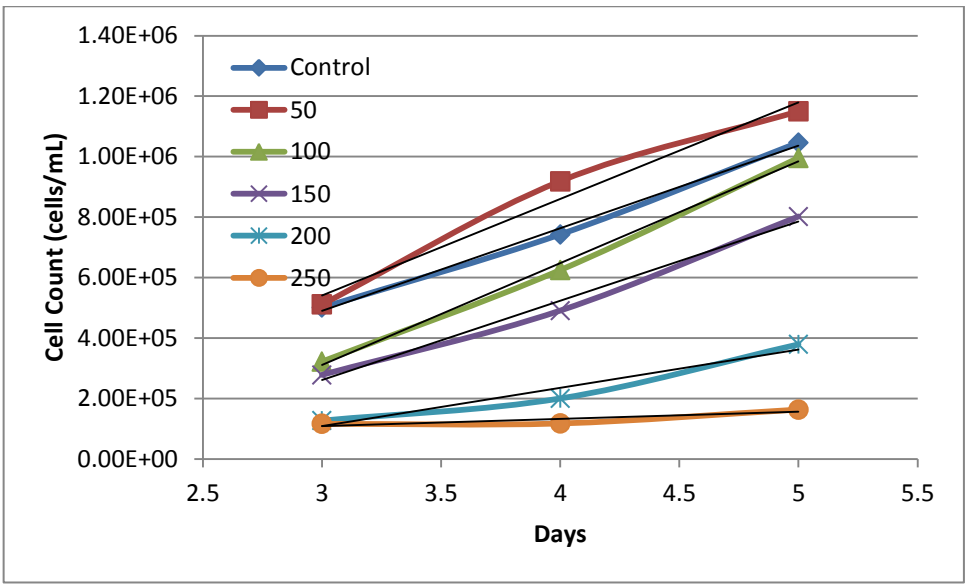

Figure 3.5- Cell growth in H_2O_2 with lines of best fit.

H_2O_2 (µM)	Relative Growth Rate
Control	1
50	1.17
100	1.23
150	0.96
200	0.46
250	0.09

Table 3.2- Gradients of lines of best fit from **Figure 3.5** relative to control.

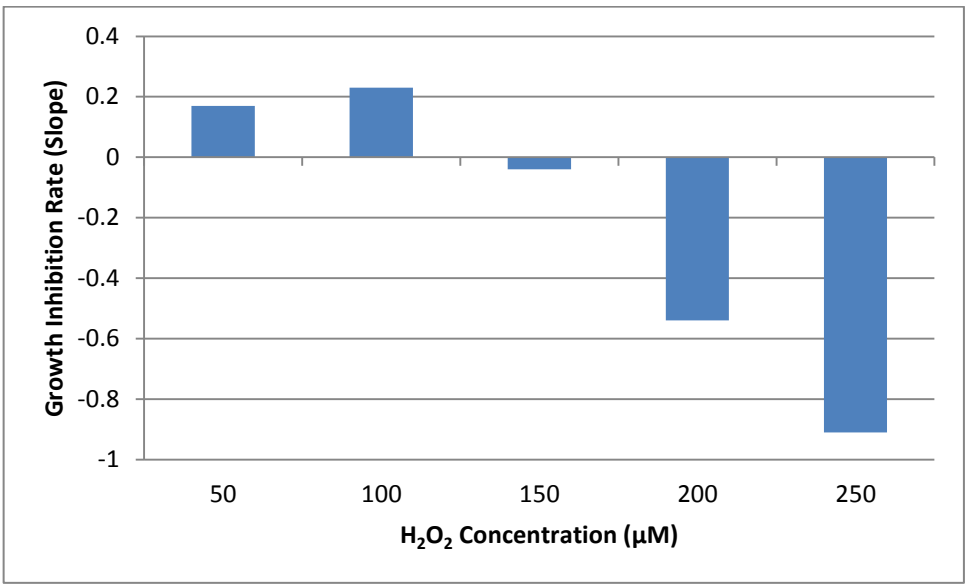

Figure 3.6- Rates of growth inhibition relative to control in H_2O_2.

3.3.3 Dose Response for Sodium Azide Treatment

Cells treated with 1, 10 and 25µM sodium azide showed growth rates comparable, if not greater than, with the control. The 200 and 250µM groups had considerably reduced growth rate through to the end of the culture period compared to the control, as shown in **Figure 3.4**

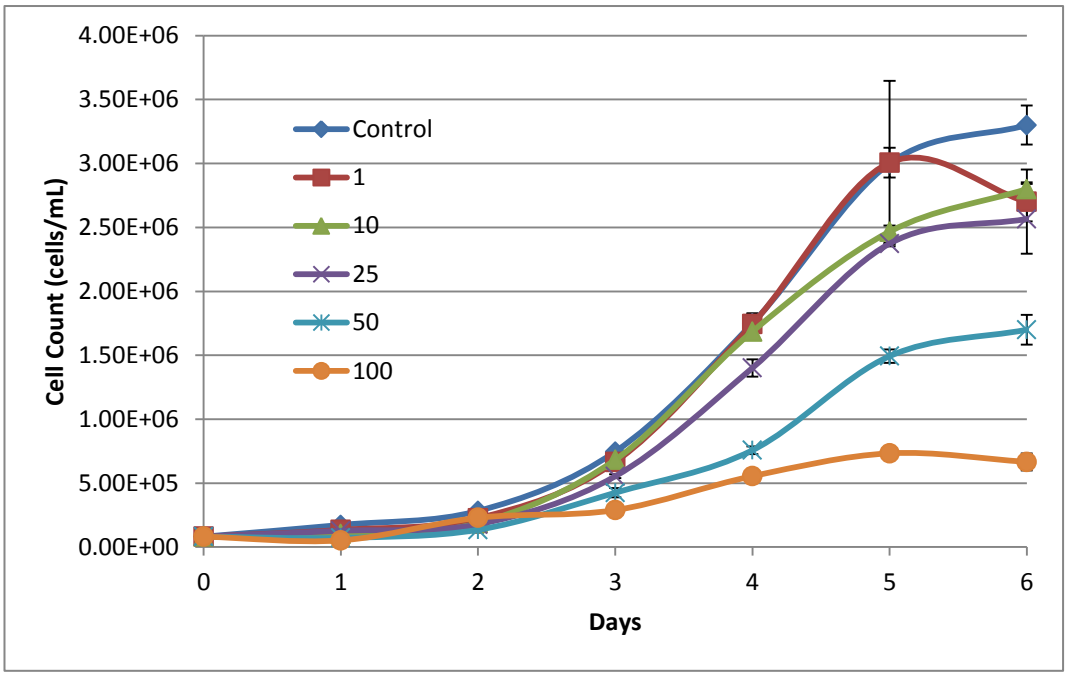

Figure 3.7- Cell growth in sodium azide (µM). Error bars showing S.E.M.

To compare cell growth across treatments, the number of cells at each time point was normalised to the number of control cells. The rate of cell growth was determined during the exponential growth phase between days 3 and 5 of the culture period. The slopes were taken from the graph over this time period, as shown in **Figure 3.8**. The gradient of the lines of best fit are expressed in **Table 3.3**. The degree of growth rate inhibition was then determined, as shown in **Figure 3.9**.

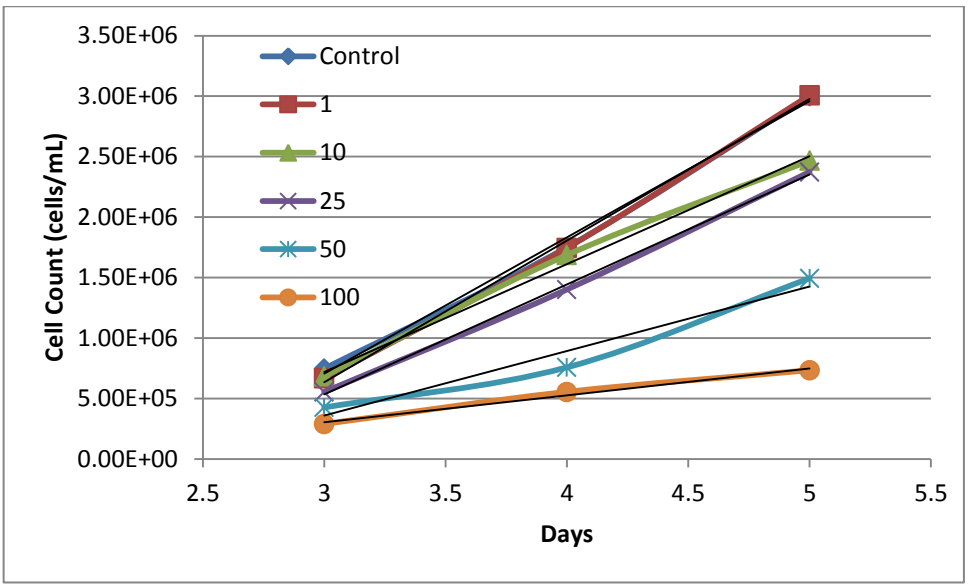

Figure 3.8- Cell growth in sodium azide with lines of best fit.

Sodium Azide (µM)	Relative Growth Rate
Control	1
1	1
10	0.89
25	0.91
50	0.53
100	0.22

Table 3.3- Gradients of lines of best fit from **Figure 3.8** relative to control.

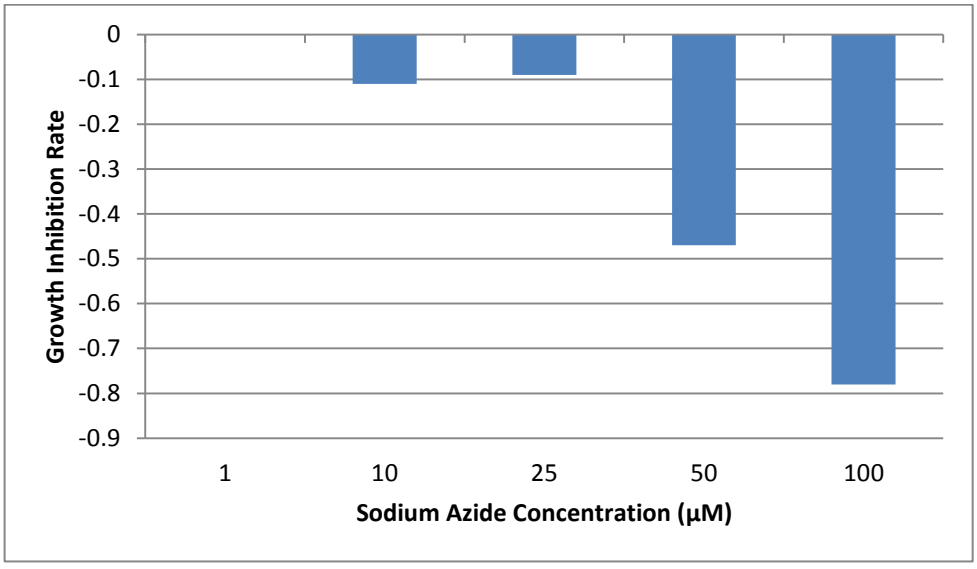

Figure 3.9- Rates of growth inhibition relative to control in sodium azide.

3.4 Discussion

The objective of this section of the study was to assess the inhibitory effects on cell growth of glucose, H_2O_2 and sodium azide on HeLa cells through dose response experiments. In this experiment, HeLa cells were incubated with a wide range of glucose, H_2O_2 and sodium azide concentrations, with varying inhibitory effects on growth rate.

As was to be expected, increasing the concentration of the treatment resulted in increased inhibition of cell growth. Slight growth inhibition resulted from treatments of 50 and 75mM glucose (11% and 30% inhibition respectively), 150μM H_2O_2 (4%), and 10 and 25μM sodium azide (11% and 9% respectively). Strong growth inhibition resulted from treatments of 100 and 125mM glucose (36% and 84% respectively), 200 and 250μM H_2O_2 (54% and 91% respectively), and 50 and 100μM sodium azide (47% and 78% respectively).

The inhibition of growth of human cells due to high glucose has previously been reported in numerous studies, where it has been postulated to be caused by impairment of the transforming growth factor-β 1 (TGF-β 1) signal pathway (Mather *et al*., 2009; Samikannu *et al*., 2006). TGF-β 1 is a secreted protein that performs functions involved in the control of cell growth, proliferation, differentiation and apoptosis. High glucose interferes with the TGF-β 1 signal pathway by inhibition of the mevalonate pathway. Downstream effects of this inhibitory effect are increased TGF-β 1 secretion and the inhibition of Ras prenylation, ultimately reducing cellular proliferation (Mather *et al*., 2009). Cell growth reportedly drastically declines after achieving 50mM glucose, which agrees with these results. However, most previous studies find a significant decline in cell growth with concentrations as low as 25mM, which was not seen in this study. In fact the glucose concentration of the stock media is 25mM. This may be explained by the differences in cell type used across studies, as HeLa cells are considered to be a remarkably hardy and robust cell type (Capes-Davis *et al*., 2010). It may also be explained by the constantly evolving nature of cell lines in culture. Through serial passage, the properties of the cell line change over time. A wide range of alterations to the behaviour and function of cells, including cell morphology, growth rates, protein expression and cell signalling have been reported (ATCC, 2007). While it is unlikely that this impacted on the final results

of these experiments, the potential still exists and is worth considering when evaluating all experiments that utilise cell culture.

H_2O_2 has been commonly used to inhibit many micro-organisms, but particularly as an anti-bacterial, due to its property of inhibiting growth (Halliwell *et al*., 2000). In human cell lines, H_2O_2 has also been reported to inhibit cell proliferation, which agrees with these results. It has been reported that sub-lethal doses of H_2O_2 result in a dose dependent inhibition of DNA synthesis, resulting in a cumulative and irreversible loss of replicative ability. As a result, doubling time increases and cells enter cellular arrest, undertaking a senescent-like state (Chen and Ames, 1994). High concentrations of H_2O_2 have also been reported to induce apoptosis through mitochondrial pathways in HeLa cells (Singh *et al*., 2007).

As an inhibitor of the mitochondrial electron transport chain, sodium azide has long been known to inhibit cell growth. It has been used as a biocide for decades due to its bacteriostatic properties (Lichstein and Seoule, 1943). As mentioned previously, in human cells, sodium azide is acutely toxic. Therefore, it is perhaps not surprising that at the micro molar concentrations used in these dose response experiments, sodium azide exhibits the same inhibitory effect on cell growth as seen in micro-organisms.

It is interesting that a degree of hormesis was present in all treatments. Hormesis is the name given to the stimulatory effects caused by low levels of potentially toxic agents (Calabrese *et al*., 2012). The 25mM glucose, and 50 and 100μM H_2O_2 treatments all resulted in increased growth rates compared to the control over the exponential growth phase. The 1μM sodium azide was found to have a comparable growth rate to the control. While it may not be surprising that the comparatively low glucose levels result in increased growth, as it would convey a greater energy source to the cell culture, it is of interest that H_2O_2 does increase growth, which agrees with results of previous studies (Burdon, 1995). H_2O_2 and its stimulatory effect on cell proliferation have been of particular interest as it has been identified that the elevated levels of H_2O_2 that result from regular exercise have a hormetic effect, indicating that minor oxidative stress may have a beneficial effect (Radak *et al*., 2008).

It should also be noted that after a few days the colour of media became yellow as treatment concentration increased. This is most likely due to the build-up of lactic

acid during glycolysis, indicating that growth inhibition is perhaps a result of mitochondrial inhibition. It can also be explained through lactate build-up, as it is known to reduce the rate of cell growth. Under the inhibitory effects of the higher treatment concentrations, cells accelerate glycolysis to compensate for reduced ATP production via oxidative phosphorylation. The reduction of pyruvate to lactate provides a means of re-oxidising excess NADH generated during glycolysis. This resulting lactate accumulation from glycolysis normally serves as the substrate for gluconeogenesis in the liver. Therefore, in this cell culture system, lactate could not be completely oxidized leading to a build-up in the culture media. Additionally, accelerated glycolysis at high treatment concentrations could lead to a faster turnover rate for glucose. Therefore substrate depletion is another factor to be considered (Lao and Toth, 2008).

To confirm that the impaired cell growth from this chapter was a result of mitochondrial inhibition, and not necrotic cell death, biochemical assays were utilised as described in **Chapter 4**.

4 Effects of Glucose, H_2O_2 and Sodium Azide on HeLa Cell Function

4.1 Introduction

The use of biochemical assays provides crucial insight as to the intracellularly functioning of cells. To further assess the growth inhibitory effects of glucose, H_2O_2 and sodium azide on HeLa cells LDH, MTT and DCFDA assays were utilised. LDH assays were used to determine if the cytotoxicity of the three treatments was due to cell lysis, representative of necrotic cell death (Decker and Lohmann-Matthes, 1988). MTT assays were undertaken to indirectly measure mitochondrial dehydrogenase activity (Marshall *et al*., 1995). Finally, DCFDA assays were carried out to quantify cellular oxidative stress (Wang and Joseph, 1999).

4.2 Methods

4.2.1 LDH Assay

Lactate dehydrogenase is a strictly cytosolic enzyme which will only be released into the surrounding media after necrotic cell death.

Near confluent HeLa cells were seeded onto a 96-well plate in 100µL of DMEM. 8 wells were treated with glucose (25-125mM), H_2O_2 (0-250µM), and sodium azide (0-100µM). The plate was then returned to incubate in standard incubation conditions for 3 days, when the cells would be in the exponential growth phase. After the 72 hours, samples were prepared as in **Chapter 2.2.1**. Briefly, one set of control cells (maximum control) was treated with 100µL 10x lysis solution and the plate was returned to standard incubating conditions for 45 minutes. After this time period, the plate was centrifuged at 250x*g* for 5 minutes at RT to pellet cell debris. 50µL of the supernatant from each well of the culture plate was transferred to the corresponding well of a 96-well enzymatic assay plate. 50µL of reconstituted substrate was then added to the supernatant in each well of the assay plate. The plate was then covered from light and incubated at RT for 30 minutes. The assay was terminated by the addition of 50µL of Stop Solution to each well of the plate. Air bubbles were removed from all wells with a needle and the absorbance was read at 490nm. The data were calculated according to **Equation 2.1** and presented as a percentage of the corresponding maximum control.

4.2.2 MTT Assay

The MTT [3-(4,5-dimethylthiazol-2-yl)-2,5-diphenyl tetrazolium bromide] assay is commonly accepted as a measure of cell viability. It is based on the activity of intracellular oxidoreductase enzymes. Of which NADH is primarily responsible for most MTT reduction (Berridge *et al*., 2005). As most oxidoreductases are located in the mitochondrial electron transport system, the MTT assay is also able to be used as an indirect measure of mitochondrial dehydrogenase activity.

Near confluent HeLa cells were seeded onto a 96-well plate in 100µL of DMEM. 8 wells were treated with glucose (25-125mM), H_2O_2 (0-250µM), and sodium azide (0-100µM). The plate was then returned to incubate in standard incubation conditions for 3 days, when the cells would be in the exponential growth phase. After the 72 hours, samples were prepared as in **Chapter 2.2.2**. Briefly, after the 72 hours the media was removed and replaced with 10µL reconstituted MTT in DMEM. The plate was then incubated at standard incubation conditions for 2 hours. After the incubation period, the culture fluid was removed and disposed of. This was followed by the addition of 100µL MTT Solubilisation Solution. The plate was then placed on a minishaker for 10 minutes to assist in dissolving the crystals. Air bubbles were then removed from all wells with a needle and the absorbance was read at 570nm and the background read at 655nm. After subtracting the averaged 655nm reading from the averaged 570nm reading, the averaged blank was also subtracted, as per **Equation 2.2.** Experimental values were then normalised to the control and expressed as a percentage of mitochondrial dehydrogenase activity (**Equation 2.3),** since dehydrogenases are predominantly situated in the mitochondria.

4.2.3 DCFDA Assay

DCFDA (2,7-dichlorofluorescein diacetate) is a fluorogenic dye that measures hydroxyl, peroxyl and other ROS activity within cells. It is a reagent capable of permeating cells, and after which, is deacetylated by cellular esterases to a non-fluorescent compound which is incapable of diffusing back out of the cell. It is later oxidized by ROS into the highly fluorescent 2, 7-dichlorofluorescin (DCF).

Near confluent HeLa cells were seeded onto a 96-well black culture plate in 100μL of DMEM. 8 wells were treated with glucose (25-125mM), H_2O_2 (0-250μM), and sodium azide (0-100μM). The plate was then returned to incubate in standard incubation conditions for time periods of 24 hours, 3 days, and 7 days. Plates incubated for 7 days had their media replaced after 3 days. At the end of the incubation period, the DMEM media was removed and the cells were washed twice with 100μL pre-warmed PBS. The cells were then incubated for a further hour in 100μL Opti-MEM containing only 2% FBS and further supplemented with 2.5μL of 400μM DCFDA. After the one hour incubation period, the media was again removed and the cells washed twice with 100μL PBS. 200μL Opti-MEM was then added, containing 2% FBS, and the plate was left to stand at RT. 10μL of 200μM H_2O_2 was added to each well, except the H_2O_2 absent control, immediately before reading the fluorescence intensity over a 30 minute period at excitation and emission wavelengths of 485nm and 520nm respectively. Data produced was standardised to the control absent of H_2O_2 and expressed relative to the control sample.

4.3 Results

4.3.1 LDH Assays

Lactate dehydrogenase is an intracellular enzyme that is only released into the media upon cell lysis, thus this assay was used to determine if the cytoxicity of glucose, H_2O_2, and sodium azide on HeLa cells at the high concentrations described in **Chapter 3** was indeed due to necrotic cell death.

After 3 days in culture, the percentage of LDH content relative to corresponding maximum control samples was calculated. It was assumed that every dead cell released an equal amount of LDH. Therefore the percentage of LDH content was interpreted as the percentage of lysed cells.

The control sample had 25.50 ± 1.31% lysed cells, and was not significantly different from the 75 and 100mM glucose groups, which had 22.76 ± 1.29% and 26.46 ± 1.00% of lysed cells, respectively. However, treatment with 125mM glucose resulted in a significantly increased ($p < 0.05$) percentage of lysed cells compared to the control; resulting in 31.46 ± 1.37% lysed cells, as shown in **Figure 4.1**.

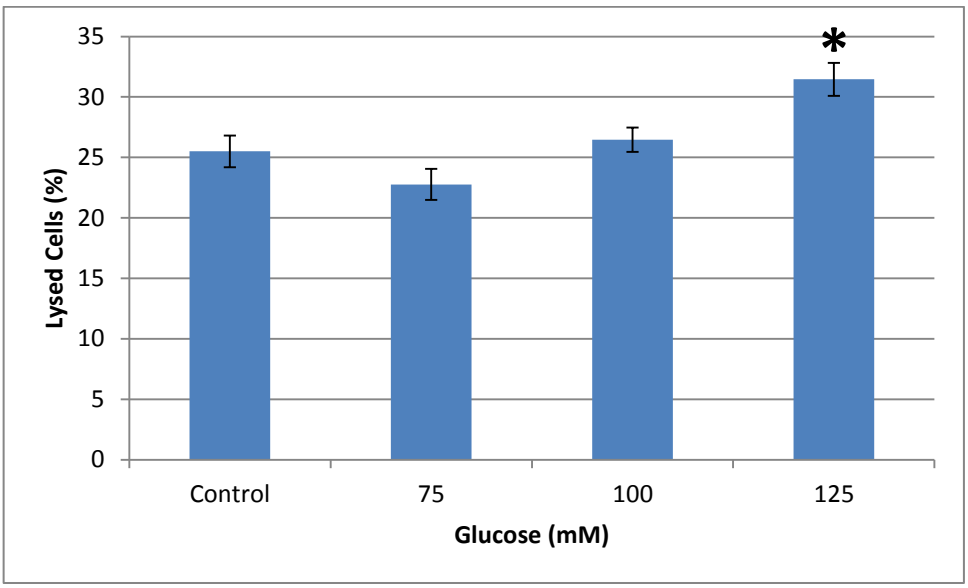

Figure 4.1- Percentage of lysed cells in the presence of glucose. Bar graph showing means ± S.E.M. * = $p < 0.05$.

The control sample had 27.84 ± 3.04% lysed cells, and was not significantly different from the 150 and 200µM H_2O_2 groups, which had 27.61 ± 2.33% and 30.69 ± 2.19% of lysed cells, respectively. However, samples treated with 250µM H_2O_2 resulted in a significantly increased ($p < 0.05$) percentage of lysed cells compared to the control; resulting in 37.71 ± 3.09% lysed cells, as shown in **Figure 4.2**.

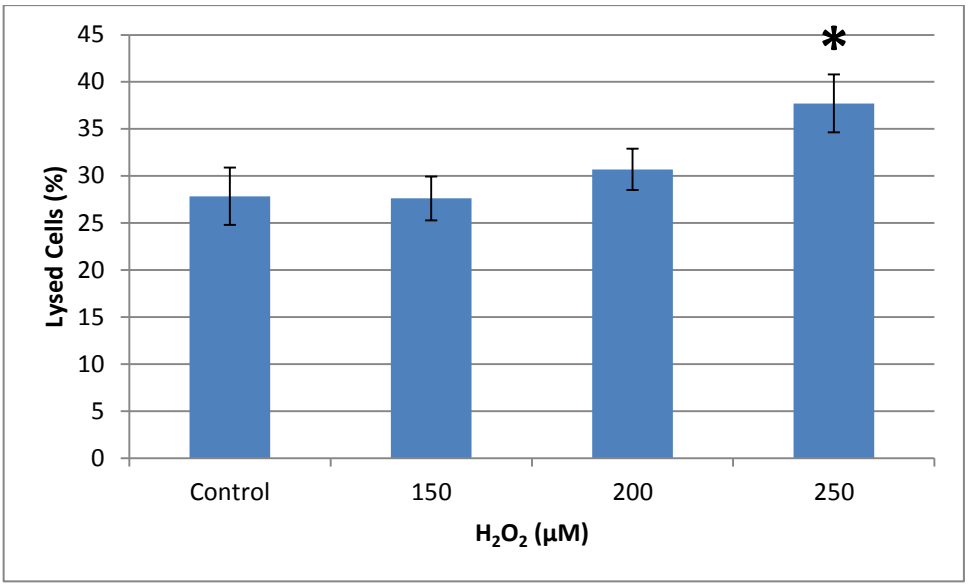

Figure 4.2- Percentage of lysed cells in the presence of H_2O_2. Bar graph showing means ± S.E.M. * = $p < 0.05$.

The control sample had 24.42 ± 1.13% lysed cells, and was not significantly different from the 25 and 50µM sodium azide groups, which had 26.80 ± 1.18% and 27.57 ± 1.51% of lysed cells, respectively. However, treatment with 100µM sodium azide resulted in a significantly increased ($p < 0.05$) percentage of lysed cells compared to the control; resulting in 32.08 ± 2.85% lysed cells, as shown in **Figure 4.3**.

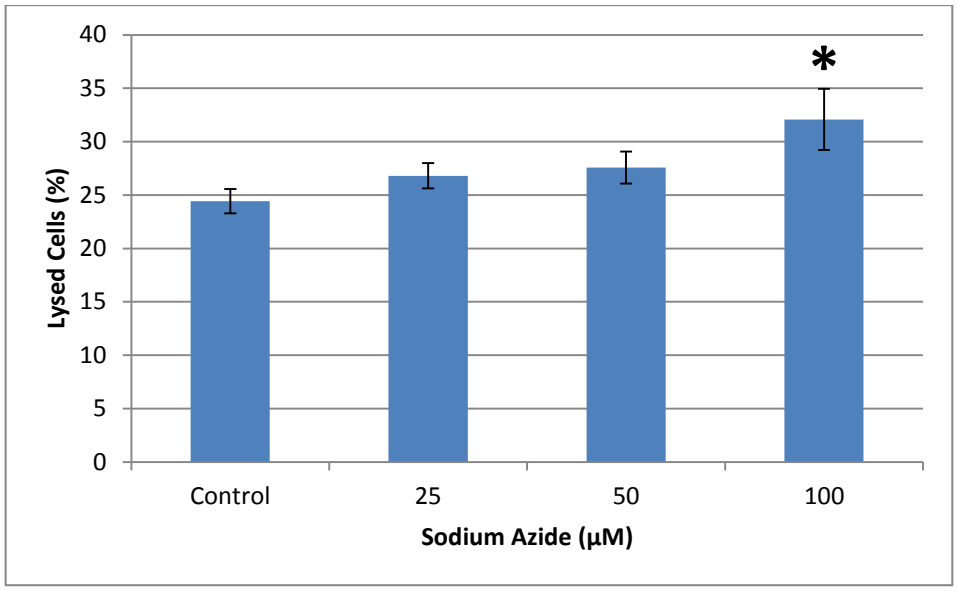

Figure 4.3- Percentage of lysed cells in the presence of sodium azide. Bar graph showing means ± S.E.M. * = $p < 0.05$.

4.3.2 MTT Assays

The MTT assay is commonly accepted as a measure of cell viability, and is also able to indirectly measure mitochondrial dehydrogenase activity. Thus it was used to determine if the inhibitory cell growth effects of glucose, H_2O_2, and sodium azide on HeLa cells was due to effects on mitochondrial activity.

After 3 days in culture, cells were incubated with MTT for 2 hours. After which the formazan crystals were solubilised, the absorbance read, and results were interpreted as a percentage of mitochondrial activity relative to the control group.

All glucose samples were found to have significantly decreased ($p < 0.05$) mitochondrial dehydrogenase activity compared to control cells. 75mM glucose resulted in 84.29 ± 1.20%, 100mM resulted in 78.21 ± 1.13%, and 125mM glucose resulted in 73.96 ± 1.12% mitochondrial dehydrogenase activity, as seen in **Figure 4.4**.

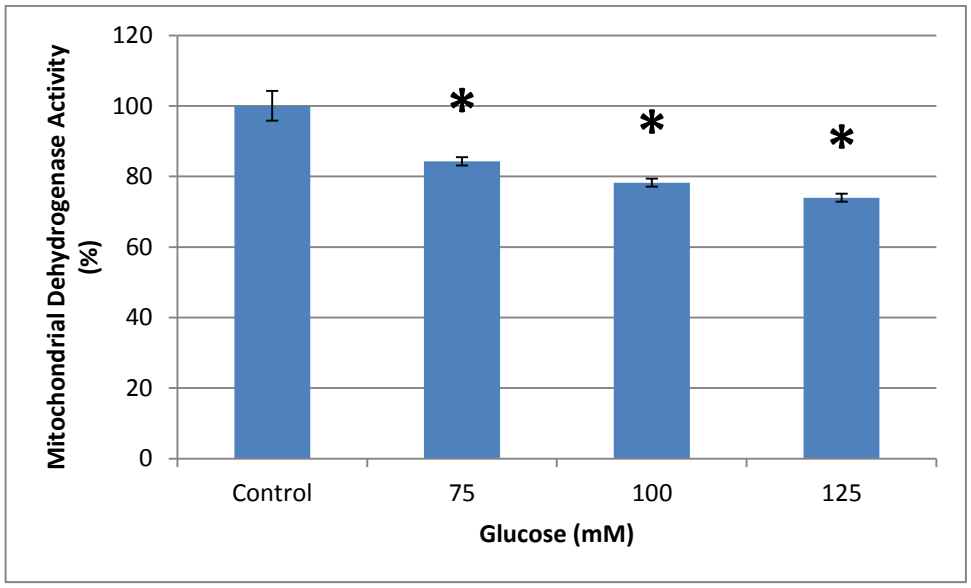

Figure 4.4- Mitochondrial dehydrogenase activity in the presence of glucose. Bar graph showing the mean ± S.E.M. * = $p < 0.05$.

All H_2O_2 samples were found to have significantly decreased ($p < 0.05$) mitochondrial dehydrogenase activity relative to control cells. 150µM H_2O_2 resulted in 87.70 ± 3.07%, 200µM resulted in 81.97 ± 1.41%, and 250µM resulted in 59.61 ± 4.21% mitochondrial dehydrogenase activity, as shown in **Figure 4.5**.

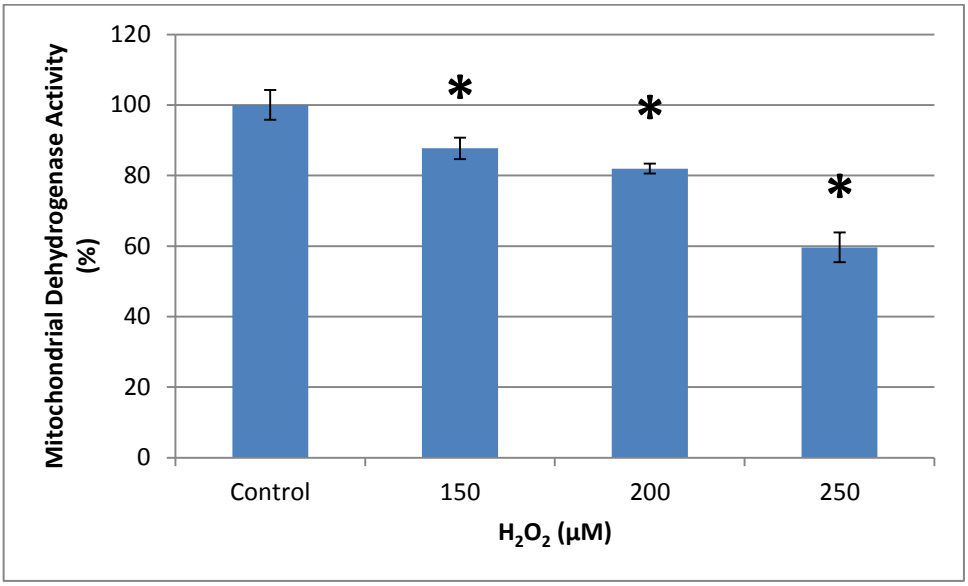

Figure 4.5- Mitochondrial dehydrogenase activity in the presence of H_2O_2. Bar graph showing the mean ± S.E.M. * = $p < 0.05$.

All sodium azide samples were found to have significantly decreased ($p < 0.05$) mitochondrial dehydrogenase activity relative to control cells. 25µM sodium azide resulted in 91.76 ± 2.27%, 50µM resulted in 73.61 ± 3.53%, and 100µM resulted in 75.33 ± 1.20% mitochondrial dehydrogenase activity, as seen in **Figure 4.6**.

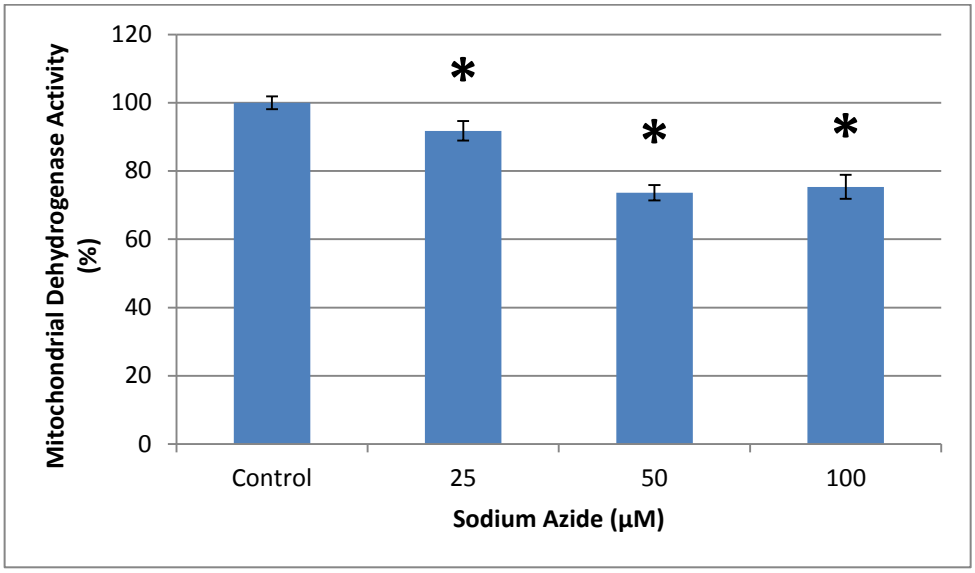

Figure 4.6- Mitochondrial dehydrogenase activity in the presence of sodium azide. Bar graph showing the mean ± S.E.M. * = $p < 0.05$.

4.3.3 DCFDA Assays

DCFDA measures hydroxyl, peroxyl and other ROS activity within cells, thus the DCFDA assay was used to determine the degree of ROS generation in HeLa cells treated with glucose, H_2O_2, and sodium azide.

After 1, 3, and 7 days in culture, cells were incubated with DCFDA for 1 hour. After which the fluorescence was read, and results were normalised to the H_2O_2 absent control. Results were interpreted as a percentage of ROS levels relative to the control group.

After 24 hours, all samples were found to have significantly increased ($p < 0.05$) ROS levels. The glucose treatment resulted in 109.06 ± 2.27%, the H_2O_2 treatment resulted in 112.93 ± 2.71%, and the sodium azide treatment resulted in 110.77 ± 2.24% ROS levels, as shown in **Figure 4.7**.

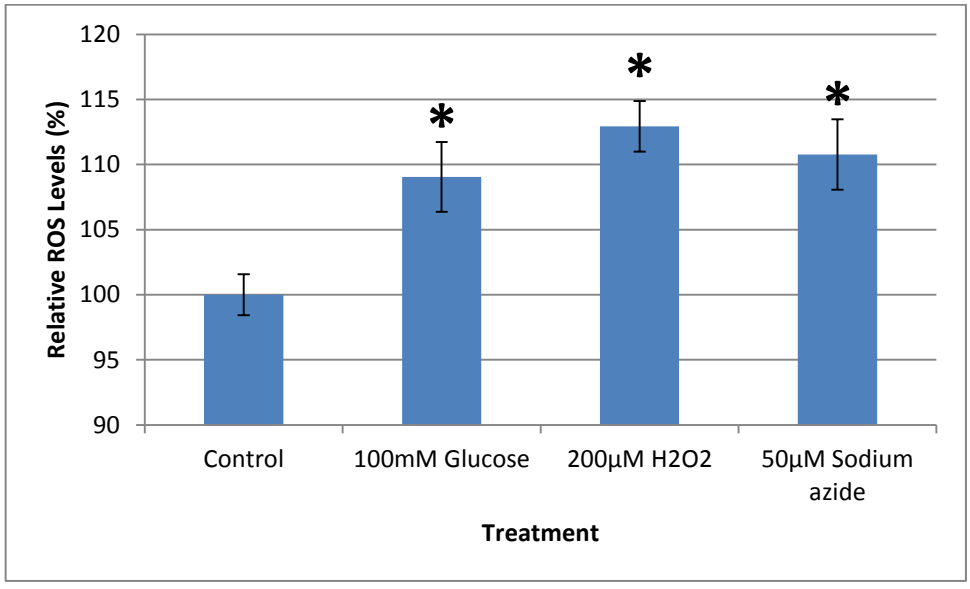

Figure 4.7- ROS levels in the presence of glucose, H_2O_2, and sodium azide over 24 hours. Bar graph showing the mean ± S.E.M. * = $p < 0.05$.

After 3 days, all samples were found to have significantly increased ($p < 0.05$) ROS levels. The glucose treatment resulted in 123.63 ± 6.24%, the H_2O_2 treatment resulted in 135.36 ± 7.33%, and the sodium azide treatment resulted in 134.77 ± 7.15% ROS levels, as seen in **Figure 4.8**.

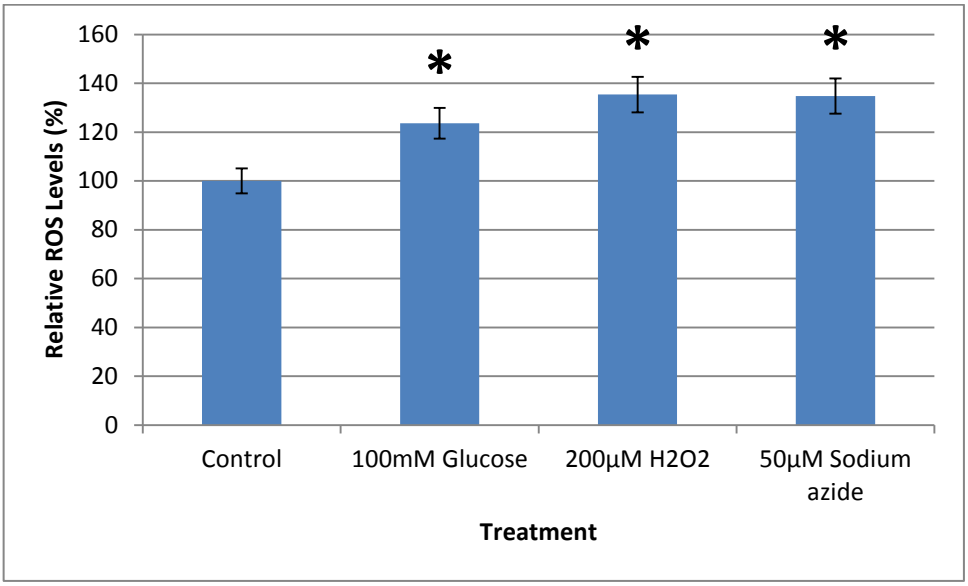

Figure 4.8- ROS levels in the presence of glucose, H_2O_2, and sodium azide over 3 days. Bar graph showing the mean ± S.E.M. * = $p < 0.05$.

After 7 days, all samples were found to have significantly increased ($p < 0.05$) ROS levels. The glucose treatment resulted in 179.95 ± 23.78%, the H_2O_2 treatment resulted in 304.56 ± 29.02%, and the sodium azide treatment resulted in 279.13 ± 43.82% ROS levels, as shown in **Figure 4.9**.

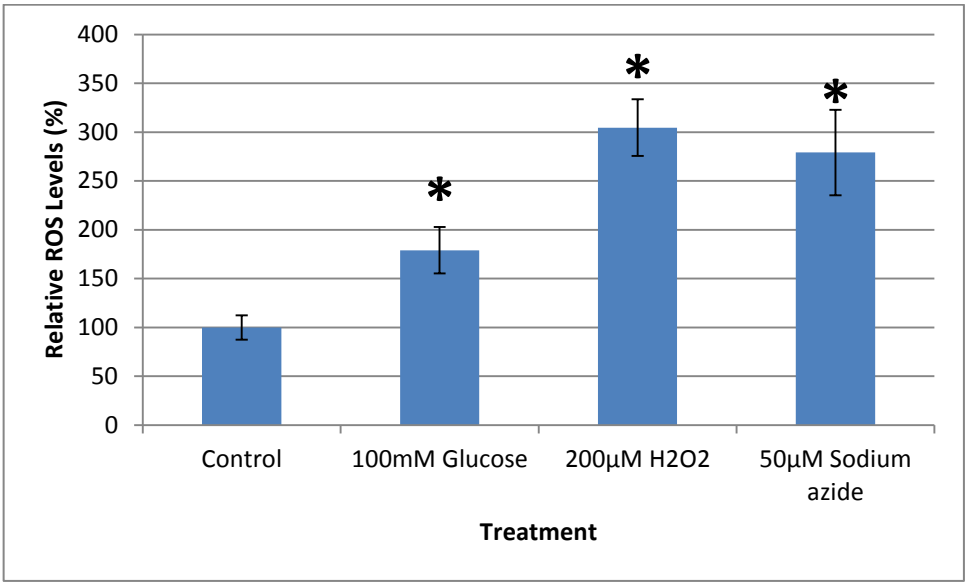

Figure 4.9- ROS levels in the presence of glucose, H_2O_2, and sodium azide over 7 days. Bar graph showing the mean ± S.E.M. * = $p < 0.05$.

4.4 Discussion

The objective of this portion of the study was to find a concentration of each of glucose, H_2O_2, and sodium azide which impaired mitochondrial activity but did not result in necrotic cell death, thus providing optimal mitochondrial stress conditions to investigate the mitochondria specific stress response that induces HSP60 expression. The concentrations of glucose, H_2O_2, and sodium azide used in these assays were only the concentrations that were deemed to result in significant growth inhibition as seen in **Chapter 3**.

The LDH assay showed that, compared with a control sample, treatment with 75 and 100mM glucose, 150 and 200μM H_2O_2, and 25 and 50μM sodium azide did not result in significantly increased cell lysis. Treatment with 125mM glucose, 250μM H_2O_2, and 100μM sodium azide did however result in significantly increased ($p < 0.05$) cell death. The MTT assay showed that, compared with control, treatment with 75, 100 and 125mM glucose, 150, 200 and 250μM H_2O_2, and 25, 50, and 100μM sodium azide all resulted in significantly reduced ($p < 0.05$) mitochondrial dehydrogenase activity.

The 125mM glucose, 250μM H_2O_2, and 100μM sodium azide treatments all indicate that cell lysis occurs at these concentrations. The MTT assay also indicates that there is reduced mitochondrial activity at these concentrations. This raises the question of whether the cell lysis experienced by these cells is due to mitochondrial inhibition, or the other way around. From this data it is impossible to tell. In future, as the LDH assay is only representative of necrotic cell death, it would be of great benefit and interest to perform assays, such as a cytochrome c assay, to assess the degree of apoptosis experienced by cells exposed to these treatments to better explain the phenomena surrounding some of these questions (Guo *et al*., 2002).

Hyperglycaemia has a number of deleterious metabolic consequences including creating advanced glycated end-products (AGE), altering signal transduction, tissue damage and abnormal gene expression, but the consequence primarily concerned with this study is increased oxidative stress (Diaz-Flores *et al*., 2004). There is an increase in intracellular ROS activity when cells are exposed to

chronic hyperglycaemia. This occurs through several mechanisms. Chronic hyperglycaemia results in elevated levels of glucose, resulting in the 'Crabtree effect'. This was first described by Herbert Crabtree in yeast, *Saccharomyces cerevisiae*, where he observed that the presence of high concentrations of glucose caused glycolysis to accelerate while inhibiting oxidative phosphorylation (Crabtree, 1928). In pertaining to this study, an increased rate of glycolysis due to hyperglycaemia would result in elevated levels of glyceraldehyde-3-phosphate, an intermediate metabolite along the glycolysis pathway. Glyceradehyde-3-phosphate undergoes auto-oxidation, and in doing so generates H_2O_2, thus increasing intracellular ROS activity (Robertson *et al*, 2003). There is also a hyperglycaemia associated decrease in the efficiency of reduction of molecular oxygen at the complex IV of the electron transport chain, increasing the amount of ROS generated (Zhang and Gutterman, 2007). However the mechanisms of this phenomenon have been poorly documented, and could well be a result of the aforementioned H_2O_2 generated by glyceraldehyde-6-phosphate auto-oxidation. The overproduction of mitochondrial ROS has been found to be associated with dynamic changes to mitochondrial morphology. Rapid fragmentation of the mitochondrion ensues, which has been found to be driven by the mitochondria's fission machinery, a known marker of apoptosis (Yu *et al*, 2008).

Hyperglycaemic conditions have been previously reported in the literature to induce cell death in a number of human cell lines through mitochondrial mediated apoptotic pathways. Reported pathways include mitochondrial fission (Yu *et al*, 2008), mitochondrial release of apoptosis-inducing factor (AIF) (Santiago *et al*., 2007) elevated production of ROSs (Peiro *et al*., 2001), and activation of proteins involved in apoptotic cell death including members of the caspase and Bcl-2 families (Allen *et al*., 2005). Based on the glucose concentrations used in previous studies, the HeLa cells used in this experiment were capable of withstanding concentrations of glucose much higher than other cell types. For instance, pancreatic islet cells undergo apoptosis when exposed to 25mM glucose concentrations (Allen *et al*., 2005). However, as mentioned in the previous chapter, HeLa cells are renowned for their robust nature. Also the potential the cells used in these experiments have evolved into a more hyperglycaemic tolerant cell line through serial passage remains a possibility. Either could explain the discrepancy between the much higher glucose concentrations the HeLa can

tolerate. In saying that, the trend still exists where with increasing glucose concentration, there is greater cell death.

High glucose concentrations also result in mitochondrial inhibition. As previously mentioned, high glucose levels results in increased levels of glyceraldehyde-6-phosphate, which undergoes auto-oxidation to generate H_2O_2 (Robertson *et al*., 2003). It has been documented that the stimulation of increased mitochondria derived ROS production in such a way correlates with mitochondrial inhibition, which a physiological state of high levels of glucose would induce (Russell *et al*., 2002). A further piece of evidence linking high glucose to oxidative stress is that high glucose has been found to induce the upregulation of antioxidant enzymes in human endothelial cells (Ceriello *et al*., 1996). It is therefore likely that the mitochondrial inhibition due to high levels of glucose as seen in this experiment was due to increased ROS levels. This aspect was further investigated using the DCFDA assay discussed later in this chapter.

H_2O_2 occurs naturally in cells as a by-product of the mitochondrial electron transport chain. At complex IV of the electron transport chain, molecular oxygen is reduced to water. However, this is not a completely efficient reaction and 1-4% of the oxygen is incompletely reduced to superoxide (O_2^-). As a ROS, O_2^- is hazardous as it may cause oxidative damage. Superoxide dismutases (SOD), and specifically SOD2 in the mitochondria, act to quickly remove this threat. The SOD2 enzyme catalyses a reaction in which O_2^- is converted into O_2 and H_2O_2. H_2O_2 is further processed by the catalase enzyme located in peroxisomes adjacent to the mitochondria. Catalase catalyses a reaction in which H_2O_2 is converted into water and oxygen. However, these reactions are not completely efficient either, and their efficiency further declines when ROS generation from the electron transport chain increases, such as during hyperglycaemia as previously detailed. H_2O_2 is capable of leaking out of the mitochondria resulting in cellular oxidative stress (Han *et al*., 2001).

If H_2O_2 is not appropriately dealt with, it is capable of causing oxidative damage. In the mitochondria, accumulating oxidative damage may affect the efficiency of the mitochondrial electron transport chain, and further increase the rate of ROS generation (Han *et al*., 2001). Oxidative damage may also occur to the DNA. Sub

lethal doses of H_2O_2 have been reported to induce oxidative DNA lesions. Such lesions may result in DNA strand breaks, and may also be mutagenic and cytotoxic (Nakamura *et al*., 2003). Ultimately, H_2O_2 has been found to induce apoptosis in cells through intrinsic cell death pathways. H_2O_2 upregulates the expression of the p73 protein, a member of the p53 protein family, which triggers apoptosis in response to DNA damaging agents. p73 in turn upregulates its downstream target Bax. The Bax protein inserts into the outer mitochondrial membrane to form an oligomeric pore. This allows for the release of cytochrome c from the mitochondria into the cytoplasm where it binds with apoptotic protease activating factor-1 (APAF-1) to form an apoptosome. The apoptosome activates caspases-9 and -3 to begin a chain reaction of intracellular protein degradation culminating in a process of controlled cell death (Singh *et al*., 2007; Wolter *et al*., 1997).

H_2O_2 has already been reported to induce cell death in human cells. As previously mentioned, high concentrations of H_2O_2 have been reported to activate mitochondrial mediated apoptosis pathways in HeLa cells (Singh *et al*, 2007). However, the concentration used to achieve apoptosis in that study was only 125μM, whereas increased cell death in this study was only achieved from 250μM, double the concentration. Like with the glucose, this could potentially be explained by the evolution of a more robust and H_2O_2 tolerant cell line resulting from serial passage, although it is not possible to verify. However, a dose dependent trend was still observed, where increasing H_2O_2 concentration resulted in increased cell death. As has been previously mentioned, oxidative stress can result in mitochondrial inhibition as determined by the MTT assay (Zeevlak *et al*., 2005). This effect was directly simulated by the addition of H_2O_2. It resulted in the observation of a dose dependent decrease in mitochondrial dehydrogenase activity as expected.

Sodium azide is a known acutely toxic compound, inhibiting the electron transport chain by irreversibly binding to the heme cofactor of complex IV. Inhibition of the mitochondrial electron transport chain, at various points, is documented to increase mitochondrial ROS generation (Quillet-Mary *et al*., 1997). As a result, oxidative stress ensues culminating in a molecular stress response. As previously

mentioned, oxidative stress activates intrinsic mitochondrial apoptotic pathways, ultimately resulting in increased cell death.

The resulting cell death of HeLa cells from micro molar concentrations of sodium azide in a dose dependent manner, as seen in these results, agrees with other cell death data in the literature, although it is of interest that other human cell types have been found to tolerate sodium azide up to milli molar levels (Gavrieli *et al*., 1992). Also as expected, sodium azide impaired mitochondrial dehydrogenase activity. This is undoubtedly through its ability to irreversibly bind to the heme cofactor complex IV, and thus block the mitochondrial electron transport chain.

By taking the LDH and MTT assay data together as in **Table 4.1**, concentrations which resulted purely in mitochondrial stress were determined as concentrations where cell death was not significantly increased according to the LDH assay but mitochondrial dehydrogenase activity was significantly reduced according to the MTT assay. Therefore optimal stress concentrations were 75 and 100mM glucose, 150 and 200μM H_2O_2, and 25 and 50μM sodium azide. To determine the optimum stress concentration, assay data was coupled with the growth inhibition data from **Chapter 3**, as seen in **Table 4.1**.

Table 4.1- Summary of LDH assay, MTT Assay, and growth inhibition results.

Treatment	Significantly Increased Cell Death?	Significantly Reduced Mitochondrial Dehydrogenase Activity?	Relative Growth Rate
75mM glucose	No	Yes	0.7
100mM glucose	**No**	**Yes**	**0.64**
125mM glucose	Yes	Yes	0.16
150μM H_2O_2	No	Yes	0.96
200μM H_2O_2	**No**	**Yes**	**0.46**
250μM H_2O_2	Yes	Yes	0.09
25μM sodium azide	No	Yes	0.91
50μM sodium azide	**No**	**Yes**	**0.53**
100μM sodium azide	Yes	Yes	0.22

The concentration of each treatment which resulted in no significant increase in cell death, but reduced mitochondrial dehydrogenase activity, and resulted in the greatest growth inhibition was 100mM glucose, 200µM H_2O_2, and 50µM sodium azide. These concentrations were determined as causing cellular stress targeted at the level of the mitochondrion, and were hence used for the remaining experiments including relative ROS levels and HSP protein expression.

The DCFDA assays showed that treatment of HeLa cells with the identified concentrations of 100mM glucose, 200µM H_2O_2, and 50µM sodium azide all result in oxidative stress, as noted by the increased levels of intracellular ROS. Over 24 hours of exposure to the treatments, there is a significant increase in ROS levels, which continues to rise drastically over both 3 and 7 day treatments, as seen in **Figure 4.10**. 200µM H_2O_2 has the greatest effect on ROS levels, followed closely by 50µM sodium azide, with 100mM glucose having the least great effect of the three.

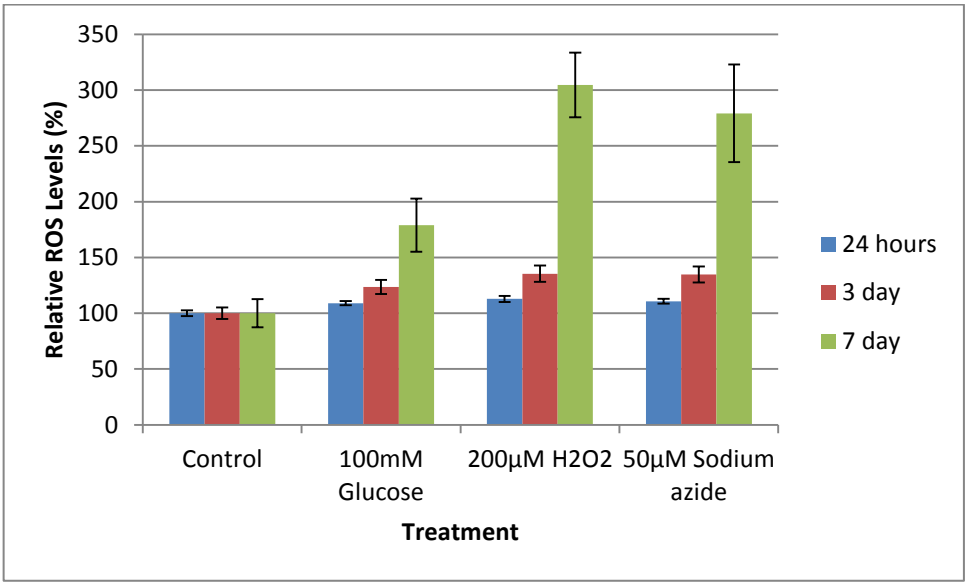

Figure 4.10- ROS levels in the presence of glucose, H_2O_2, and sodium azide over 24 hours, 3, and 7 days. Bar graph showing the mean ± S.E.M. * = $p < 0.05$.

Elevated levels of ROS activity in cells is known to be indicative of mitochondrial compromised cells. Within mitochondria, the primary site of ROS generation is the electron transport chain. At complex IV of the electron transport change molecular oxygen is reduced to water. However, this is not a completely efficient reaction and 1-4% of the oxygen is incompletely reduced to O_2^-. O_2^- can then

generate other ROS species, such as H_2O_2, through various enzymatic and nonenzymatic reactions. The proportion of oxygen incompletely reduced to O_2^- increases in dysfunctional mitochondria, therefore increasing mitochondrial ROS generation. Physiologically, this dysfunction may result from hyperglycaemia and/or free fatty acid flux (Zhang and Gutterman, 2007). Hyperglycaemia may also result in ROS generation through increased concentrations of glyceraldehyde-6-phosphate undergoing auto-oxidation to generate H_2O_2, as previously mentioned (Robertson *et al*, 2003).

The DCFDA assay has shown that the 100mM glucose treatment was in fact resulting in increased ROS production, providing supplementary evidence to the MTT assay results. Over 24 hour, 3 day, and 7 day treatment periods, exposure of HeLa cells to 100mM glucose resulted in 109.06, 123.63, and 178.95% increases in ROS activity respectively. As previously mentioned, high glucose concentrations have been proposed to result in mitochondrial dysfunction through increased ROS production, which this data certainly supports.

The DCFDA assay results also lend support to the MTT assay results for the H_2O_2 and sodium azide treatments. Both the 200μM H_2O_2 and 50μM sodium azide led to substantial increases in intracellular ROS levels over a 7 day time period. Over 24 hour, 3 day, and 7 day treatment periods, exposure of HeLa cells to 200μM H_2O_2 resulted in 112.93, 135.36, and 305.56% increases in ROS activity respectively. Over 24 hour, 3 day, and 7 day treatment periods, exposure of HeLa cells to 50μM sodium azide resulted in 110.77, 134.77, and 279.13% increases in ROS activity respectively. Due to their previously described properties that lead them to interrupt mitochondrial respiration and culminate in mitochondrial dysfunction, the DCFDA assay provides further evidence of cellular stress targeted at the level of the mitochondrion by both these stressors. In saying that, the ROS levels of H_2O_2 treated HeLa cells represents a combination of residual H_2O_2 that escaped the wash protocol and ROS generated due to oxidative stress, so cannot be exclusively deemed to be generated by the cell's mitochondria.

5 Effects of Glucose, H_2O_2 and Sodium Azide on HeLa Cell HSP Expression

5.1 Introduction

The previous chapters identified optimal conditions in which cells were subjected to treatments which resulted in mitochondria specific cell stress, as determined in **Chapter 4**. It is known that part of the cellular stress response culminates in the induction of HSP expression. Specifically, HSP60 induction is evidence of mitochondria specific stress and HSP70 induction is indicative of a general cellular stress (Martinus *et al*., 1996). On this basis, we therefore wanted to assess the level of HSP60 and HSP70 expression in HeLa cells upon exposure to glucose, H_2O_2, and sodium azide at sub-lethal concentrations optimised for mitochondrial impairment. The level of HSP60 and HSP70 expression was determined by western blot.

5.2 Methods

5.2.1 Heat Shock Control Cells

As a means of obtaining a positive control, a heat shock treatment was also utilised following much of the same protocol of Martinus and colleagues from 1996. HeLa cells were grown in a culture flask for 3 days, so as to reach the exponential growth stage. The media was then replaced with DMEM pre-warmed to 45˚C, and placed into a 45˚C incubator for 20 minutes. Following heat treatment, the media was again replaced, this time with DMEM pre-warmed to 37˚C. The culture was returned to standard incubating conditions for 6 hours. After this time, the cells were harvested for protein extraction.

5.2.2 Protein Extraction

Harvested HeLa cells treated with glucose (100µM), H_2O_2 (200µM), sodium azide (50µM) and a control sample grown over 3 and 7 days, along with the heat shock cells, were treated with 100µL TENT buffer freshly supplemented with 1µL 40mM PMSF. The cells were ruptured by vortexing, and were subsequently incubated at 4°C for 30 minutes before being spun down at 10,000rcf for 5 minutes at 4°C to pellet cell debris. The supernatant was transferred to a new tube and protein concentration was estimated. Samples were stored at -20˚C.

5.2.3 Protein Estimation

Protein concentration was estimated using the BCA Protein Assay kit. 200µL was added to 10µL of sample protein, as well as a 1:10 dilution of samples. The plate was then mixed briefly on a minishaker for 30 seconds before incubating at 37°C for 30 minutes. The plate was then read at 570nm. The concentration of each protein sample was determined by entering the absorbance value into the line of best fit equation determined by the BSA standard curve, as mentioned in **Chapter 2.3.2.**

5.2.4 Protein Separation and Transfer

Total protein was separated on 10% polyacrylamide gels, made as described in **Chapter 2.3.3**. 20µg total protein was made up to 20µL with protein loading buffer. The samples were denatured in boiling water for approximately 5 minutes before loading into the wells. 2µL of protein ladder was run alongside the samples. The gel was electrophoresed at a constant 20mA as the bands ran through the stacking gel, and 30mA through the resolving gel. The end point was determined as when the loading dye ran off the gel. The protein was then transferred to a PVDF membrane via semi-dry transfer was 3-buffer system. The transfer cell was run at 15V for 35 minutes. Efficient transfer was then confirmed with Ponceau S staining.

5.2.5 Western Blotting

Membranes were blocked in 10% skim milk in TBST overnight. After six 5 minute washes in TBST, they were incubated in primary antibody (rabbit anti-HSP60/70/actin) diluted 1:250 in 5% skim milk in TBST overnight at 4˚C. They were again washed 6 x 5 minutes before being incubated in secondary antibody (anti-rabbit) diluted 1:1000 in 5% skim milk in TBST for 5 hours at RT on a gyro rocker. After another 6x5 minute washes the membrane was incubated with SuperSignal west substrate for 5 minutes, and then visualised. Bands were quantified and normalised to actin (**Chapter 2.3.4**).

5.3 Results

5.3.1 HSP60

After total protein was separated on a polyacrylamide gel and transferred to a PVDF membrane, Ponceau S staining was used to show the standard HSP60 band to be at 60kDa and that protein loading was even. After western blot, a single band for each sample was seen and the bands appeared to be the same size as the standard HSP60 protein band. The bands were then quantitated using the Gel Quant software, and the relative expression to the control was plotted.

HSP60 protein expression was found to be upregulated in all treatments over 3 days. The heat shocked cells had a 2.23 fold increase in HSP60 expression, while the 100mM glucose, 200µM H_2O_2, and 50µM sodium azide had 1.61, 1.54 and 2.12 fold increases respectively. All were significantly different to the control ($p < 0.05$).

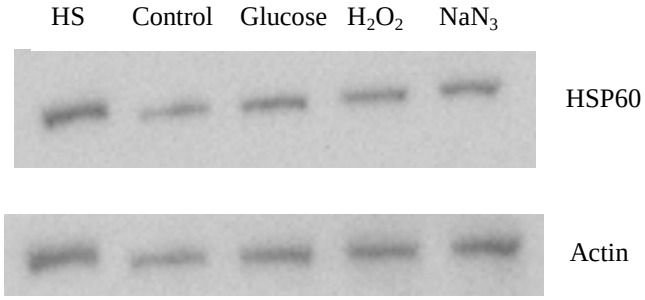

Figure 5.1- Western blots of HSP60 and actin in cells treated with heat shock, glucose (100mM), H_2O_2 (200µM), and sodium azide (50µM), respectively, over 3 days.

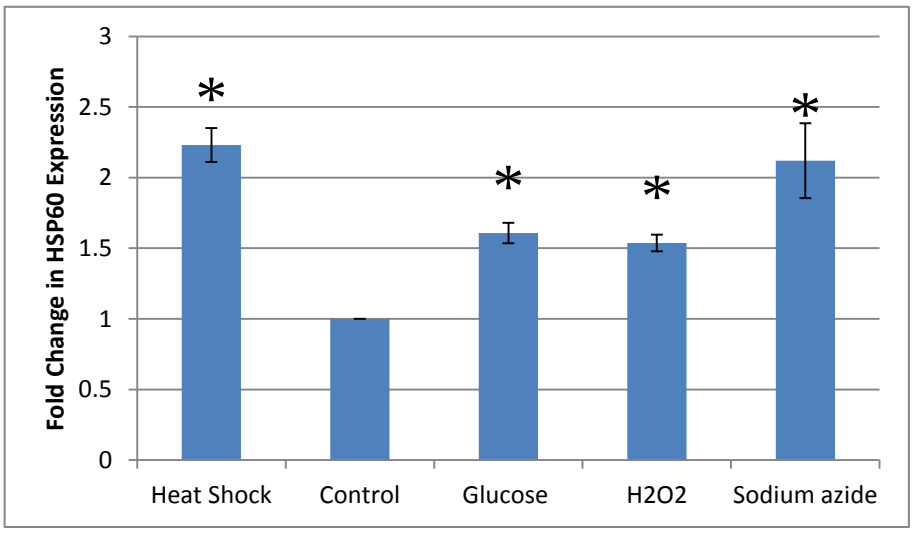

Figure 5.2- Relative HSP60 expression in cells treated with heat shock, glucose (100mM), H_2O_2 (200µM), and sodium azide (50µM) over 3 days. Bar graph showing the mean ± S.E.M. * = $p < 0.05$.

Additionally, HSP60 protein expression was found to be further upregulated in all treatments over a 7 day treatment period. The heat shocked cells had a 2.38 fold increase in HSP60 expression according to these membranes. The 100mM glucose, 200µM H_2O_2, and 50µM sodium azide had 2.43, 3.58 and 4.74 fold increases respectively, and each was significantly different from the control ($p < 0.05$).

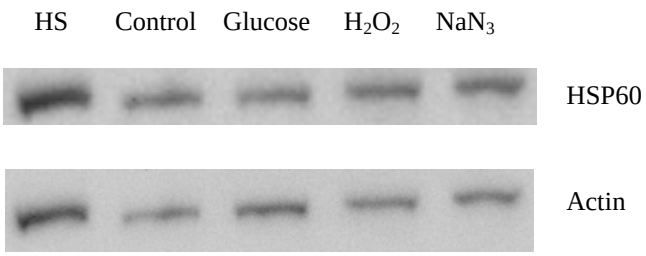

Figure 5.3- Western blots of HSP60 and actin in cells treated with heat shock, glucose (100mM), H_2O_2 (200µM), and sodium azide (50µM) over 7 days.

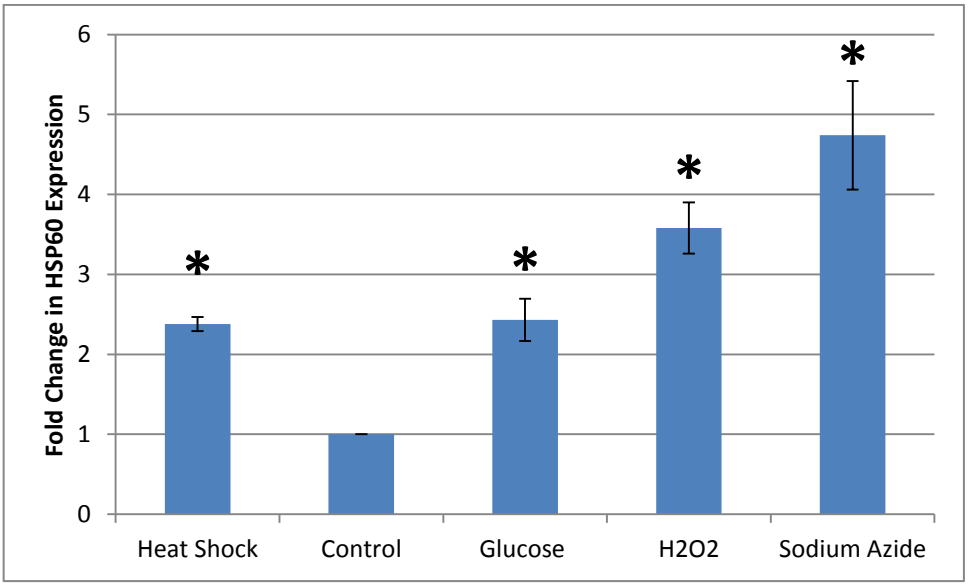

Figure 5.4- Relative HSP60 expression in cells treated with heat shock, glucose (100mM), H_2O_2 (200µM), and sodium azide (50µM) over 7 days. Bar graph showing the mean ± S.E.M. * = $p < 0.05$.

5.3.2 HSP70

After the HSP60 western blot, the PVDF membrane was stripped of the bound antibodies and was again blocked. A western blot for HSP70 was then carried out, and a single band for each sample was seen. The bands were then quantitated using the Gel Quant software, and the relative expression to the control was plotted.

HSP70 protein expression was also found to be upregulated in all treatments over 3 days. The heat shocked cells had a 2.50 fold increase in HSP70 expression, while the 100mM glucose, 200µM H_2O_2, and 50µM sodium azide had 1.85, 1.71 and 2.23 fold increases respectively. Each sample was significantly different from the control ($p < 0.05$).

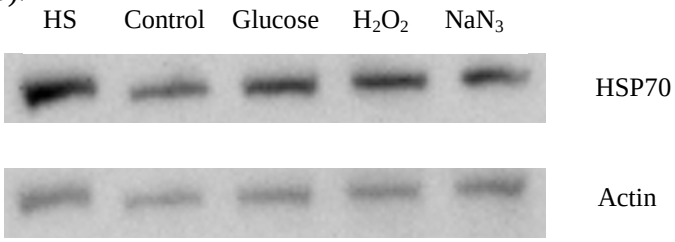

Figure 5.5- Western blots of HSP70 and actin in cells treated with heat shock, glucose (100mM), H_2O_2 (200µM), and sodium azide (50µM) over 3 days.

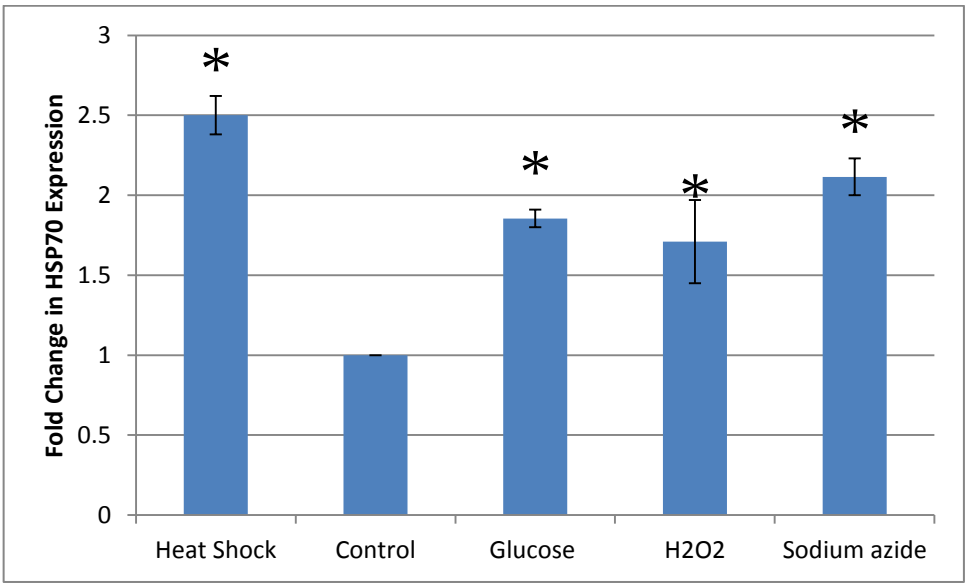

Figure 5.6- Relative HSP70 expression in cells treated with heat shock, glucose (100mM), H_2O_2 (200µM), and sodium azide (50µM) over 3 days. Bar graph showing the mean ± S.E.M. * = $p < 0.05$.

Additionally, HSP70 protein expression was found to be further upregulated in all treatments over a 7 day treatment period. The heat shocked cells had a 2.50 fold increase in HSP70 expression. The 100mM glucose, 200µM H_2O_2, and 50µM sodium azide had 2.75, 3.98 and 5.08 fold increases respectively, and each was found to be significantly different from the control ($p < 0.05$).

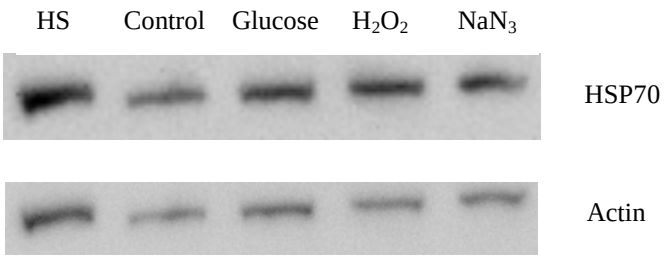

Figure 5.7- Western blots of HSP70 and actin in cells treated with heat shock, glucose (100mM), H_2O_2 (200µM), and sodium azide (50µM) over 7 days.

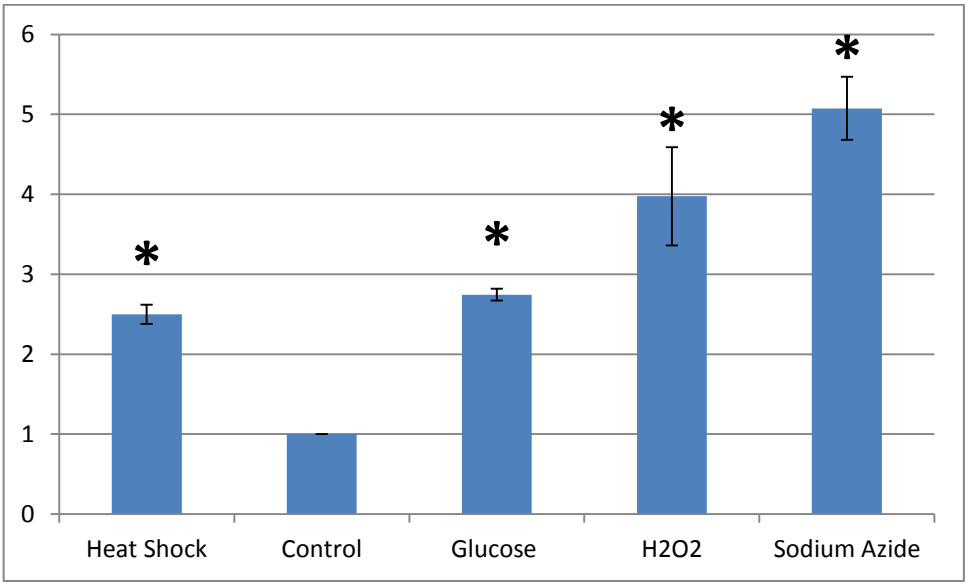

Figure 5.8- Relative HSP70 expression in cells treated with heat shock, glucose (100mM), H_2O_2 (200µM), and sodium azide (50µM) over 7 days. Bar graph showing the mean ± S.E.M. * = $p < 0.05$.

5.4 Discussion

In this section of the study, HSP60 and HSP70 protein expression was measured in HeLa cells treated with 100mM glucose, 200µM H_2O_2, and 50µM sodium azide for 3 and 7 days.

It is of interest that the protein levels of both HSP60 and HSP70 continued to increase under all treatment conditions from 3 to 7 days of treatment. This is clearly shown in **Figure 5.9** and **Figure 5.10**. As both HSP60 and HSP70 are upregulated under these conditions, it can be assumed that a number of stress responses are occurring, including a mitochondria specific response as well as a more general cellular response.

.

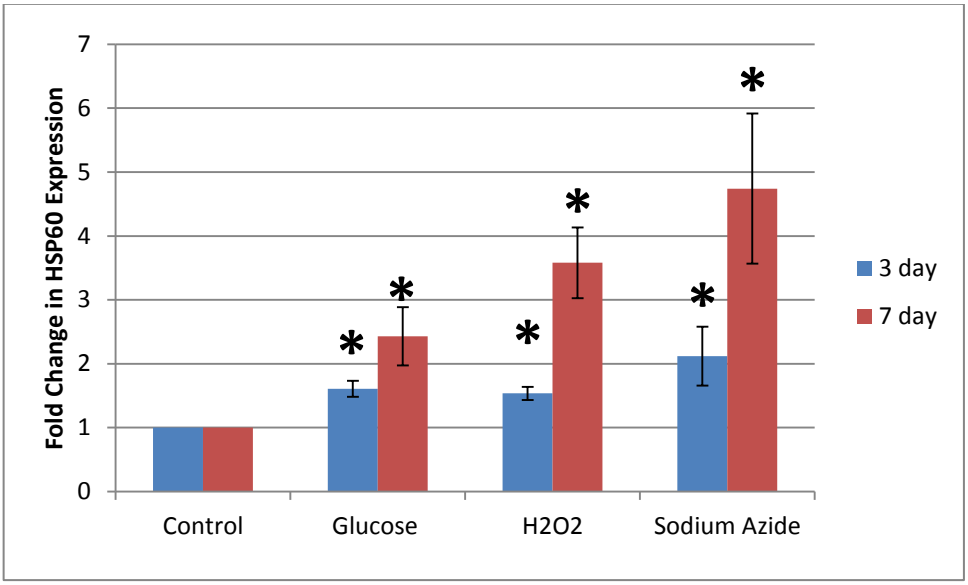

Figure 5.9- Relative HSP60 expression in cells treated with heat shock, glucose (100mM), H_2O_2 (200µM), and sodium azide (50µM) over both 3 and 7 days. Bar graph showing the mean ± S.E.M. * = $p < 0.05$.

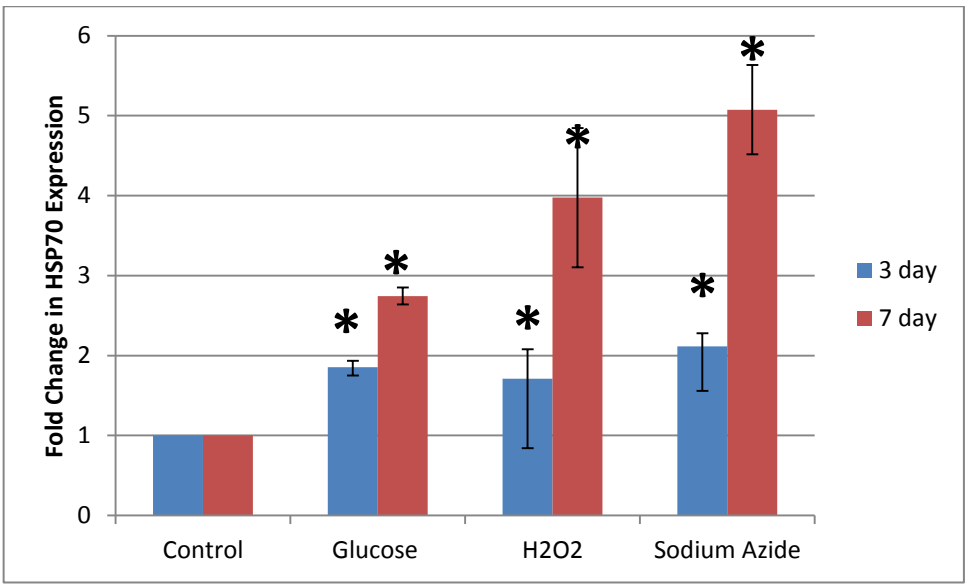

Figure 5.10- Relative HSP70 expression in cells treated with heat shock, glucose (100mM), H_2O_2 (200µM), and sodium azide (50µM) over both 3 and 7 days. Bar graph showing the mean ± S.E.M. * = $p < 0.05$.

As previously discussed in **Chapter 1.5**, HSP60 plays a critical role in the molecular cellular stress response targeted at the level of the mitochondrion. The primary role of HSPs is that of a molecular chaperone, where they act to mediate the folding, assembly or translocation across the intracellular membranes of other polypeptides; and a role in protein degradation, making up some of the essential components of the cytoplasmic ubiquitin-dependent degradative pathway (Burel et al., 1992). Additionally, when exposed to a various proteotoxic stressors, the expression of HSPs is induced in order to minimise cellular damage, as well as to stave off apoptosis, by stabilising compromised proteins.

Due to the universal and fundamental nature of the molecular stress response which culminates in HSP upregulation, compiling a complete list of stressors that do activate it is a difficult, expensive, and time consuming task. Known stressors include exposure to various cytotoxins, infection, inflammation, exercise, hypoxia, and water deprivation (Santoro, 2000).

The known stressor that particularly applies to this set of experiments is oxidative stress, as increased levels of intracellular ROS have been previously documented to have HSP inducing properties (Vayssier and Polla, 1998). As previously mentioned in C**hapter 1.5**, the inducible HSP component of a cell's total HSP

pool is regulated by HSFs, of which HSF-1 is the major regulator. In the absence of cellular stress, HSF-1 is inhibited due to its association with HSPs and is therefore maintained in an inactive state. If and when a cellular stress does occur, the HSPs bind to any misfolded proteins, and subsequently dissociate from HSF-1. This allows the HSF-1 monomers to oligomerise and form active trimers, regaining their DNA binding activity. The trimers undergo stress-induced serine phosphorylation and are translocated to the nucleus (Prahlad and Morimoto, 2008). Upon nuclear localisation, HSF-1 binds to the HSE situated upstream of heat shock responsive genes, which results in HSP gene transcription. However, the mechanisms for stress sensing and signalling to activate HSF-1 have not been fully elucidated. However, there is growing evidence in the literature that this mechanism is mediated by ROS, and in particular H_2O_2 (Ahn and Thiele, 2002).

H_2O_2 has been found to induce a concentration-dependent transactivation and DNA-binding activity of HSF-1, although to a lesser extent than that of the classical heat shock treatment (Jacquier-Sarlin and Polla, 1996). Sensing of the oxidative stress requires two cysteine residues within the HSF-1 DNA-binding domain that are engaged in redox-sensitive disulfide bonds. HSF-1 derivatives in which either or both of these cysteine residues are mutated have been found to be defective in stress-inducible trimerization and DNA binding, stress-inducible nuclear translocation and HSP gene trans-activation, and in the protection of mouse cells from stress-induced apoptosis (Ahn and Thiele, 2002). In this way, H_2O_2 exerts two effects on the activation and the DNA-binding activity of HSF; H_2O_2 favours the nuclear translocation of HSF, while also altering the HSFs DNA-binding activity, which is achieved by oxidizing the two critical cysteine residues within the DNA-binding domain (Jacquier-Sarlin and Polla, 1996).

It would appear, based on the results from **Chapters 4 and 5** and the evidence in the literature, that the HSP60 and HSP70 upregulation resulting from treatment of HeLa cells with high glucose, H_2O_2, and sodium azide is the result of an increase in intracellular ROS activity. That is to say that it appears the degree of oxidative stress induced by the treatment is proportional to the degree of HSP induction. This is shown in **Figure 5.11**.

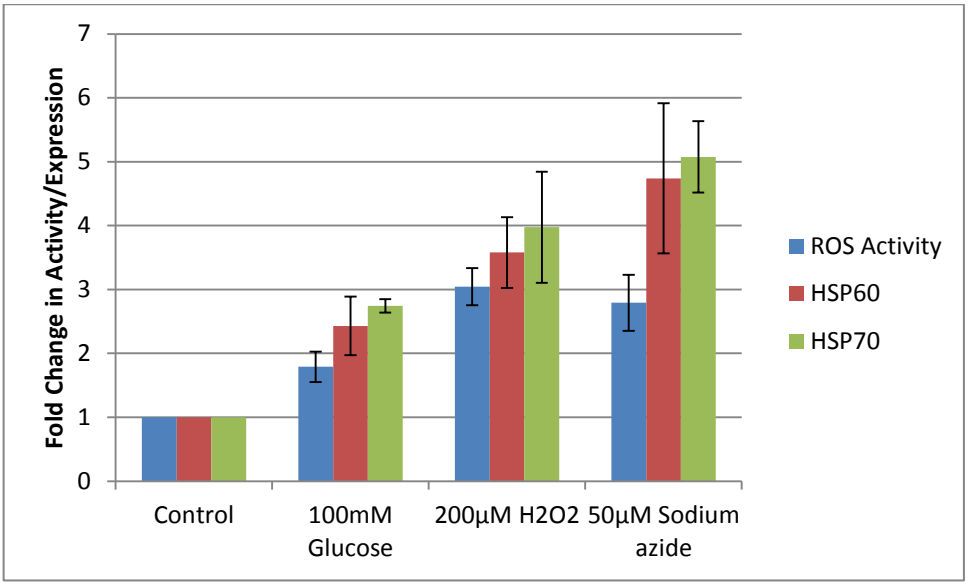

Figure 5.11- Relative ROS activity, HSP60 expression, and HSP70 expression in cells treated with glucose (100mM), H_2O_2 (200µM), and sodium azide (50µM) over 7 days. Bar graph showing the mean ± S.E.M. * = $p < 0.05$.

After 7 days of treatment with 100mM glucose the intracellular ROS activity had increased by 178.95%, the HSP60 expression had experienced a 2.43 fold increase, and the HSP70 a 2.75 fold increase. As discussed in **Chapter 4**, hyperglycaemia has been reported to increase oxidative stress by increasing the rate of glycolysis while inhibiting oxidative phosphorylation (Crabtree, 1928). The build-up, and subsequent auto-oxidation, of glyceraldehyde-6-phosphate which ensues from increased glycolysis results in the generation of H_2O_2. As a result, the mitochondrion experiences an increase in ROS generation. As mentioned earlier in this chapter, activation of HSF-1, the major regulator of HSPs, is redox dependent. Thus, the induction of HSP60 and 70 expression may be explained by the increased oxidative stress that the 100mM glucose treatment resulted in.

After 7 days of treatment with 200µM H_2O_2 the intracellular ROS activity had increased by 304.56%, the HSP60 expression had experienced a 3.48 fold increase,

and the HSP70 a 3.98 fold increase. While the results of the DCFDA assay from **Chapter 4** reflects the ROS that has been truly generated from within the cell for the high glucose and sodium azide treatments, for the H_2O_2 treatment it is not so clear cut seeing as H_2O_2 is a ROS in itself. Therefore, the ROS levels of H_2O_2 treated HeLa cells, as measured by the DCFDA assay, represents a combination of residual H_2O_2 that escaped the wash protocol and ROS generated due to oxidative stress. As a result, the induction of HSP expression is not as pronounced as one may have predicted, which indicates that it is perhaps ROS generated from within the cell by the mitochondria as a result of the simulated oxidative that has the most significant effect on HSF-1 activation and therefore HSP induction.

After 7 days of treatment with 50μM sodium azide the intracellular ROS activity had increased by 279.13%, the HSP60 expression had experienced a 4.74 fold increase, and the HSP70 a 5.08 fold increase. Unlike the other two treatments, sodium azide actively inhibits the mitochondrial electron transport system by binding irreversibly to the heme group of complex IV. Not only does this result in inefficient reduction of molecular oxygen by the electron transport chain resulting in increased ROS generation like the other two treatments, but it also prevents ATP generation by preventing the maintenance of the hydrogen ion gradient across the inner mitochondrial membrane. This may help to explain why treatment with sodium azide resulted in a greater induction of HSP60 and HSP70 expression.

6 Final Summary and Future Directions

This study looked at several aspects of high glucose, H_2O_2, and sodium azide treatment on human HeLa cells. At low levels each treatment had a hormetic effect on HeLa cell growth; however at high concentrations growth was significantly inhibited. Additionally, high treatment concentrations resulted cell lysis as determined by the LDH assay. The 100mM glucose, 200μM H_2O_2, and 50μM sodium azide treatments were the only treatment concentrations that did not result in significantly different levels of cell lysis when compared to a control sample. On the other hand, the 125mM glucose, 250μM H_2O_2, and 100μM sodium azide treatments were the only treatment concentrations that resulted in significantly increased levels of cell lysis when compared to a control sample. Mitochondrial dehydrogenase activity was also found to be significantly decreased at high treatment concentrations. Thus, the 100mM glucose, 200μM H_2O_2, and 50μM sodium azide treatments were identified as optimal conditions for mitochondria targeted cell stress as each of these treatments impaired cell growth and inhibited mitochondrial while having not significantly increasing the degree of cell lysis.

The 100mM glucose, 200μM H_2O_2, and 50μM sodium azide treatments were then investigated for the intracellular ROS activity they culminated in over treatment periods of 24 hours, 3 and 7 days. After 7 days of treatment, the 200μM H_2O_2 and 50μM sodium azide treatments resulted in approximately 3 times greater ROS activity, while the 100mM glucose treatment resulted in almost twice as much ROS.

Finally, the effects of 100mM glucose, 200μM H_2O_2, and 50μM sodium azide treatments on HSP60 and 70 expression was also examined over 3 and 7 day time periods. After the 7 day treatment period, the 100mM glucose treatment had induced a 2.43 fold increase in HSP60 expression and a 2.75 fold increase in HSP70 expression, the 200μM H_2O_2 induced a 3.48 fold increase in HSP60 expression and a 3.98 HSP70 expression, and finally the 50μM sodium azide induced a 4.74 fold increase in HSP60 expression and a 5.08 fold increase in HSP70 expression.

As a result, this study has come close to achieving the development of a model to study HSP60 expression in human cells under conditions of mitochondrial

impairment. Three different treatments have been optimised to result in mitochondria specific cell stress, but not necrotic cytotoxicity, of human HeLa cells. However, these treatments also result in the induction of both HSP60 and HSP70 expression. This indicates that while there is a mitochondria specific stress response occurring, there is also a general cellular stress response taking place too. Therefore, the treatment protocols must still be modified to achieve a strictly mitochondria specific stress response. Once this has been achieved, treatments can be further exploited to study the downstream mechanisms and effects of HSP60, particularly pertaining to its extracellular expression.

The results of this study agree with the literature, that increased intracellular ROS activity in cells with compromised mitochondria activates a HSP response. This has implications for T2D and obesity in particular, as increased levels of circulating HSP60 has been documented in individuals diagnosed with these metabolic diseases (Märker *et al*, 2012; Shamaei-Tousi *et al*, 2006). This study indicates that the hyperglycaemia and elevated oxidative stress, which are both associated with these diseases, are both possible stressors that lead to the observed increased extracellular HSP expression. This is of particular interest as HSP60 has been linked to the development of atherosclerosis, and patients of T2D and obesity are predisposed to developing CVDs. HSP60 may therefore represent the molecular link between the two.

As mentioned in **Chapter 5**, seeing as these treatments result in the activation of multiple stress responses, it would be of interest to investigate if any early apoptotic signalling is occurring. Such developments towards a commitment to apoptosis could be determined in a number of ways, such as a cytochrome c assay. Cytochrome c is an appropriate way of measuring apoptosis as it is usually strictly located in the mitochondria. However, when a cell is entering apoptosis cytochrome c is leaked into the cytoplasm through the Bax protein channels that insert into the outer mitochondrial membrane upon stress detection (Guo *et al*, 2002).

It would also be of benefit to run additional long term treatments for the HSP western blots, say 14 and 21 days, to give a better indication of chronic exposure to such conditions, as is the case in metabolic conditions like T2D and obesity.

Along with new time periods, new treatments should also be investigated. It would be of particular interest to target mitochondrial impairment at different sites of inhibition. Such points may include mitochondrial protein synthesis, using azidothymadine (AZT), mitochondrial DNA replication, using ethidium bromide, and other components of the electron transport chain, using rotenone. Furthermore, it may be of interest to look at mitochondrial redox-rescue strategies aimed at maintaining treated cells with impaired mitochondrial capacity.

Extracellular HSP60 has been implicated in having deleterious immunogenic effects, as previously discussed in **Chapter 1.5**. In particular, HSP60 has been purported to promote the CVD development in T2D and obesity. Therefore, it would be of interest to determine if the increased expression of HSPs intracellularly with treatments of 100mM glucose, 200μM H_2O_2, and 50μM sodium azide is matched with an increase of HSPs in the media. It would also be of interest to look at any change as to the surface expression of HSP60 with these treatments using confocal microscopy. There is also little known as to the translocation and secretory mechanisms of HSP60 which confocal microscopy could also be used to address.

It would also be of benefit to see how universal the effects of these treatments are across various human cell lines. Due to the suspected role HSP60 plays in atherosclerotic development, it would be of particular interest to investigate this in human monocytes, such as the human acute monocytic leukaemia THP-1 cell line. If it is indeed a universal effect and THP-1 cells are found to upregulate HSP60 expression in response to high glucose, H_2O_2, and sodium azide, an exciting experiment to conduct would be that of a co-culture. The experiment would involve co-culturing THP-1s, stressed with these various stressors, with an endothelial cell line, such as HUVECs, in a biochip capable of simulating the shear stress present in human blood vessels. By monitoring the HUVECs for the induction of pro-inflammatory factors, such as TNF-α, as well as atherosclerotic plaque formation, it can be observed whether the exposure of monocytes, which have been stressed to induce HSP60 expression, to HUVECs culminates in atherosclerotic development. If this too is found to be positive, characterising the receptor/s that HSP60 binds to and the signal transduction pathway that responds to receptor binding to illicit a pro-inflammatory response could be of immense importance in the development of treating and preventing the development of

CVDs in at risk individuals, particularly individuals diagnosed with T2D and obesity.

References

Aguilar-Zavala, H., Garay-Sevilla, M.E., Malacara, J.M. and Perez-Luque, E.L. (2008), Stress, Inflammatory Markers And Factors Associated In Patients With Type 2 Diabetes Mellitus. *Stress and Health* , 24(1):49-54.

Ahn, S.G. and Thiele, D.J. (2002), Redox Regulation Of Mammalian Heat Shock Factor 1 Is Essential For Hsp Gene Activation And Protection From Stress. *Genes and Development*, 17:516-528.

American Type Culture Collection. (2007), Passage Number Effects In Cell Lines. ATCC Technical Bulletin no. 7.

Akira, S., Takeda, K. and Kaisho, T. (2001), Toll-like Receptors: Critical Proteins Linking Innate And Acquired Immunity. *Nature Immunology*, 2(8):675-680.

Alard, J.E., Dueymes, M., Mageed, R.A., Saraux, A., Youinou, P. and Jamin, C. (2009), Mitochondrial Heat Shock Protein (HSP) 70 Synergizes With HSP60 In Transducing Endothelial Cell Apoptosis Induced By Anti-HSP60 Autoantibody. *Faseb Journal*, 23(8):2772-2779.

Allen, D.A., Yaqoob, M.M. and Harwood, S.M. (2005), Mechanisms Of High Glucose-Induced Apoptosis And Its Relationship To Diabetic Complications. *The Journal of Nutritional Biochemistry*, 16(12):705-713.

Bailey, C.J. (2008), Metformin: Effects On Micro And Macrovascular Complications In Type 2 Diabetes. *Cardiovascular drugs and Therapy*, 22(3):215-224.

Bangen, J.M., Schade, F.U. and Flohe, S.B. (2007), Diverse Regulatory Activity Of Human Heat Shock Proteins 60 And 70 On Endotoxin-Induced Inflammation. *Biochemical and Biophysical Research Communications*, 359(3):709-715.

Bausinger, H., Lipsker, D., Ziylan, U., Manie, S., Briand, J.P., Cazenave, J.P., Muller, S., Haeuw, J.F., Ravanat, C., de la Salle, H. and Hanau, D. (2002), Endotoxin-Free Heat-Shock Protein 70 Fails To Induce APC Activation. *European Journal of Immunology*, 32(12):3708-3713.

Beekhuizen, H. and van Furth, R. (1993), Monocyte Adherence To Human Vascular Endothelium. *Journal of Leukocyte Biology*, 54:363-378.

Beere, H.M., Wolf, B.B., Cain, K., Mosser, D.D., Mahboubi,A., Kuwana, T., Tailor, P., Morimoto, R.I., Cohen, G.M. and Green, D.R. (2000), Heat-Shock Protein 70 Inhibits Apoptosis By Preventing Recruitment Of Procaspase-9 To The Apaf-1 Apoptosome. *Nature Cell Biology*, 2(8):469-475.

Berridge, M.V., Herst, P.M. and Tan, A.S. (2005), Tetrazolium Dyes As Tools In Cell Biology: New Insight Into Their Cellular Reduction. *Biotechnology Annual Review*, 11(11):127-152.

Binder, R.J., Vatner, R. and Srivastava, P. (2004), The Heat-Shock Protein Receptors: Some Answers And More Questions. *Tissue* Antigens, 64(4):442-451.

Bjorbaek, C. and Kahn, B.B. (2004), Leptin Signaling In The Central Nervous System And The Periphery. *Recent Progress in Hormone Research*, 59:305-331.

Bray, A.G. (1985), Complications Of Obesity. *Annals of Internal Medicine*, 103(6):1052-1062.

Bray, A.G. (1999), Etiology And Pathogenesis Of Obesity. *Clinical Cornerstone*, 2(3):1-15.

Brownlee, M. (2001), Biochemistry And Molecular Cell Biology Of Diabetic Complications. *Nature,* 414(6865): 813-820.

Burdon, R.H. (1995), Superoxide And Hydrogen Peroxide In Relation To Mammalian Cell Proliferation. *Free Radical Biology and Medicine*, 18(4):775-794.

Burel, C., Mezger, V., Pinto, M., Rallu, M., Trigon, S. and Morange, M. (1992), Mammalian Heat Shock Protein Families. Expression And Functions. *Cellular and Molecular Life Sciences*, 48(7):629-634.

Burnet, F.M. (1959), The Clonal Selection Theory Of Acquired Immunity. *Vanderbilt University Press*, Nashville.

Calabrese, E.J., Iavicoli, I. and Calabrese, V. (2012), Hormesis: Its Impact On Health And Medicine. *Human and ExperimentalToxicology*, electronically published ahead of print.

Capes-Davis, A., Theodosopoulos, G., Atkin, I., Drexler, H.G., Kohara, A., MacLeod, R.A., Masters, J.R., Nakamura,Y., Reid, Y.A., Reddel, R.R. and Freshney, R.I. (2010), Check Your Cultures! A List Of Cross-Contaminated Or Misidentified Cell Lines. *International Journal of Cancer*, 127(1):1-8.

Ceriello, A., dello Russo, P., Amstad, P. and Cerutti, P. (1996), High Glucose Induces Antioxidant Enzymes in Human Endothelial Cells in Culture: Evidence Linking Hyperglycemia and Oxidative Stress. *Diabetes*, 45(4):471-477.

Chang, S. and Lamm, S.H. (2003), Human Health Effects Of Sodium Azide Exposure: A Literature Review And Analysis. *International Journal of Toxicology*, 22:175-186.

Chanseaume, E. and Morio, B. (2009), Potential Mechanisms Of Muscle Mitochondrial Dysfunction In Aging And Obesity And Cellular Consequences. *International Journal of Molecular Sciences*, 10:306-324.

Chen, Q. and Ames, B. N. (1994), Senescence-Like Growth Arrest Induced By Hydrogen Peroxide In Human Diploid Fibroblast F65 Cells. *Proceedings of the National Academy of Sciences*, 91(10):4130-4134.

Chen, W., Syldath, U., Bellmann, K., Burkart, V. And Kolb, H. (1999), Human 60-kDa Heat-Shock Protien: A Danger Signal To The Innate Immune System. *The Journal of Immunology*, 162:3212-3219.

Cheng, M.Y., Hartl, F.U. and Horwich, A.L. (1990), The Mitochondrial Chaperonin HSP60 Is Required For Its Own Assembly. *Nature*, 348:455-458.

Cicconi, R., Delphino, A., Piselli, P., Castelli, M. and Vismara, D. (2004), Expression Of 60 kDa Heat Shock Protein (HSP60) On Plasma Membrane Of Daudi Cells. *Molecular and Cellular Biochemistry*, 259(1-2):1-7.

Decker, T., and Lohmann-Matthes, ML., (1988), A Quick And Simple Method For The Quantitation Of Lactate Dehydrogenase Release In Measurements Of Cellular Cytotoxicity And Tumor Necrosis Factor (TNF) Activity. *Journal of Immunological Methods*, 15(1):61-69.

Eckel, R.H., Kahn, S.E., Ferrannini, E., Goldfine, A.B., Nathan, D.M., Shwartz, M.W., Smith, R.J. and Smith, S.R. (2011), Obesity And Type 2 Diabetes: What Can Be Unified And What Needs To Be Individualised? *The Journal of Clinical Endocrinology and Metabolism*, 96(6):1654-1663.

Ezzati, M., Vander Hoorn, S., Lawes, C.M.M., Leach R. and James W.P.T. (2005), Rethinking The "Diseases Of Affluence" Paradigm: Global Patterns Of Nutritional Risks In Relation To Economic Development. *PLoS Med*, 2(5):e133.

Fabian, T.K., Gaspar, J., Fejerdy, L., Kaan, B., Balint, M., Csermely, P. and Fejerdy, P. (2004), HSP70 Is Present In Human Saliva. *Medical Science Monitor*, 9(1):BR62-65.

Fenton, W.A., Kashi, Y., Furtak, K. and Horwich, A.L. (1994), Residues In Chaperonin GroEL Required For Polypeptide Binding And Release. *Nature*, 371(6498):614-619.

Flier, J.S. (2004), Obesity Wars: Molecular Progress Confronts An Expanding Epidemic. *Cell*, 116:317-350.

Flaherty, K.M., DeLuca-Flaherty, C. and McKay, D.B. (1990), Three-Dimensional Structure Of The ATPase Fragment Of A 70K Heat-Shock Cognate Protein. *Nature*, 346(6285):623-628.

Furukawa, S., Fujita, T., Shimabukuro, M., Iwaki, M., Yamada, Y., Nakajima, Y., Nakayama, O., Makishima, M., Matsuda, M. and Shimomura, I. (2004), Increased Oxidative Stress In Obesity And Its Impact On Metabolic Syndrome. *The Journal of Clinical Investigation*, 114(12): 1752-1761.

Gao, B. and Tsan, M.F. (2003), Endotoxin Contamination In Recombinant Human Heat Shock Protein 70 (HSP70) Preparation Is Responsible For The Induction Of Tumor Necrosis Factor Alpha Release By Murine Macrophages. *The Journal of Biological Chemistry*, 278(1):14-179.

Gao, B.C., and Tsan, M.F. (2003), Recombinant Human Heat Shock Protein 60 Does Not Induce The Release Of Tumor Necrosis Factor Alpha From Murine Macrophages. *The Journal of Biological Chemistry*, 278(25):22523-22529.

Gavrieli, Y., Sherman, Y. and Ben-Sasson, S.A. (1992), Identification Of Programmed Cell Death In Situ Via Specific Labeling Of Nuclear DNA Fragmentation. *The Journal of Cell Biology*, 119(3):493-501.

Giacco, F. and Brownlee, M. (2010), Oxidative Stress And Diabetic Complications. *Circulation Research*, 107:1058-1070.

Girard, J. (1997), Is Leptin The Link Between Obesity And Insulin Resistance? *Diabetes and Metabolism*, 3:16-24.

Grundtman, C. and Wick, G. (2011), The Autoimmune Concept Of Atherosclerosis. *Current Opinion in Lipidology*, 22:327-334.

Grundtman, C., Kreutmayer, S.B., Almanzar, G., Wick, M.C. and Wick, G. (2011), Heat Shock Protein 60 And Immune Inflammatory Responses In Atherosclerosis. *Arteriosclerosis, Thrombosis, and Vascular Biology*, 31:960-968.

Guertin, M.J. and Lis, J.T. (2010), Chromatin Landscape Dictates HSF Binding To Target DNA Elements. *PLoS Genetics*, 6(9).

Guertin, M.J., Petesch, Z.J., Zobeck, K.L., Min, I.M. and Lis, J.T. (2010), Drosophila Heat Shock System As A General Model To Investigate Transcriptional Regulation. *Cold Spring Harbor Symposia on Quantitative Biology*, 75:1-9.

Guo, Y., Srinivasula, S.M., Druilhe, A., Fernandes-Alnemri, T. and Alnemri, E.S. (2002), Caspase-2 Induces Apoptosis By Releasing Proapoptotic Proteins From Mitochondria. *The Journal of Biological Chemistry*, 277:13430-13437.

Gupta, R.S. (1995), Evolution Of The Chaperonin Families (HSP60, HSP10 and TCP-1) Of Proteins And The Origin Of Eukaryotic Cells. *Molecular Microbiology*, 15(1):1-11.

Gupta, S. and Knowlton, A.A. (2006), Exosome Dependent HSP60 Secretion In Rat Cardiac Myocytes. *Journal of Molecular and Cellular Cardiology*, 40(6):875-876.

Habich, C., Baumgart, K, Kolb, V. And Burkart, V. (2002), The Receptor For Heat Shock Protein 60 On Macrophages Is Saturable, Specific, And Distinct From Receptors For Other Heat Shock Proteins. *The Journal of Immunology*, 168:569-576.

Habich, C., Kempe, K., van der Zee, R., Burkart, V. and Kolb, H. (2003), Different Heat Shock Protein 60 Species Share Pro-Inflammatory Activity But Not Binding Sites On Macrophages. *FEBS Letters*, 533(1-3):105-109.

Habich, C., Kempe, K., van der Zee, R., Rumenapf, R., Akiyama, H., Kolb, H. and Burkart, V. (2005), Heat Shock Protein 60: Specific Binding Of Lipopolysaccharide. *Journal of Immunology*, 174(1):875-876.

Habich, C. and Burkart, V. (2007), Heat Shock Protein 60: Regulatory Role On Innate Immune Cells. *Cellular and Molecular Life Sciences*, 64(6):742-51.

Halliwell, B., Clement, M.V. and Lonh, L.H. (2000), Hydrogen Peroxide In The Human Body. *Federation of European Biochemical Societies Letters*, 486(1)10-13.

Han, D., Williams, E. and Cadenas, E. (2001), Mitochondrial Respiratory Chain-Dependent Generation Of Superoxide Anion And Its Release Into The Intermembrane Space. *Biochemical Journal*, 353(2):411-416.

Henderson, B. and Mesher, J. (2007), The Search For The Chaperonin 60 Receptors. *Methods*, 43(3):223-228.

Hochleitner, B.W., Hochleitner, E.O., Obrist, P., Eberl, T., Amberger, A., Xu, Q.B., Margreiter, R. and Wick, G. (2000), Fluid Shear Stress Induces Heat Shock Protein 60 Expression In Endothelial Cells In Vitro And In Vivo. *Arteriosclerosis, Thrombosis and Vascular Biology*, 20(3):617-623.

Jacquier-Sarlin, M.R. and Polla, B.S. (1996), Dual Regulation Of Heat-Shock Transcription Factor (HSF) Activation And DNA Binding Activity By H_2O_2 : Role Of Thioredoxin. *Biochemical Journal*, 318:187-193.

Janeway, C.A. (1992), The Immune System Evolved To Discriminate Infectious Nonself From Non-Infectious Self. *Immunology Today*, 13(1):11-16.

Jensen, M.D. (2006), Adipose Tissue As An Endocrine Organ: Implications Of Its Distribution On Free Fatty Acid Metabolism. *European Heart Journal Supplements*, 8:B13-B19.

Kaal, E.C.A., Vlug, A.S., Versleijen, M.W.V., Kuilman, M., Joosten, E.A.J and Dop Bär, P.R. (2000), Chronic Mitochondrial Inhibition Induces Selective Motoneuron Death In Vitro: A New Model For Amyotrophic Lateral Sclerosis. *Journal of Neurochemistry*, 74:1158-1165.

Kim, J., Yongzhong, W. and Sowers, J.R. (2008), Role Of Mitochondrial Dysfunction In Insulin Resistance. *Circulation Research*, 102:401-414.

Kissebah, A.H., Vydelingum, N., Murray, R., Evans, D.J., Kalkhoff, R.K. and Adams, P.W. (1982), Relation Of Body Fat Distribution To Metabolic Comlications Of Obesity. *The Journal of Clinical Endocrinology and Metabolism*, 54(2):254-260.

Kershaw, E.E., and Flier, J.S. (2004), Adipose Tissue As An Endocrine Organ. *The Journal of Clinical Endocrinology and Metabolism*, 89(6):2548-2556.

Kol, A., Lichtman, A.H., Finberg, R.W., Libby, P. and Kurt-Jones, E.A. (2000), Cutting Edge: Heat Shock Protein (HSP) 60 Activates The Innate Immune Response: CD14 Is An Essential Receptor For Hsp60 Activation Of Mononuclear Cells. *Journal of Immunology*, 164(1):13-17.

Laclaustra, M., Corella, D. and Ordovas, J.M. (2007), Metabolic Syndrome Pathophysiology: The Role Of Adipose Tissue. *Nutrition, Metabolism and Cardiovascular Diseases*, 17:125-139.

Lao, M. and Toth, D. (2008), Effects Of Ammonium And Lactate On Growth And Metabolism Of A Recombinant Chinese Hamster Ovary Cell Culture. *Biotechnology Progress*, 13(5):688-691.

Levy-Rimler, G., Viitanen, P., Weiss, C., Sharkia, R., Greenberg, A., Niv, A., Lustig, A., Delarea, Y. and Azem A. (2001), The Effect Of Nucleotides And Mitochondrial Chaperonin 10 On The Structure And Chaperone

Activity Of Mitochondrial Chaperonin 60. *European Journal of Biochemistry*, 268(12):3465-3472.

Liao, D.F., Jin, Z.G., Baas, A.S., Daum, G., Gygi, S.P., Aebersold, R. and Berk, B.C. (2000), Purification And Identification Of Secreted Oxidative Stress-Induced Factors From Vascular Smooth Muscle Cells. *Journal of Biological Chemistry*, 275(1):189-196.

Libby, P. (2002), Inflammation In Atherosclerosis. *Nature*, 420(6917):868-874.

Llorca, O., Martin-Benito, J., Ritco-Vonsovici, M., Grantham, J., Hynes, G.M., Willison, K.R., Carrascosa, J.L. and Valpuesta, J.M. (2000), Eukaryotic Chaperonin cct Stabilizes Actin And Tubulin Folding Intermediates In Open Quasi-Native Conformations. *EMBO Journal*, 19(22): 5971-5979.

Lowell B.B. and Shulman G.I. (2005), Mitochondrial Dysfunction And Type 2 Diabetes. *Science*, 307(5708): 384-387.

Ludewig, B. and Laman, J.D. (2004), The In And Out Of Monocytes In Atherosclerotic Plaques: Balancing Inflammation Through Migration. *Proceedings of the National Academy of Sciences of the United States of America*, 101(32):11529-11530.

Märker, T., Sell, H., Zilleßen., P, Glöde, A., Kriebel, J., Ouwens, D.M., Pattyn, P., Ruige, J., Famulla, S., Roden, M., Eckel, J. and Habich, C. (2012), Heat Shock Protein 60 As A Mediator Of Adipose Tissue Inflammation And Insulin Resistance. *Diabetes*, 61(3):615-625.

Marshall, N.J., Goodwin, C.J. and Holt, S.J. (1995), A Critical-Assessment Of The Use Of Microculture Tetrazolium Assays To Measure Cell-Growth And Function. *Growth Regulation*, 5(2):69-84.

Martinus, R.D., Garth, G.P., Webster, T.L., Cartwright, P., Naylor, D.J., Hoj, P.B. and Hoogenraad, N.J. (1996), Selective induction Of Mitochondrial Chaperones In Response To Loss Of The Mitochondrial Genome. *European Journal of Biochemistry*, 240:98-103.

Maslin, C.L., Kedzierska, K., Webster, N.L., Muller, W.A. and Crowe S.M. (2005), Transendothelial Migration Of Monocytes: The Underlying

Molecular Mechanisms And Consequences Of Hiv-1 Infection. *Current HIV Research*, 3(4):303-317.

Mather, A., Chen, X.M., McGinn, S., Field, M.J., Sumual, S., Mangiafico, S., Zhang, Y., Kelly, D.J. and Pollock, C.A. (2009), High Glucose Induced Endothelial Cell Growth Inhibition Is Associated With An Increase In TGFbeta1 Secretion And Inhibition Of Ras Prenylation Via Suppression Of The Mevalonate Pathway. *The International Journal of Biochemistry and Cell Biology*, 41(3):561-569.

Matzinger, P. (1998), An Innate Sense Of Danger. *Seminars in Immunology*, 10(5):399-415.

Merendino, A.M., Bucchieri, F., Campanella, C., Marciano, V., Ribbene, A., David, S., Zummo, G., Burgio, G., Corona, D.F.V., Conway de Macario, E., Macario, A.J.L. and Capello, F. (2010), HSP60 Is Actively Secreted By Human Tumor Cells. *PLoS One*, 5(2):e9247.

Ministry of Health. (2004). Tracking The Obesity Epidemic, New Zealand 1977-2003: Public Health Intelligence Occasional Bulletin No. 24. Wellington: Ministry of Health.

Ministry of Health. (2007), Diabetes Surveillance: Population-Based Estimates And Projections For New Zealand, 2001–2011: Public Health Intelligence Occasional Bulletin No. 46. Wellington: Ministry of Health.

Ministry of Health. (2008), Diabetes and Cardiovascular Disease Quality Improvement Plan. Wellington: Ministry of Health.

Ministry of Health. (2011), Targeting Diabetes and Cardiovascular Disease: Better Diabetes and Cardiovascular Services. Wellington: Ministry of Health.

Morimoto, R.I. (1993), Cells In Stress: Transcriptional Activation Of Heat Shock Genes. *Science*, 259(5100):1409-1410.

Mulder, H. and Ling, C. (2009), Mitochondrial Dysfunction In Pancreatic β-cells In Type 2 Diabetes. *Molecular and Cellular Endocrinology*, 297:34-40.

Nakamura, J., Purvis, E.R. and Swenberg, J.A. (2003), Micromolar Concentrations Of Hydrogen Peroxide Induce Oxidative DNA Lesions More Effectively Than Millimolar Concentrations In Mammalian Cells. *Nucleic Acids Research*, 31(6):1790-1795.

Newman, G. and Crooke., E. (2000), Dnaa, The Initiator Of *Escherichia coli* Chromosomal Replication, Is Located At The Cell Membrane. *Journal of Bacteriology*, 182(9):2604-2610.

Nishikawa, M., Takemoto, S. and Takakura, Y. (2008), Heat Shock Protein Derivatives For Delivery Of Antigens To Antigen Presenting Cells. *International Journal of Pharmacology*, 354(1-2):23-27.

Osterloh, A., Meier-Steigen, F., Veit, A., Fleischer, B., von Bonin, A. and Breloer, M. (2004), Lipopolysaccharide Free Heat Shock Protein 60 Activates T Cells. *Journal of Biological Chemistry*, 279(46):47906-47911.

Osterloh, A., Kalinke, U., Weiss, S., Fleischer, B. and Breloer, M. (2007), Synergistic And Differential Modulation Of Immune Responses By HSP60 And Lipopolysaccharide. *Journal of Biological Chemistry*, 282(7):4669-4680.

Osterloh, A. and Breloer, M. (2008), Heat Shock Proteins: Linking Danger And Pathogen Recognition. *Medical Microbiology and Immunology*, 197(1):1-8.

Passlick, B., Flieger, D. and Zieglerheitbrock, H.W.L. (1989), Identification And Characterization Of A Novel Monocyte Subpopulation In Human Peripheral-Blood. *Blood*, 74(7):2527-2534.

Peiro, C., Lafuente, N., Matesanz, N., Cercas, E., Llergo, J.L., Vallejo, S., Rodriguez-Mañas, L. and Sanchez-Ferrer, C.F. (2001), High Glucose Induces Cell Death Of Cultured Human Aortic Smooth Muscle Cells Through The Formation Of Hydrogen Peroxide. *British Journal of Pharmacology*, 133(7):967-974.

Peterson, M. (2003), Economic Costs Of Diabetes In The US In 2002. *Diabetes Care*, 26(3):917-932.

Pfister, G., Stroh, C.M., Pershinka, H., Kind, M., Knoflach, M., Hinterdorfer, P. and Wick, G. (2005), Detection Of HSP60 On The Membrane Surface Of Stressed Human Endothelial Cells By Atomic Force And Confocal Microscopy. *Journal of Cell Science*, 118:1587-1594.

Pirkkala, L., Nykanen, P. and Sistonen, L. (2001), Roles Of The Heat Shock Transcription Factors In Regulation Of The Heat Shock Response And Beyond. *FASEB Journal*, 15(7): 1118-1131.

Pockley, A.G., Bulmer, J., Hanks, B.M. and Wright B.H. (1999), Identification Of Human Heat Shock Protein 60 (HSP60) And Anti-HSP60 Antibodies In The Peripheral Circulation Of Normal Individuals. *Cell Stress Chaperones*, 4(1):29-35.

Pockley, A.G., Wu, R., Lemne, C., Kiessling, R., de Faire, U. and Frostegard, J. (2000), Circulating Heat Shock Protein 60 Is Associated With Early Cardiovascular Disease. *Hypertension*, 36(2):303-307.

Pockley, A.G. (2002), Heat Shock Proteins, Inflammation, And Cardiovascular Disease. *Circulation*, 105(8):1012-1017.

Pockley, A.G. (2003), Heat Shock Proteins As Regulators Of The Immune Response. *Lancet*, 362(9382): 469-476.

Pockley, A.G., Georgiades, A., Thulin, T, de Faire, U. and Frostegard, J. (2003), Serum Heat Shock Protein 70 Levels Predict The Development Of Atherosclerosis In Subjects With Established Hypertension. *Hypertension*, 4:235-238.

Prahlad, V. and Morimoto, R.I. (2008), Integrating The Stress Response: Lessons For Neurodegenerative Diseases From *C. elegans. Trends in Cell Biology*, 19(2):52-61.

Quillet-Mary, A., Jaffrezou, J.P., Mansat, V., Bordier, C., Naval, J. and Laurent, G. (1997), Implication Of Mitochondrial Hydrogen Peroxide Generation In Ceramide-Induced Apoptosis. *The Journal of Biological Chemistry*, 272(34)21388-21395.

Radak, Z., Chung, H.Y., Koltai, E., Taylor, A.W. and Goto, S. (2008), Exercise, Oxidative Stress And Hormesis. *Ageing Research Reviews*, 7:34-42.

Ranford, J.C., Coates, A.R.M. and Henderson, B. (2000), Chaperonins Are Cell-Signalling Proteins: The Unfolding Biology Of Molecular Chaperones. *Expert Reviews in Molecular Medicine*, 2:1-17.

Ritossa, F.M. (1996), Discovery Of The Heat Shock Response. *Cell Stress and Chaperones*, 1(2):97-98.

Robertson, R.P., Harmon, J., Tran, P.O., Tanaka, Y. and Takahashi, H. (2003), Glucose Toxicity In β-Cells: Type 2 Diabetes, Good Radicals Gone Bad, And The Glutathione Connection. *Diabetes*, 52(3):581-587.

Rolland, F., Winderickx, J. and Thevelein, J.M. (2001), Glucose-sensing mechanisms in eukaryotic cells. *Trends in Biochemical Sciences*, 26(5):310–317.

Rolo, A.P. and Palmeira, C.M. (2006), Diabetes And Mitochondrial Function: Role Of Hyperglycaemia And Oxidative Stress. *Toxicology and Applied Pharmacology*, 212:167-178.

Russell, J.W., Golovoy, D., Vincent, A.M., Mahendru, P., Olzmann, J.A. and Feldman, E.L. (2002), High Glucose-Induced Oxidative Stress And Mitochondrial Dysfunction In Neurons. *FASEB Journal*, 16(13):1738-1748.

Santiago, A.R., Cristovão, A.J., Santos, P.F., Carvalho, C.M. and Ambrosio, A.F. (2007), High Glucose Induces Caspase-Independent Cell Death In Retinal Neural Cells. *Neurobiology of Disease*, 25(3):464-472.

Santoro, M.G. (2000), Heat Shock Factors And The Control Of The Stress Response. *Biochemical Pharmacology*, 59(1):55-63.

Samikkannu, T., Thomas, J.J., Bhat, G.J., Wittman, V. and Thekkumkara, T.J. (2006), Acute Effect Of High Glucose On Long-Term Cell Growth: A Role For Transient Glucose Increase In Proximal Tubule Cell Injury. *American Journal of Physiology – Renal Physiology*, 291(1):F162-F175.

Schlesinger, M.J. (1990), Heat Shock Proteins. *The Journal of Biological Chemistry*, 265(21): 12111-12114.

Singh, M., Sharma, H. and Singh, N. (2007), Hydrogen Peroxide Induces Apoptosis In HeLa Cells Through Mitochondrial Pathway. *Mitochondrion*, 7:367-373.

Soltys, B.J. and Gupta, R.S. (1997), Cell Surface Localisation Of The 60 kDA Heat Shock Chaperonin Protein (HSP60) In Mammalian Cells. *Cell Biology International*, 21:315.

Stebbing, A.R.D. (1982), Hormesis - The Stimulation Of Growth By Low Levels Of Inhibitors. *Science of the Total Environment*, 22(3):213-234.

Tavaria, M., Gabriele, T., Kola, I. and Anderson, R.L. (1996), A Hitchhiker's Guide To The Human HSP70 Family. *Cell Stress Chaperones*, 1(1):23-28.

Triantafilou, M. and Triantafilou, K. (2002), Lipopolysaccharide Recognition: CD14, TLRs And The LPS-Activation Cluster. *Trends in Immunology*, 23(6):301-304.

Tsan, M.F. and Gao, B.C. (2004), Cytokine Function Of Heat Shock Proteins. *American Journal of Physiology-Cell Physiology*, 286(4): C739-C744.

Tsan, M.F. and Gao, B.C. (2009), Heat Shock Proteins And Immune System. *Journal of Leukocyte Biology*, 85(6):905-910.

Vabulas, R.M., Ahmad-Nejad, P., da Costa, C., Miethke, T., Kirschning, C.J., Havker, H. and Wagner, H. (2001), Endocytosed Hsp60s Use Toll-Like Receptor 2 (TLR2) And TLR4 To Activate The Toll/Interleukin-1 Receptor Signalling Pathway In Innate immune cells. *Journal of Biological Cemistry*, 276(33):31332-31339.

van Wijk, F. and Prakken, B. (2010), Heat Shock Proteins: Darwinsitic Immune Modulation On Dangerous Grounds. *Journal of Leukocyte Biology*, 88(3):431-434.

Varming, T., Drejer, J., Frandsen, A. and Schousboe, A. (1996), Characterisation Of A Chemical Anoxia Model In Cerebellar Granule Neurons Using

Sodium Azide: Protection By Nifedipine And MK-801. *Journal of Neuroscience Research*, 44:40-46.

Vayssier, M. and Polla, B.S. (1998), Heat Shock Proteins Chaperoning Life An d Death. *Cell Stress and Chaperones*, 3(4):221-227.

Wegele, H., Muller, L. and Buchner, J. (2004), HSP70 And HSP90- A Relay Team For Protein Folding. *Reviews of Physiology, Biochemistry and Pharmacology*. 151:1-44.

Wallin, R.P.A., Lundqvist, A., More, S.H., von Bonin, A., Kiessling, R, and Ljunggren, HG. (2002), Heat-Shock Proteins As Activators Of The Innate Immune System. *Trends in Immunology*, 23(3):130-135.

Wang, H. and Joseph, J.A. (1999), Quantifying Cellular Oxidative Stress By Dichlorofluorescein Assay Using Microplate Reader. *Free Radical Biology and Medicine*, 27(5-6)316-616.

Wolter, K.G., Hsu, Y., Smith, C.L., Mechushtan, A., Xi, X. and Youle, R.J. (1997), Movement Of BAX From Cytosol To Mitochondria During Apoptosis. *The Journal of Cell Biology*, 139(5):1281-1292.

World Health Organisation. (2006), Definition And Diagnosis Of Diabetes Mellitus And Intermediate Hyperglycemia: Report Of A WHO/IDF Consultation.

World Health Organisation. (2008), Waist Circumference and Waist–Hip Ratio: Report of a WHO Expert Consultation.

World Health Organisation. (2011), New WHO Report: Deaths From Noncommunicable Diseases On The Rise, With Developing World Hit Hardest.

World Health Organisation. (2011), Use Of Glycated Haemoglobin (Hba1c) In The Diagnosis Of Diabetes Mellitus: Abbreviated Report Of A WHO Consultation.

World Health Organisation. (2011), Diabetes Factsheet.

World Health Organisation. (2011), Diabetes Factsheet.

World Health Organisation. (2012), Obesity And Overweight Factsheet.

Wright, B.H., Corton, J.M., El-Nahas, A.M., Wood, R.F.M. and Pockley, A.G. (2000), Elevated Levels Of Circulating Heat Shock Protein 70 (HSP70) In Peripheral And Renal Vascular Disease. *Heart and Vessels*, 15(1):18-22.

Xu, Q., Schett, G., Perschinka, H., Mayr, M., Egger, G., Oberhollenzer, F., Willeit, J., Kiechl, S. and Wick, G. (2000), Serum Soluble Heat Shock Proetin 60 Is Elevated In Subjects With Atherosclerosis In A General Population. *Circulation*, 102:14-20.

Yu, T., Sheu, S.S., Robotham, J.L. and Yoon, Y. (2008), Mitochondrial Fission Mediates High Glucose-Induced Cell Death Through Elevated Production Of Reactive Oxygen Species. *Cardiovascular Research*, 79(2):341-351.

Zarich, S.W. (2009), Potential Of Glucose-Lowering Drugs To Reduce Cardiovascular Events. *Current Diabetes Reports*, 9(1):87-94.

Zeevlak, G.D., Bernard, L.P., Song, C., Gluck, M. and Ehrhart, J. (2005), Mitochondrial Inhibition And Oxidative Stress: Reciprocating Players In Neurodegeneration. *Antioxidant and Redox Signalling*. 7(9-10):1117-1139.

Zhang, D.X. and Gutterman, D.D. (2007), Mitochondrial Reactive Oxygen Species-Mediated Signaling In Endothelial Cells. *American Journal of Physiology – Heart and Circulatory Physiology*, 292: H2023-H2031.

Zheng, L., He, M., Long, M., Blomgran, R. and Stendahl, O. (2004), Pathogen-Induced Apoptotic Neutrophils Express Heat Shock Proteins And Elicit Activation Of Human Macrophages. *The Journal of Immunology*, 173:6319-6326.